F.L.C.S.

Fabric **L**aser **C**utting **S**ystem

Department of Electrical and Computer Engineering
Department of Optics and Photonics
EEL 4914 – Senior Design I
Fall 2025 – Spring 2026

Group 2 Team:

Jacqueline Harper	Nolphky Nicolas	Michael Rodriguez
Photonic Science and Engineering	*Computer Engineering*	*Photonic Science and Engineering*

Review Committee:

Dr. Peter Delfyett	CREOL	Pegasus Professor
Prof. Maddox	ECE	Instructor
Dr. Suboh Suboh	ECE	Associate Lecturer

Advisors:

Dr. Saleem Sahawneh	ECE	Lecturer
Dr. Aravinda Kar	CREOL	Professor

List of Figures

List of Tables

Chapter 1: Executive Summary (Jacqui)

Textiles have played a foundational role in human culture for thousands of years, serving not only as practical tools for protection and warmth but also as one of the most powerful mediums for personal and cultural expression. Fabric, clothing, and crafted textile goods carry meaning—communicating identity, creativity, and heritage. As global interest in handmade goods, customized fashion, and small-batch production continues to grow, there is an increased demand for tools that allow more people to participate in fabric creation and manipulation at a high level of precision and quality. Despite advances in digital design and manufacturing, one of the most fundamental steps in textile work, fabric cutting, remains largely manual, skill-dependent, and often inaccessible.

This project proposes the design and implementation of an accessible, highly reliable fabric laser cutting system intended to transform how individuals or small organizations approach textile fabrication. Traditional cutting methods require physical dexterity, trained technique, and significant time investment, all of which can prevent beginners, hobbyists, or users with limited mobility from engaging fully with textile work. Additionally, manual cutting introduces variability, leading to inconsistencies in pattern shapes, seam allowances, and repeated batches—issues that directly impact product quality. Industrial laser cutters address many of these challenges but remain financially and technically out of reach for most small businesses, schools, and individual creators.

The goal of this project is to bridge this gap by developing a compact and user-friendly fabric laser cutting solution that brings professional-level precision to a wider audience. The system leverages automated motion control, optimized laser parameters for various fabrics, and intuitive software that allows users to upload or design patterns with minimal setup time or computer knowledge. By eliminating the need for aligning, or repetitive scissor work, the system drastically reduces labor while enhancing accuracy and repeatability. Safety considerations—such as enclosed laser operation, ventilation controls, and material-specific presets—ensure that the device remains approachable even for users with no prior experience in laser machining.

The broader impact of this technology extends into multiple sectors. For hobbyists, small businesses, and independent designers, accessible laser cutting significantly increases productivity and consistency, enabling them to compete with larger manufacturers without requiring industrial infrastructure. For hobbyists or individuals with physical limitations, the system opens pathways to creativity that were previously restricted by the physical demands of traditional cutting methods. In our educational setting, it provides students with hands-on experience in digital fabrication and textile engineering, encouraging innovation and interdisciplinary learning.

By enabling access to precision cutting, this fabric laser cutting system advances both the creative and practical aspects of textile work. It supports cultural expression, empowers entrepreneurship, and modernizes one of the oldest human crafts through thoughtful engineering and accessible design. The resulting impact is a meaningful contribution to the evolving intersection of technology, creativity, and human expression in the textile arts.

Chapter 2: Project Description

2.1 Motivation & Background (Jacqui)

The idea of F.L.C.S. is a solution solver. The design of this fabric laser cutter will appeal to those who do not have advanced understanding of computers or computer software. Instead of needing a cutting software or specific file or a laptop to upload the desired cut pattern, we can instead use image acquisition and processing to differentiate the desired cut lines from the fabric. This product is for those "old-fashioned" hobbyists or even business owners who might want some technology to assist them in physically cutting, without needing the background knowledge needed for operating software and uploading files.

F.L.C.S can be useful for all types of hobbyists, designers, and manufacturers who desire quick cutting of pieces of fabric at the tap of a screen. By drawing using a black marker on light fabric or white on dark fabric, the user can outline the desired shape of their fabric and click the touchscreen module to cut the desired lines once the fabric is inside the machine. It is large enough to have a variety of practical applications in terms of the large area we are able to cut. If needed, the system can run multiple cuts on the object.

In senior design our objective is to gather and work as a group. With this project multiple subsystems will be utilized, including a laser diode system, mirror guidance system, power systems, and a user-friendly touchscreen. The beam from the laser diode is focused and collimated using the lens system and is directed by the mirror system. The housing includes a user-friendly touchscreen as well as an optical system emergency stop switch. F.L.C.S's design allows for expansion of its' subsystems if needed, to accommodate the students in the group. For users, this system will be easy to use and understand. It will fit on your work desk or fabric station and will not require you to connect your laptop or PC for fabric cutting.

2.2 Existing Projects & Prior Related Work

2.2.1 Open Source Buildlog.net 2.x Laser [1] (Nick)

The Buildlog 2.x laser is a second generation open-source laser cutter that employs a 2-axis rail-based XY gantry system, with an additional manually adjustable vertical axis. Unlike our proposed fabric laser cutter, the Buildlog 2.x does not have a Human-Machine Interface (HMI). Instead, it relies on tethered computer control for job setup and execution. Our design introduces an onboard Raspberry Pi touchscreen HMI to enable stand-alone operation, real-time job management, and user feedback without requiring a connected computer. In addition, while the Buildlog design delivers the laser via a moving gantry, our project employs mirrors that will steer the beam to the appropriate destination. This approach should reduce the mechanical load of moving the entire laser head and potentially enabling faster operation, though it introduces new challenges in precision alignment and control. Despite these differences, the Buildlog 2.x website provides valuable reference material for general mechanical layout, enclosure design, and community-tested best practices that we can include in our own system.

2.2.2 Commercial Epilog Fusion Pro Lasers [2] (Nick)

The Epilog Fusion Pro is a professional, industry-level laser cutter that integrates a built-in touchscreen HMI, similar to what we intend to implement in our project. Its 7" display allows a user to select between stored jobs, adjust parameters, auto-focus the laser, and rerun previous cuts directly from the machine without requiring a tethered computer. In addition, the Fusion Pro incorporates an overhead camera system, which provides a real-time view of the work area. These features align with our project goals for the FLCS system. By adding an onboard touchscreen interface, our cutter will provide stand-alone job management and ease of use comparable to the Fusion Pro. Although we will not reach the same industrial-grade specifications; we seek to emulate their machine on a smaller and cheaper scale.

2.2.3 DENER FiBER LASER [3] (Nick)

The DENER FiBER LASER is a high-performance 2D metal sheet cutter designed for industrial applications. It uses an XYZ moving gantry laser system, allowing for precise and efficient cutting across large sheet areas. The machine integrates with custom CAD/CAM software, enabling operators to import digital designs and automatically generate optimized toolpaths, ensuring consistent quality, fast processing, and minimal material waste.

Our project follows a similar principle, but with a different workflow and application. Instead of relying on digital design files and specialized software, the cutting path is physically drawn directly onto the fabric. Our system will interpret these hand-drawn lines and guide the laser accordingly, eliminating the need for intermediate design software. This makes the process more intuitive, accessible, and adaptable.

2.2.4 Wattsan 6090 LT [4]

The Wattsan 6090 LT is a versatile laser engraver and cutter designed for precise work across a medium-format area, using an XYZ gantry system. It relies on digital design files that are transferred by software and processed by its controller. This allows the laser to follow exact paths for cutting a variety of materials.

Like that laser system, our project is based on this same principle, but the design input takes a different form. Instead of software-controlled paths, our system locates hand-drawn markings directly on fabric. This approach combines the precision of gantry-based laser cutting with the creative freedom of drawing patterns physically, rather than needing to generate them digitally.

2.2.5 APALES – Senior Design Group 5, Fall 2023 to Spring 2024 [5]

This past Senior Design project by UCF students named "Automated Parameter Adjusting Laser Engraving System" serves as an example of what we seek to build. This project used specific laser power and scan speed for each distinct material to be engraved. Each unique material was identified by a spectrometer, and the laser's power and speed were adjusted to operate on that material. Shapes could be engraved, but also a particular image could be uploaded to an application to have that engraved.

Our laser system will require more power because we will cut through certain fabrics instead of merely engraving them. Our project will have presets for the distinct parameters of varying materials. Similarly, thinking about safety, we will incorporate a fume extraction system to handle toxic fumes.

2.3 Project Goals & Objectives

2.3.1 Goals

- Basic goals
  - Laser beam cuts through fabric with kerf size of less than .5 millimeters
  - Beam from the laser diode is delivered to mirrors safely, and later the fabric
  - Human Machine Interface (HMI) boots with a functional, intuitive user interface
  - HMI clearly display operational options and system status
  - HMI clearly display job progress
  - Touchscreen shall be secure through a rigid panel mount that prevents loosening or flex
  - Touchscreen boots directly into a functional user interface without manual login or terminal interaction
  - Touchscreen options are clear and understandable to the user
  - Capture back-reflections from the fabric
  - Confidently identify marker on fabric canvas
  - Capture clear image of entire fabric canvas in the frame
  - Beam can cleanly cut through fabric
  - Mirror system guides laser beam to target precisely
- Advanced goals
  - Beam is expanded by >5x before reaching mirrors
  - Focused .1-.15mm diameter spot size using a four-lens system: 3 lenses and 2 prisms before the mirrors and one lens after
  - Collimated beam before contacting mirrors
  - HMI displays real time job preview from the camera
  - HMI displays descriptive error messages for user diagnostic
  - Include buzzer or speaker for events such as job completion or system errors
  - Store library of default or frequently used cutting jobs in internal storage
  - Confidently identify lines on multiple fabric types
  - Identify sketches from multiple marker colors
  - Generate coordinate points from capture for smooth operation
- Stretch goals
  - Sensor system integration that can identify reflectance and corresponding required passes for the fabric
  - Adjust power to account for different types of fabrics
  - Support job file upload via USB or wireless transfer
  - Log previous job parameters and error history for diagnostics

    - Integrate with a companion app for remote job upload and monitoring
    - Adjustable power/speed for differing thicknesses of fabric
    - Identify sketches from UV fluorescent markers for no visible marker residue

2.3.2 Objectives

- Basic
    - Laser diode driver distributes current of 2.1A to laser diode, not reaching 3A operating current
    - Fused silica dielectric mirrors used to reflect 99% beam light
    - X-y moving gantry used to move components redirecting the beam
    - Camera placed
    - Anamorphic prism pair corrects beam shape from elliptical to circular
    - The touchscreen shall withstand normal push force akin to the force a user would normally apply during normal operation
        - Under a typical finger press, visible bezel/frame motion shall be ≤0.2 mm
    - The Raspberry Pi Display 2 shall boot and launch the laser-cutter UI automatically through a kiosk-mode configuration within 30 seconds of powering on and will be fully interactable
    - Design the touchscreen UI layout with clearly labelled icons, consistent color coding, and font sizes
        - Conduct a user test with at least 3 people outside of the team. The interface passes if each person can correctly and confidently use the UI without external aid
- Advanced
    - Galilean beam expander expands beam by a factor greater than 7 prior to contact with mirrors
    - Wattage incident on mirrors is >.5 watts
    - Display live job preview or camera feed for alignment verification
    - Log system faults automatically to system's internal storage in a first in first out manner based on available storage
    - Recall default jobs or material presets from internal storage without the need of any markings
    - Implement and onboard buzzer or speaker to provide audible feedback for key system notices such as job completion, errors, and emergency stops
        - Generate distinct audible tones for at least 3 system events (job completion, errors, emergency stop)
        - Ensure that each signal is audible at ≥70 dB some distance from the enclosure
        - Response latency ≤ 200ms between event trigger and audio activation
    - Implement color coded and descriptive error messages that specify the fault type (overheating, UART faults, visual loss from camera) and provide recovery instructions
        - Simulate 3 distinct error conditions and confirm that each generate a message within 1s of detection and remains visible until acknowledged by the user

    - Implement automatic restart of the system's UI if the OS crashes, ensuring continuous operation without user intervention
    - Display real-time job progression on the touchscreen through dynamic progress bars, numeric representation, or elapsed time indicators with estimated time to completion indicator
        - During testing, observe that the interface updates job completion metrics every ≤2s while the laser is active
- Stretch
    - Wireless job upload and download system that allows users to share G-code or job metadata via a companion mobile or web application
        - Demonstrate successful upload of a job file ≤ 1MB from the laser system to the app, and successful download and transfer of that same file to a second device over Wi-Fi or Bluetooth, with total transfer latency of ≤ 2s
    - Develop app functionality that allows a user to remotely monitor active jobs, system status, and error alerts in real time through a Wi-Fi or Bluetooth connection
        - App shall display live job progression, elapsed time, and system state (idle, running, or error) updated at ≤ 2s intervals. Information such as laser power and estimated time to completion will also be shown
        - App shall generate push notifications for any critical errors within ≤ 3s of detection
        - Connection shall remain stable for at least 10 minutes
    - Enable the onboard microcontroller to receive and execute downloadable G-code jobs transmitted from the main Raspberry Pi 4B via UART or USB
        - Confirm end-to-end data transfer integrity by verifying that at least 99% of the data sent from the Pi 4B are received by the microcontroller without corruption and that downloaded jobs execute identically to local jobs
    - Implement an onboard data logging system that records job metadata (duration, laser power, material type, completion status) and all system errors
        - Log entries shall include timestamp, job ID, and error code fields
        - System shall maintain a minimum of 50 records in local storage without corruption. Which a replacement system of first in first out
        - Logged data shall be exportable as a .txt file

2.4 Features & Functionalities

2.4.1 Optical Systems Diagram (Jacqui & Mike)

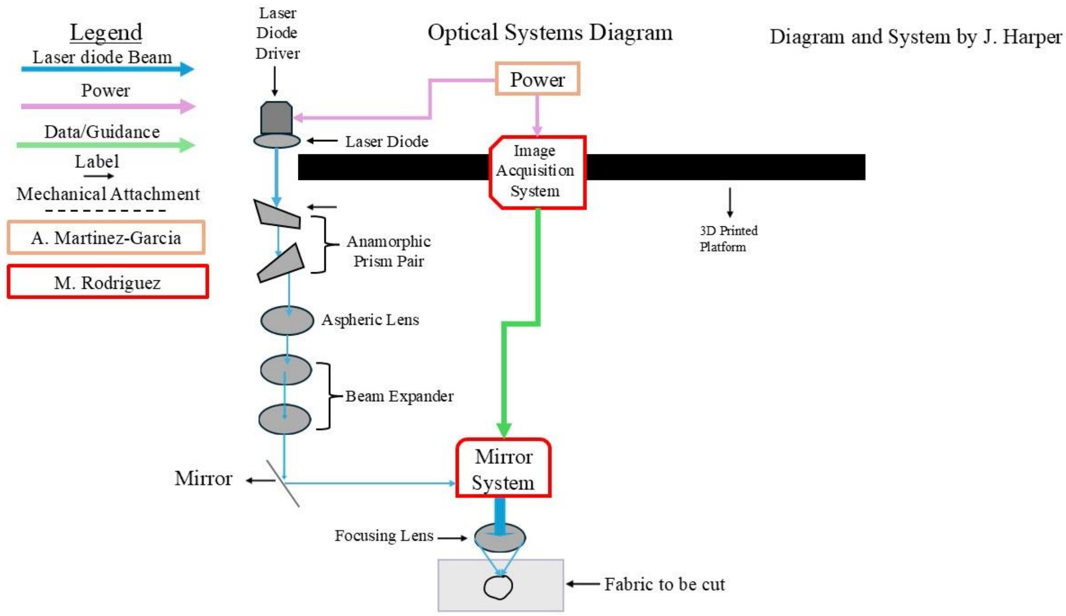

Figure 1: Optical Systems Diagram (Jacqui)

The laser diode system shown in Figure 1 uses an anamorphic prism pair and three lenses, all secured by 3D printed mounts, to keep the laser diode beam collimated and enlarged as it approaches the mirror guidance system with the focusing lens. Collimation of the beam is essential because it minimizes divergence, or widening, of the beam as it travels. The initial lens of the system is aspheric, which will collimate the beam into the anamorphic prism pair that corrects the beam shape. Followed by the beam expander system composed of two lenses, expanding the beam size incident on the mirrors. The beam expander in this system ensures the beam spot size on fabric will be small because the beam incident on the focusing lens is large.

To move the mirrors and redirect the laser beam onto any specific spot of the fabric canvas the user desires to cut, there are two viable mechanisms that were investigated: a moving gantry and galvo motor system. Both mechanisms quickly and efficiently direct the beam and have their advantages and disadvantages.

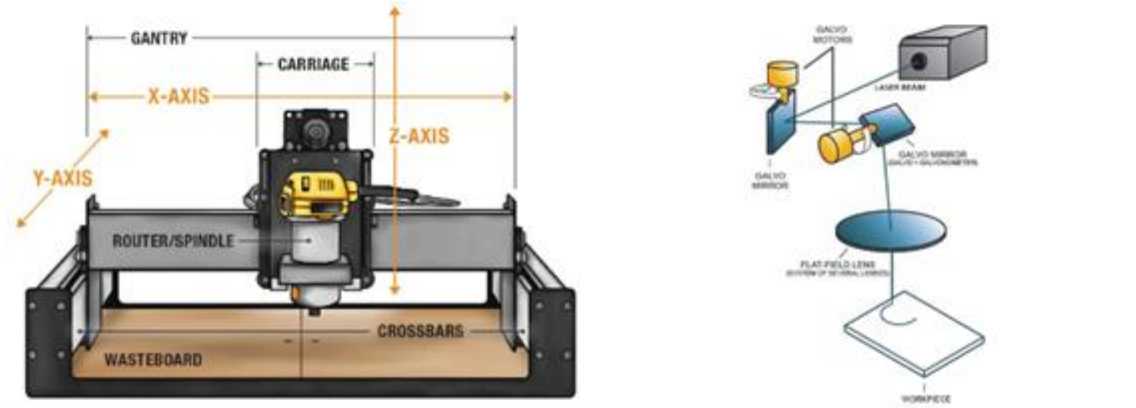

Figure 2: Illustrations of the galvanometer system [23,24] (Mike)

A galvanometer system uses two small fast-moving mirrors mounted onto galvo motors to precisely control the direction of a laser beam onto a specific point on a two-dimensional plane. By rotating the motors with electric signals, the angle of the mirrors change, and the direction of the reflected laser beam changes. The mirrors are used together, one for the x-axis and one for the y-axis. This system works quickly and precisely to rapidly move a laser on a 2D plane, needing very few mechanical parts and with a very compact design. To make sure the beam is focused at the same spot size and reduce distortion on the edges of the field, an f-theta lens is used after the mirrors.

This system is much superior to moving gantry systems on small fields, but as field sizes increase, the galvanometer system becomes a lot less practical. This system has a limited scanning angle. Since the size of the mirrors limits the max scanning angle, larger mirrors would be required to prevent the laser from clipping. The entire 350 mm x 350 mm field may not be accessible to the system in the confined space of the enclosure. The light entering an f-theta lens is usually between 15 to 20 degrees, and no larger than 28 degrees. [25, 26] Based on the area of the field, the focal length of the desired f-theta-lens can be determined:

$$\frac{350}{2\tan(\theta)} = f$$

Even at the maximum angle, the required focal length is 330 mm, which is very large. In fact, none of the f-theta lenses available on Thorlabs or Edmund Optics can cover the entire field except for one; with a focal length of 650 mm and a scan angle of 24 degrees, it could cover a maximum field area of 410 mm x 410 mm. There are only two downsides, the wavelength range is near infrared, and the cost for a single lens is over seven thousand dollars. [25, 26]

A moving gantry system would be much more practical and economical for this field size since it can be scaled up for larger areas without requiring larger optics but instead just scaling the beam sizes to the size of the field area.

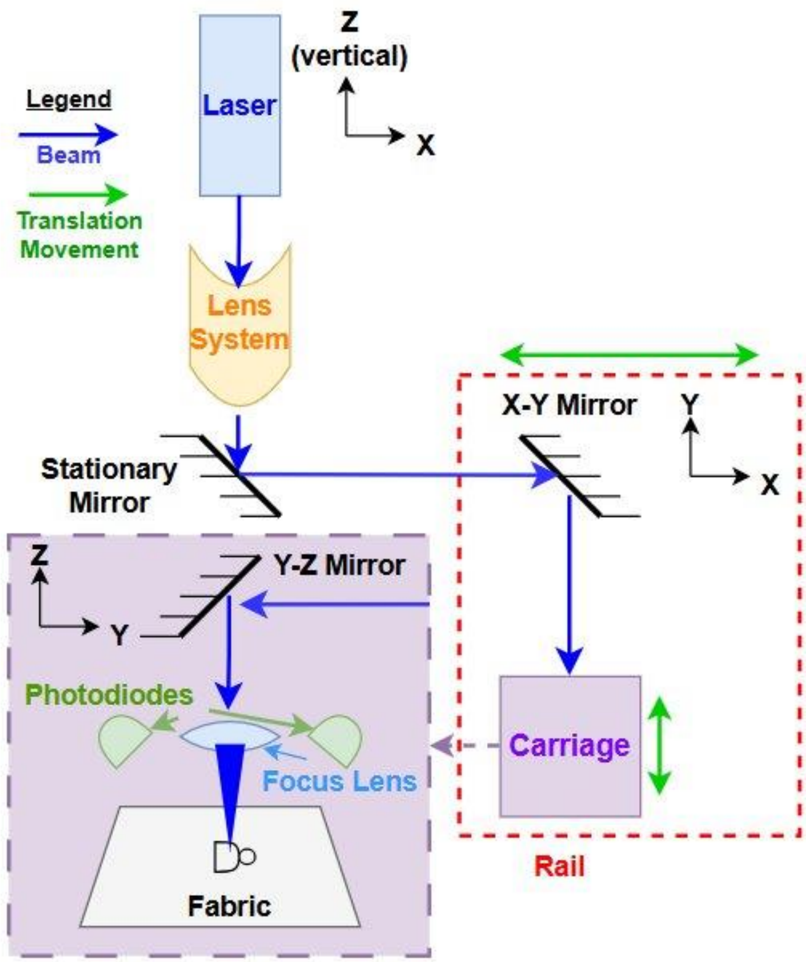

Figure 3: Beam Guidance System Diagram

To best guide this beam with the least amount of divergence and distortion possible, a moving XY gantry mirror system (Figure 2) will be implemented for scanning the entire 350 x 350 mm field. Both mirrors will move in the x-direction together on a shiftable crane component above the fabric, dictating the x-position of the beam. A second downward-facing mirror will move independently in the y-direction along the crane component itself, dictating the y-position of the beam and directing the beam onto the fabric. This makes it possible for the beam to reach any x-y position on the fabric canvas.

At this stage, the beam is still large and collimated with low intensity. Mounted on the same unit as the second mirror, directly under it, is a convex lens to focus this beam to get the final small beam spot and high optical intensity on the desired line to be cut. Since the thickness of the fabrics may differ, the focus lens will be able to translate up and down in the z-direction, ensuring uniform focus spot of high intensity and high precision cutting on a multitude of fabrics.

To be able to detect and locate the lines, a camera mounted overhead will capture an image of the entire fabric canvas in bright ambient lighting before the job is initiated. To avoid distortion at the edges of the image, a narrow FOV camera will be used over a foot above the fabric. Once the image is captured, it is analyzed, the lines are confidently discerned from the fabric, and the pixels will be mapped into coordinates for the beam guiding system to follow.

2.4.2 Subsystem Features

- Laser Diode System (Jacqui)
  - Laser Diode (LD)
    - Beam exiting diode is elliptical and diverges as it travels
    - Beam from LD is guided by mirror system to burn/cut through textiles
  - Laser Diode Driver
    - Delivers constant current to LD, staying below max current threshold of 3A
    - Delivers operating voltage to LD, staying below the maximum voltage value of 5.2 and ensuring a reverse voltage of 2 volts.
  - Lens System
    - Aspheric lens focuses beam into the anamorphic prism pair that corrects the beam shape meaning the slow (horizontal) and fast (vertical) axis of the beam exiting the laser diode
    - Dual lens beam expander system enlarges beam before contacting mirrors with focusing lens
- Beam Guiding System (Mike)
  - Plane mirrors
    - Mirrors fixed at 45° angle with respect to the beam for redirection in each axis
      - Reflect >99% of the incoming beam
    - Gantry rail/motors
      - Smooth precise movement of mirrors
    - Focus lens
      - Maximizes beam intensity on fabric
      - Adjustable height to compensate for fabric thickness
  - Image Acquisition System (Mike)
    - Camera
      - Capture entire fabric canvas area
      - Minimal/no edge distortion
      - Capture high quality images
    - Image processing
      - Reliably contrast/filter lines from the rest of the fabric, if not then error
      - Convert line pixels into gantry coordinates with <1% error
    - Ambient lighting
      - Steady ambient lighting during image capture
  - Touchscreen (Nick)
    - Interactive User Interface
      - 7” multi-touch capacitive touchscreen with intuitive menu navigation

        - Large buttons/Icons to avoid unintended actions
    - Job Management
        - Upload job files via USB flash drive (stretch)
        - Display job preview before starting
        - Select from default jobs integrated into the machine (advanced)
        - Select from stored jobs previously used that were uploaded into the machine
    - Cutting Controls
        - Start, pause, resume, and stop a job from the screen
        - Adjust laser speed and power
    - Status Feedback
        - Real-time progress display to show percent completed and estimated time remaining
        - Descriptive error messages
        - Indicators of the current state of the machine (running, idle, error)
        - Audio feedback via buzzer or speaker
    - Safety
        - Automatic stop when errors occur
        - Emergency stop button

2.5 Component Specifications

Table 1: Component Specifications

Component	Parameter	Specification	Unit
Housing (Jacqui)			
Honeycomb Base	a) Dimensions b) Thickness	a) 400 x 400 b) 22	a) Millimeters b) Millimeters
System Housing	Dimensions	600 x 600 x 600	Millimeters
Camera	Height	441	Millimeters
Laser Diode System (Jacqui)			
Laser Diode	a) Wavelength b) Optical Power Output c) Beam Diameter d)Threshold Current e) Operating Voltage f) Operating Current	a) 445-465 b) 3500 c) TBD d) .25 - .3 e) 4.4-5.2 f) 2.1-2.4 g)3	a) Nanometers b) Milliwatts c) TBD d) Amps e) Volts f) Amps g) Amps

	g) Max Current h) Operating Temperature	h) 0-60	h) Celsius
Laser Diode Driver	a) Current Delivered b) Max Voltage c) Operating Temperature	a) TBD b) TBD c) TBD	a) Amps b) Volts c) Celsius
Aspheric Lens (Thorlabs-C140TMD-A)	a) Focal Length b) Diameter c) Coating d) Diameter with Mount	a) 1.5 b) 2.4 c) ThorlabsA: 300-750 d) 6.2	a) Millimeters b) Millimeters c) Nanometers d) Millimeters
Anamorphic Prism Pair (Thorlabs-PS873-A)	a) Focal Length b) Size c) Coating d) Diameter with Mount	a) N/A b) < 12x12 c) Thorlabs ARC: 350-700	a) N/A b) Millimeters c) Nanometers
Plano-Concave Lens (Thorlabs-LC1975)	a) Focal Length b) Diameter c) Coating	a) -23.9 b) 6 c) Uncoated	a) Millimeters b) Millimeters c) N/A
Bi-Convex Lens (Thorlabs- LB1945-AB)	a) Focal Length b) Diameter c) Coating d) Exiting Beam Diameter	a) 200 b) 1 c)Thorlabs A: 300-750 d) 1.32	a) Millimeters b) Inches c) Nanometers d) Millimeters
Mirror Guiding & Focusing System (Mike)			
Mirror A	a) Reflectivity b) Diameter c) Wavelength	a) >99% b) 7 c) 400-750	a) N/A b) Millimeters c) Nanometers
Mirror B	a) Reflectivity b) Diameter c) Wavelength	a) >99% b) 7 c) 400-750	a) N/A b) Millimeters c) Nanometers
Focusing Lens	a) Focal Length b) Diameter c) Coating	a) 17.9 (at 455 nm) b) 6.5 c) AR	a) Millimeters b) Millimeters c) N/A

	d) Beam Size	d) TBD	d) TBD
Camera-Tracking System (Mike)			
Camera	a) Resolution b) Field of View c) Shutter Speed d) Aperture	a) 1920×1080 b) ~40-60 c) 1/100 d) TBD	a) Pixels b) Degrees c) Seconds d) f/#
Touchscreen System (Nick)			
Screen	a) Touch b) Brightness c) Input latency d) Resolution e) Viewing Angle f) Size	a) Five-touch capabilities b) ≥500 c) ≤100 d) 720 x 1280 e) ≥80 f) 7	a) Pressure Points b) Nits c) Milliseconds d) Pixels e) Degrees f) Inches
Controller/Processor	a) CPU Speed b) RAM c) Power Draw d) Boot Time	a) 1.5 b) 4 c) ~3.4 - 7 d) ~25	a) Gigahertz b) Gigabytes c) Watts d) Seconds
Storage	a) Type b) Size c) Read speed d) Write speed	a) High Endurance b) 256 c) 100 d) 40	a) Class b) GB c) Megabytes per second
Buzzer	a) Frequency b) Trigger Latency	a) 2000 - 4000 b) <1	a) Hertz b) Millisecond
Power System (Tony)			
Power Supply	a) Efficiency b) Load Regulation	a) ≥74 b) ≤8	a) Percentage b) Percentage

Table 2: Engineering and Performance Specifications

Engineering Requirement	Requirement Specification	Unit

<table>
<tr><th colspan="3">Housing System (Jacqui)</th></tr>
<tr><td>The camera will sit at the height to have the full view of the honeycomb laser bed.</td><td>463</td><td>Millimeters, from the bottom</td></tr>
<tr><td>The 3D printed platform will sit at this height to ensure separation of key components from the laser system, accounting for thickness of the platform</td><td>110-137</td><td>Millimeters, From the top</td></tr>
<tr><th colspan="3">Laser Diode System (Jacqui)</th></tr>
<tr><td>The maximum power of the laser diode delivered to the fabric</td><td>3</td><td>Watts</td></tr>
<tr><td>The maximum current delivered to the laser diode, varying depending on the fabric</td><td><1</td><td>Amp</td></tr>
<tr><td>The constant voltage delivered to the laser diode</td><td>4.5</td><td>Volts</td></tr>
<tr><td>The beam diameter size incident on mirrors</td><td><7</td><td>Millimeters</td></tr>
<tr><td>The laser beam can cut through fabric with an initial thickness of</td><td><1</td><td>Millimeters</td></tr>
<tr><th colspan="3">Beam Guiding System (Mike)</th></tr>
<tr><td>Laser redirection speed</td><td>>10, depends on fabric type and thickness</td><td>Millimeters per second</td></tr>
<tr><td>Mirror reflectivity</td><td>>99</td><td>Percent</td></tr>
<tr><td>Final focus spot size</td><td><100</td><td>Microns</td></tr>
<tr><td>Focus lens</td><td>17.9</td><td>Millimeters</td></tr>
<tr><th colspan="3">Image Acquisition System (Mike)</th></tr>
<tr><td>Sensor resolution</td><td>4608 × 2592</td><td>Pixels</td></tr>
<tr><td>Processing Time</td><td>~500</td><td>Milliseconds</td></tr>
</table>

Horizontal FOV	66	Degrees
Vertical FOV	41	Degrees
Depth of field	10 - ∞	Centimeters
Touchscreen System (Nick)		
The system shall boot within and show the system UI within a reasonable amount of time	≤30	Seconds
The system shall show clear images from the camera system and clearly show written text.	720 x 1280	Pixels
The system shall provide user feedback on errors and job progression	≥90% of errors produce an onscreen message	Percentage
The system shall provide audio feedback on job completion and errors	≥70	dB

2.6 Hardware Block Diagram (Tony)

The figure below shows the hardware block diagram for the overall project design. The hardware block diagram involves three main subsystems: the power supply unit, the laser system and the printed circuit board (PCB). The power supply unit serves to provide and distribute stable power to all of the components. The laser system contains several components that will be instrumental in enabling the laser to cut fabrics. All of the subsystems work in tandem to deliver the final product. Each given part of the design is color-coded to establish who in the team will be responsible for that task.

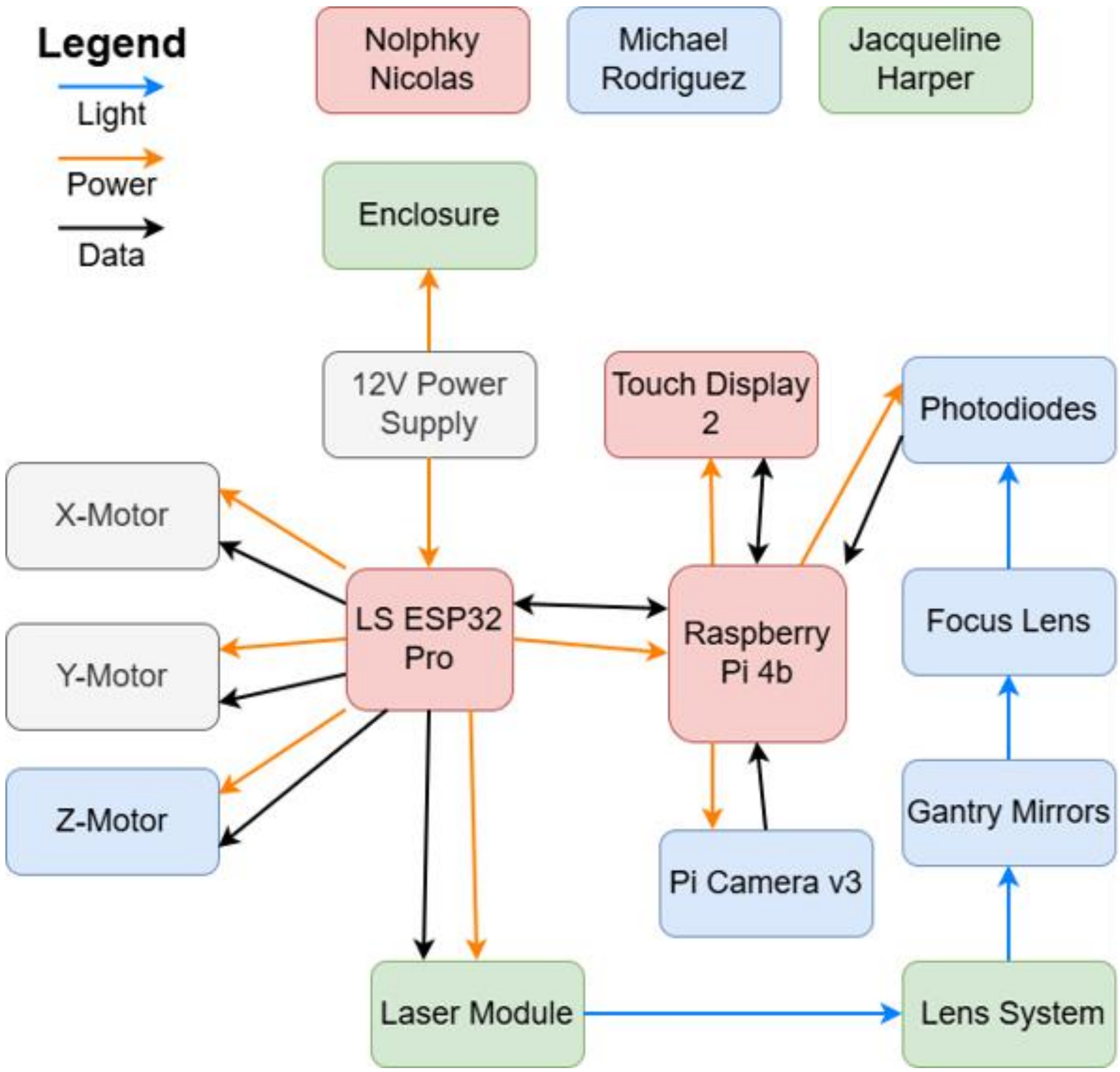

Figure 4: Hardware Block Diagram

2.7 Software Diagram (Nick)

2.7.1 Touchscreen Flowchart & Description

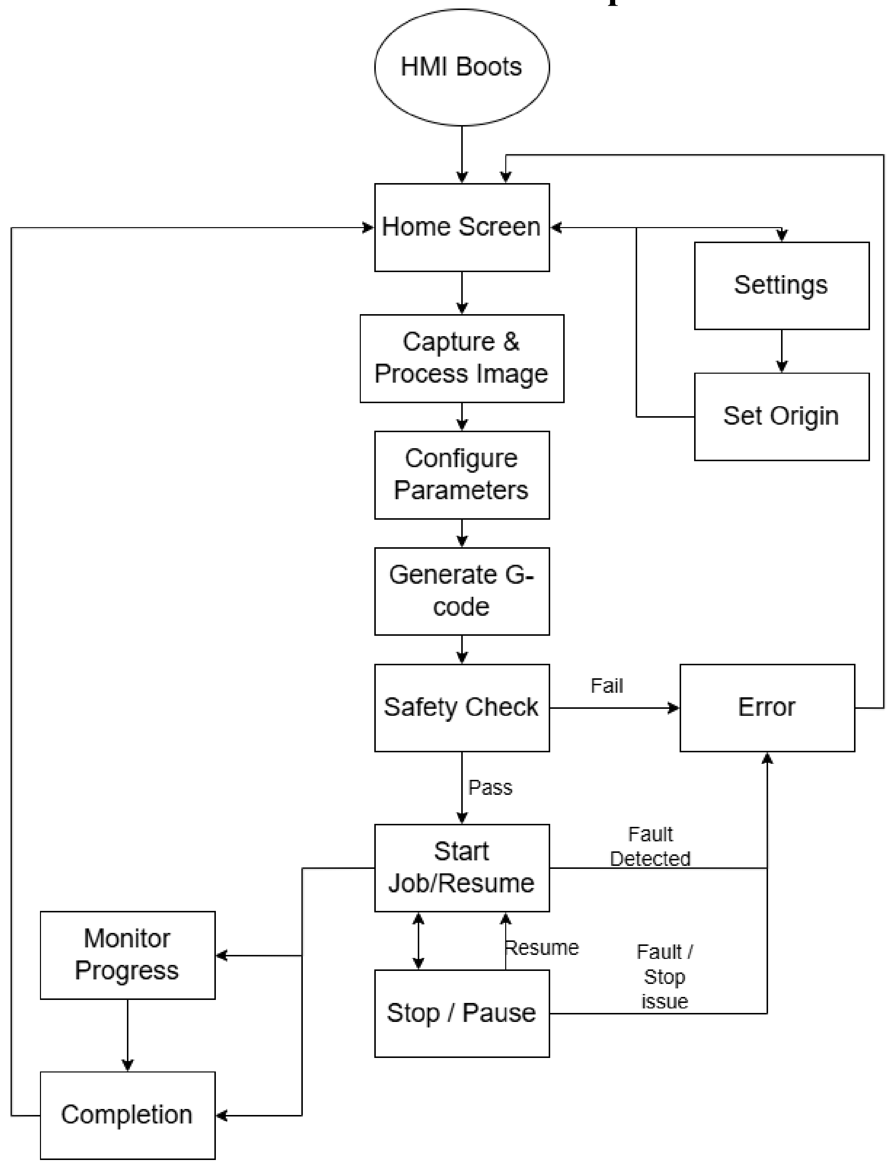

Figure 5: Touchscreen Flowchart

- **Home Screen**
  - Access Settings
    - Control over system preferences
    - Configure camera system (alignment, job preview, calibration)
    - Load job – Selects a cutting job from the camera system or, as a stretch goal, via USB drive or Bluetooth file transfer
- **Load Job**
  - Captured by the camera system (preview image available)
- **Set Parameters**

- Allows for users to configure power, speed, and number of passes
  - Includes material presets for common fabrics
- **Safety Check**
  - The software verifies critical safety check
  - Any failures will lead to an error screen
- **Error Handling**
  - Displays descriptive warnings
  - Prevents the system from starting until conditions are corrected
- **Start Job/Resume**
  - Sends job parameters and cutting commands to the controller
  - Initializes job timer and enables real-time monitoring
- **Monitor Progress**
  - Displays percent completed, estimated time remaining, and live status
  - Emergency stop and pause options are also available on this screen
- **Stop/Pause**
  - User can halt or pause the cutter mid-operation
  - Software ensures the laser powers down safely
- **Completion**
  - Once a job is finished, a confirmation message is displayed. The software logs the job and returns the user to the home screen
  - Provides an option to review job statistics

2.8 Prototype Illustrations (Jacqui)

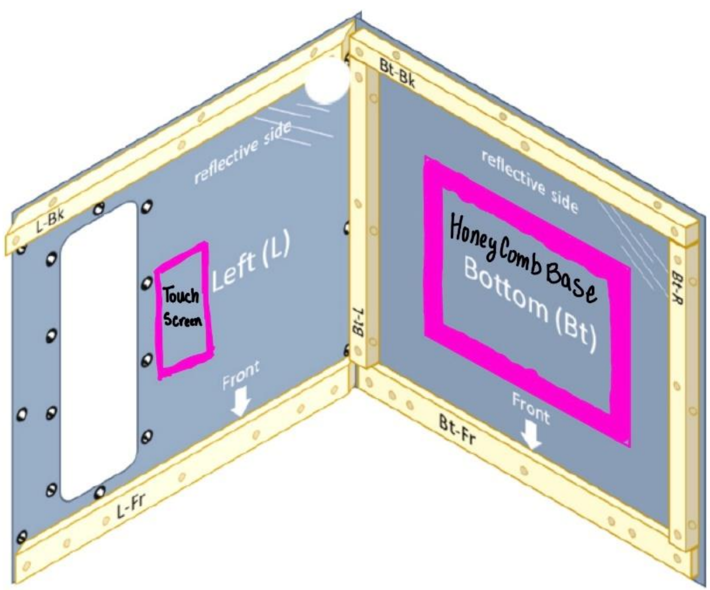

Figure 6: Partially Assembled Prototype with Touchscreen and Honeycomb Base

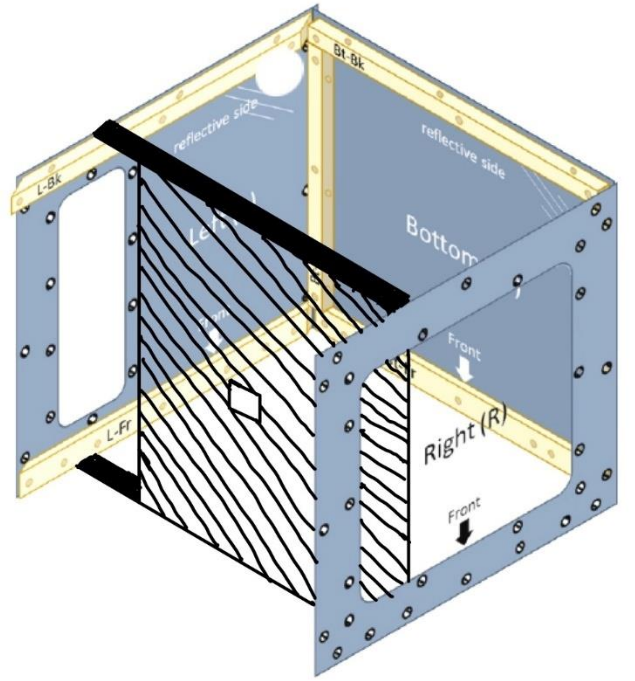

Figure 7: Partially Assembled Prototype with Platform

Since we are purchasing this enclosure, we know the size will be 600x600x600 mm. The enclosure is equipped with OD6+ laser safety windows instead of the clear windows shown in the figures above. This enclosure gives us space to secure each of our subsystems, protects our laser cutting area from outside forces, and gives us easy access to adjust these subsystems once the project is built. We will be utilizing the UCF manufacturing lab to cut extra space in the panel or side of the enclosure for our touchscreen and possible fan system.We will be placing a 400x400mm honeycomb base at the bottom of the cutting system so that there is minimal contact between the fabric and metal as the fabric is being cut by the laser. The honeycomb base and the touchscreen are shown in Figure 6. We will be constructing a 3D-printed platform to separate the gantry system from the power system and anything required to run the touchscreen and camera system. The power systems will be on top of this platform and it will have a space cut so that the optical system rail can be on one side of the enclosure pointing down, with the laser diode above the platform and beam exiting below the platform. There will be a hole-like notch to fit the camera and hold it in place at the height needed to view the entire honeycomb base, shown in Figure 7. We also may add small holes in the platform to aide in airflow.

2.9 House of Quality (Tony)

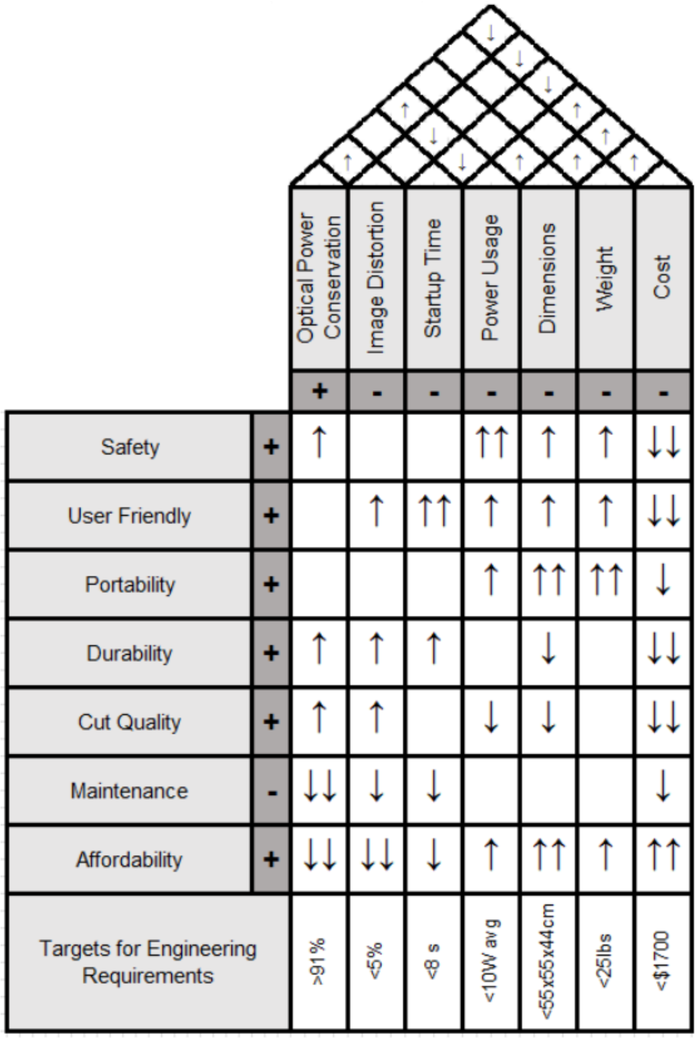

Figure 8: House of Quality

2.10 System Architecture Overview (Nick)

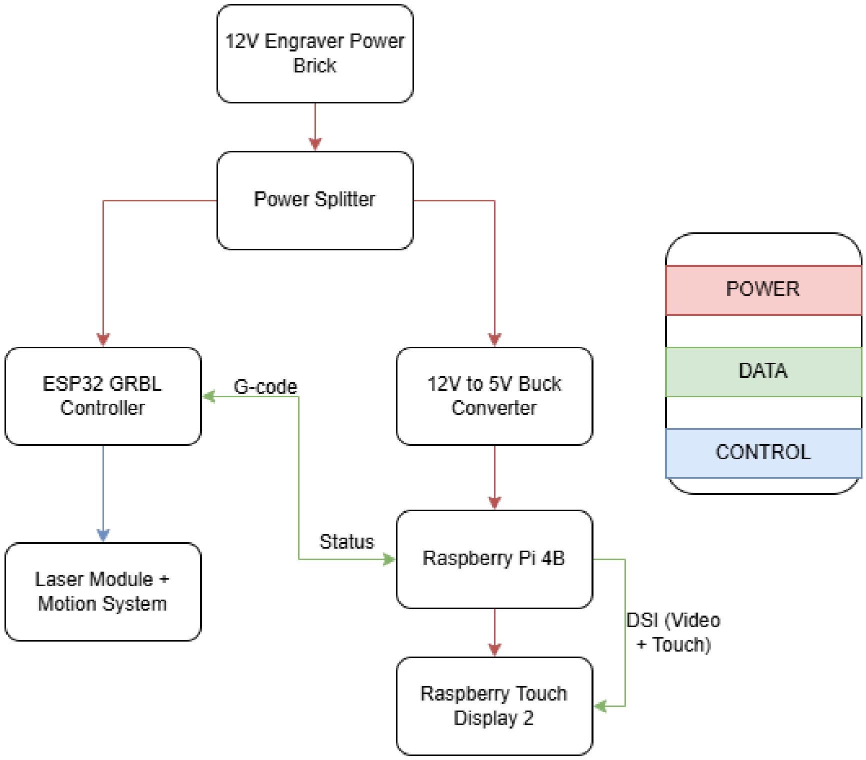

Figure 9: System Architecture

The system is powered by a 12 V power supply that is split between the laser engraver and a 12V to 5V buck converter for the Raspberry pi 4B. The Raspberry Pi hosts the touchscreen HMI and communicates with the ESP32-based GRBL controller via USB serial using G-code commands. The GRBL controller executes motion control and laser operations, while the Raspberry pi manages high level tasks such as suer interaction, image processing, and job configuration. The touchscreen display is interfaced through a DSI connection for video and touch input and powered by the Raspberry pi via its 5V and GND pins.

Chapter 3: Research

3.1 Hardware Research

3.1.1 Housing Comparison Table & Description (Jacqui)

Table 3: Housing Comparison Table

Enclosure/Housing			
Name or Product (Brand)	Laser Engraver Cover (Creality)	Professor Laser Engraver Enclosure (Makergadgets)	Innovator 3D Printer/Engraver Enclosure (Makergadgets)
Material	Flame-retardant fabric	Aluminum	Aluminum

Dimensions (mm)	700x720x400	724x699x292	600x600x600
Acrylic Window Dimensions (mm)	255x255	200x600	(2) 216x356
Additional Features	Zipper, lightweight, OD6+ viewing window, Hinged door on top	Door on top, OD6+ viewing window	Hinged side door, OD6+ viewing window
Cost (USD)	59.99	Originally 99.99, 125.00 with OD6+ window	99.99 base price, up to 180.00

When considering how to build our housing, this group was limited due to the absence of a mechanical engineer. To avoid mistakes in designing the main structure for our system, we opted to purchase an enclosure to house our system. After noticing the fabric material used in the Creality Laser Engraver Cover, we decided to focus our efforts on finding housing that would be an affordable metal such as aluminum. This was done to eliminate concerns when using flammable materials. By filtering our scope based on our desired material we were able to limit our other options to two enclosures offered by Makergadgets.

Between our available options, we prefer the "Innovator", this enclosure has a side door that will allow us to mount the camera and laser diode module towards the top of the interior, staying stationary, while allowing the user to open and close the door as needed and easily view the cutting system at work. These Makergadgets brand options are larger than our initial dimensions, but this extra space will be taken up by necessary electronic components, the mirror and focusing guidance system, as well as stabilizing components to ensure movement of our guidance system does not move the fabric. The "Innovator" comes equipped with a two-phase air purification system that absorbs harmful compounds and fumes using high efficiency particulate air filters or HEPA filters. These types of filters have been confirmed by NASA as well as the University of Minnesota to remove 99.99% of nanometer-sized particulates [6]. For this enclosure to be the most practical, we will be cutting out some of the aluminum to make space for our touchscreen and possible supplemental fan system. We will be cutting this aluminum using the manufacturing lab at UCF.

3.1.2 Touchscreen Comparison Table & Description (Nick)

Table 4: Touchscreen Comparison Table

	Raspberry Pi Touch Display 2 (7")	**Generic 7" HDMI touchscreen**	**10.1" HDMI Touchscreen**
Resolution	720x1280	1024x600	1280x800
Size	7"	7"	10.1"

Touch Spec	Capacitive (5-point)		Capacitive (5-10 point) Capacitive (5-10 point)
Connection to Pi	DSI ribbon (video) + 5 V GPIO (power/touch)	HDMI (video) + USB (touch) + 5 V barrel/USB (power)	HDMI (video) + USB (touch) + 5 V barrel/USB (power)
Driver Support	Native in Raspberry Pi OS, no config needed	USB HID (works as generic mouse) usually plug & play	USB HID (works as generic mouse) usually plug & play
Cable Management	Very clean (only ribbon + jumper)	Messy (HDMI + USB + power cable)	Messy (HDMI + USB + power cable)
Power Draw	~2.4-3 W	~3-5W	~5-8W
Ease of Mounting	Panel mount, slim	Often thicker, may need custom bezel	Bulkier, needs larger cutout
UI Real Estate	Limited (good for menus and buttons)	More space for menus/status	More space; can show job preview or even webcam feed
Cost	~$80	~40-70	~$80-130
Best for	Clean integration, guaranteed support, low hassle	Slightly higher resolution on same footprint	Larger UX, multi-window layouts, more “industrial” look
Link	Raspberry Pi Touch Display 2	$48 Amazon $42 elecrow $44 waveshare	Amazon link around $84

Three candidate touchscreen options were considered: the Raspberry Pi Touch Display 2, a set of generic 7-inch HDMI panels (such as the Waveshare and Elecrow 1024x600 models), and a 10.1-inch HDMI touchscreen (such as the ROADOM 1280x800 display). The HDMI panels provide slightly higher resolution than the official Pi display, with the 10.1-inch screen offering more UI real estate for previews and menus. However, both HDMI options require multiple connections (HDMI for video, USB for touch, and separate 5 V power), which complicates cable management inside the enclosure and introduces potential signal interference if cables are unshielded[7][8].

In contrast, the Raspberry Pi Touch Display 2 uses a native MIPI-DSI ribbon for video and draws power directly from the Pi’s GPIO header, yielding a compact, lightweight assembly with minimal cable clutter[9]. This tight integration also reduces potential mechanical strain on connectors and improves long-term reliability in an enclosed system where space is limited. Because the official display is supported natively within Raspberry Pi OS, no external USB drivers or calibration utilities are required, ensuring plug-and-play operation and long-term maintainability[10].

Long-term reliability is a nice addition that comes with the touch display 2. Since it is produced and supported by Raspberry Pi Ltd., its drivers are bundled directly within official Raspberry Pi OS releases. This ensures continued compatibility with future kernel updates and firmware revisions without requiring external configuration or third-party patches.

From a thermal and power perspective, the official display is also advantageous. Drawing power directly from the Pi's regulated 5 V rail ensures stable voltage levels and avoids the potential ground loops or noise that can occur with separate HDMI and USB power lines. With a measured draw of approximately 2.5 W during normal operation[11], it contributes less heat to the enclosure and maintains overall system efficiency, which is an important factor in a closed laser-cutter chassis where airflow is limited.

The DSI connection also reduces electromagnetic interference within the control enclosure. HDMI and USB cabling can act as radiating loops (especially when unshielded) that introduce signal noise into nearby low-voltage PWM and sensor lines. The MIPI-DSI ribbon uses short, low-voltage differential pairs that minimize radiated emissions and susceptibility to noise, which is advantageous in systems involving precision laser timing and analog sensing.

From an ergonomic standpoint, a 7-inch display size provides sufficient screen space for large, easily navigable icons and menus without taking too much space on the available side-panel dimensions of the enclosure. A higher resolution 10.1-inch screen is visually appealing but is not necessary and conflicts with the system's compact form factor.

Finally, extensive community forums and official resources further supported the choice to use the Raspberry Pi Display 2 over the others. Because it is part of the Raspberry Pi's ecosystem, guides, libraries, and troubleshooting information are available through documentation and developer forums. This greatly reduces potential integration issues and lowers development time compared to lesser-known third-party HDMI panels.

3.1.3 Controller Comparison Table & Description (Nick)

Table 5: Touchscreen Controller Comparison Table

	Raspberry Pi 4B	**Raspberry Pi 5**	**Arduino Mega 2560 Rev3**	**NVIDIA Jetson Nano**	**ESP32-WROOM**

Ram	4GB LPDDR4 SDRAM	LPDDR4X-4267 SDRAM 4GB	8kb SRAM	4GB 64-bit LPDDR4 25.6GB/s	520 KB SRAM, 4 MB Flash
Processor	Broadcom BCM2711, a quad-core Cortex-A72 (ARM v8) 64-bit SoC @ 1.5GHz	Broadcom BCM2712, a Quad-core 2.4 GHz Arm Cortex-A76	ATmega2560	Quad-core ARM® Cortex®-A57 MPCore processor @ 1.43GHz	two low-power Xtensa®32-bit LX6 microprocessors
Graphics/Display	VideoCore VI 3D Graphics	VideoCore VII	none	128-core NVIDIA Maxwell™ architecture GPU	none
Connectivity	2.4 GHz and 5.0 GHz IEEE 802.11b/g/n/ac wireless LAN, Bluetooth 5.0, BLE Gigabit Ethernet 2 × USB 3.0 ports 2 × USB 2.0 ports	2.4 GHz and 5.0 GHz IEEE 802.11b/g/n/ac	54 digital I/O pins 4 hardware	Gigabit Ethernet 4 x USB 3.0 ports	Wi-Fi 802.11 Bluetooth v4.2 BR/EDR and BLE

					wireless Bluetooth 5.0, BLE Gigabit Ethernet 2 × USB 3.0 ports 2 × USB 2.0 ports	UARTS USB B connector	Micro USB/USB C HDMI 2.0 Display port	specification NZIF receiver with –97 dBm sensitivity SD card, UART, SPI, SDIO, I2C, LED PWM, Motor PWM, I2S, IR, pulse counter, GPIO, capacitive touch sensor, ADC, DAC
Cost	$59.99				$60.00	$49.90	$129.00	
Power Requ	5V 3A (USB-C power supply)	5v 5A (USB-C	5V 7V-12V	5V	3V - 3.6V			

ireme nt		power supply)	(recom mende d input)		
Oper ating Temp eratu re	0–50ºC	0–50ºC	–40 °C ~+85 °C	–25 °C ~+85 °C	–40 °C ~+85 °C

In evaluating potential controllers for this project, five options were considered: the Raspberry Pi 5, Raspberry Pi 4B, Arduino Mega 2560, and ESP32-WROOM. The Arduino Mega 2560, while inexpensive and reliable for low-level embedded control, lacks an operating system, GPU, and sufficient memory, making it unsuitable for a system requiring a touchscreen interface. Similarly, the ESP32-WROOM, recommended by a peer for its strong bluetooth and WI-FI capabilities and ease of programming through the CP2102 USB-to-UART bridge, excels in IoT and wireless applications but falls short in onboard computing power, GPU support, and OS capabilities. It is better suited for real-time, low-level control, whereas this subsystem requires a supervisory-level controller capable of running a graphical interface and managing multiple software processes.

The Jetson Nano offers significant graphical and AI-processing performance, but its higher cost, greater power consumption, and lack of onboard wireless connectivity would add unnecessary complexity, particularly if the project's stretch goal of Bluetooth communication is pursued. Between the two Raspberry Pi options, the Pi 4B provides a proven balance of cost, community support, and performance, while the pi 5 offers improved CPU and GPU resources and higher RAM options, making it a more future-proof choice. Ultimately, the Raspberry Pi family was selected as the most suitable controller platform due to its ability to run a full Linux operating system, support a native touchscreen interface, and balance affordability with the required computational capabilities. Between the two, however, the Pi 4B is chosen because it requires a smaller power supply, has lower cost, and is more field proven than the newer Pi 5.

3.1.4 Microcontroller Comparison Table & Description (Nick)

Table 6: Microcontroller Comparison Table

Microcontroller	Process/ clock	Key Features	Pros	Cons	Fit for project

Raspberry Pi Pico 2	Dual-core ARM Cortex-M33 @ 150 MHz	520 KB on-chip SRAM USB drag and drop programming	• Excellent timing precision (< 1 µs interrupt latency) • Low cost (< $10) • Easy USB programming • Strong community and Raspberry Pi integration	• Limited flash/RAM • No RTOS (bare-metal or simple scheduler)	**Selected** – provides reliable real-time control for laser PWM and safety interlocks
Arduino Mega 2560	8-bit AVR @ 16 MHz	54 GPIO, UART, SPI, I²C	• Widely used and beginner-friendly • Excellent Arduino library support	• 8-bit MCU with limited speed; not ideal for precise timing or heavy serial traffic	Slower; insufficient timing resolution for laser PWM
STM32 F4 Series	32-bit ARM Cortex-M4 @ 180 MHz	Advanced timers, DMA, RTOS support	• High-performance MCU with rich peripherals • Can run FreeRTOS for multitasking	• Higher cost • Requires more complex toolchain and setup	Viable but adds unnecessary complexity for a student project
ESP32	Dual-core Xtensa	Wi-Fi, Bluetooth,	High clock speed, wireless	Nondeterministic timing due to background	Implemented as it came with

	LX6 @ 240 MHz	FreeRTOS support	connectivity, low power	Wi-fi/Bluetooth tasks	the engraver

After evaluating multiple microcontrollers such as the Arduino Mega 2560 and STM32 F4 Series, the team considered the Raspberry Pi Pico 2 for the real-time control layer. Compared to the Arduino Mega's slower 16 MHz clock speed, the Pico 2's dual-core ARM Cortex-M33 processor running at 150 MHz provides microsecond-level timing, ideal for laser PWM gating and safety interlocks. Using the fundamental clock-period equation T=1/f, this corresponds to approximately 6.7 nanoseconds per cycle, demonstrating the Pico 2's capabilities to handle sub-microsecond interrupts with deterministic precision.
While the STM32 F4 Series offers even higher performance, it introduces greater cost and toolchain complexity than required for this project. The Pico 2 delivers a strong balance of performance, cost, and ecosystem support with 520 KB of on-chip SRAM, simple USB drag-and-drop programming, and full compatibility with the Raspberry Pi SDK. These factors make it a reliable and affordable choice for deterministic real-time control without adding unnecessary complexity to the overall system.

However, during system integration, the design shifted to utilize an ESP32-based GRBL-compatible controller integrated within the engraver hardware. This controller is responsible for executing G-code commands, generating motion trajectories, and controlling output through PWM signals. Although it was not originally selected for strict real-time control due to potential nondeterminism from background tasks, the ESP32 proved to be highly effective in practice due to the optimized GRBL firmware environment. GRBL provides precise motion planning, stepper motor control, and laser modulation, eliminating the need to implement these features from scratch.

In the final architecture, the Raspberry Pi 4B acts as a high-level supervisory controller, handling the human machine interface (HMI), image processing and G-code generation. The ESP32 controller executes low-level motion control tasks, forming a distributed system that balances computational flexibility with reliable machine control.

This approach simplifies development while leveraging proven firmware, resulting in a robust and practical implementation aligned with project requirements.

3.1.5 Communication Interface Selection (Nick)

Table 7: Communication Interface Table

Interface	Typical Speed	Wiring Complexity	Processor Overhead	Determinism	Debugging Ease	Fit for project

UART	Up to ~1 Mbps	2 lines (TX/RX)	Low	High	Excellent (serial monitor)	Considered: reliable, low-latency control link
SPI	Up to ~10 Mbps	4 lines + CS (with more peripherals)	Moderate	High	Moderate (logic analyzer)	High speed but requires more pins
I²C	Up to 400 kbps	2 lines (SDA/SCL)	Moderate	Medium (shared bus)	Difficult (shared addressing)	Simpler wiring but less robust timing
USB	12 Mbps (Full) / 480 Mbps (High)	2 differential pairs	High (stack driver)	Low	Complex (driver-dependent)	Good for firmware update

In the final system implementation, communication between the Raspberry Pi 4B and the laser engraver controller is achieved using USB serial communication. The engraver is driven by an ESP32-based GRBL compatible controller, which exposes a virtual serial interface over USB. This eliminates the need for direct hardware level protocol such as SPI or I²C.

Although UART was initially considered for a direct microcontroller to microcontroller link, the use of USB simplifies integration by providing a standardized communication interface with built-in driver support. The Raspberry Pi transmits G-code commands over this serial interface which are interpreted and executed by the GRBL firmware on the controller.

This approach offers several advantages including ease of debugging through serial monitoring, reliable data transmission, and compatibility with existing tools such as LaserGRBL. While USB introduces slightly higher overhead compared to UART, it is not a limiting factor for this application due to the low bandwidth requirements of G-code streaming. Overall, USB serial communication provides a robust and practical solution for coordinating motion control in the system.

3.1.6 Timing Budget and Determinism Requirements (Nick)

In real-time embedded systems, each subsystem operates under different latency and determinism requirements. Human-interface actions, such as touchscreen input or menu updates, can tolerate delays in the order of tens of milliseconds without affecting usability, while laser gating and motion control demand precise, repeatable timing at the microsecond scale.

In the F.L.C.S. architecture, this requirement is addressed by delegating all timing-critical operations to the ESP32-based GRBL controller. The GRBL firmware internally manages stepper motor pulse generation, motion planning, and laser PWM modulation with deterministic timing. This eliminates the need for real-time guarantees on the Raspberry pi, which operates as a high-level supervisory system.

A timing budget is therefore established to distinguish between non-real-time tasks executed on the Raspberry Pi and real-time tasks handled internally by the GRBL controller. This separation ensures reliable system performance while maintaining flexibility for user interaction, image processing, and job configuration.

Table 8: Timing Budget Table

Operation Type	Example Task	Target Latency (max)	Allowable Jitter	Runs On	Rationale
Image Processing /Job Preparation	Generate G-code from captured image and job configurations	>100 ms	N/A	Pi 4B (Linux)	Computationally intensive, not time-critical.
UI/HMI	Touch press. Button highlight; screen refresh	≤ 100 ms	≤ 20 ms	Pi 4B (Linux)	Human-perceptible but tolerant to delay

Job I/O & Logging	File operations, loging	10 - 100 ms	≥ 10 ms	Pi 4B (Linux)	Not real time critical
Command dispatch	Stream G-code to controller	≤ 10 ms (per command)	≤ 5 ms	Pi 4B via USB Serial	Ensures smooth command flow to GRBL
Motion Control Execution	Stepper motion, trajectory planning	Microsecond scale (internal)	Deterministic (internal)	ESP32 GRBL Controller	Hnadled internally by GRBL firmware
Laser Power Control	Laser PWM MODULATION	Microsecond-scale (internal)	Deterministic (internal)	ESP32 GRBL Controller	Ensures consistent energy delivery
Safety interlocks	Emergency stop	Immediate (hardware/firmware)	Deterministic	ESP32 GRBL Controller + hardware	Critical for safe operation
Controller Monitoring	Status reporting (“ok”, errors)	≤ 50 ms	≤ 10 ms	ESP32 to Pi	Supports UI updates and fault detection

3.1.7 Motors

The movement of the laser is of great importance to achieve a fine and precise cut. The movement will be dependent upon the functionality of particular types of motors and motor controllers. The motors to be implemented will move using X and Y coordinates to move the laser accordingly. The type of motor to be used will need to provide the necessary torque to consistently cut in an optimal manner. Most importantly, precision will be best tailored by a motor that can provide small, gradual, calculated movement.

The two main categories of motors are alternating current (AC) motors and direct current (DC) motors. From there, each category has several different kinds of motors. DC motors will best suit this project due to the fact that much of the hardware operates on direct current. It must also be noted that it is simpler to handle control systems with DC motors than with AC motors. Each varied motor will have its advantages and disadvantages. Ultimately, the type of motor to be implemented will have features that most effectively meet the project’s needs.

3.1.7.1 Brushed DC Motor

The main parts of this motor include a stator, rotor, brushes and a commutator. The stator produces a static magnetic field around the rotor. The rotor's winding(s) generate a magnetic field when they are supplied with energy. The poles generated from the rotor's magnetic field will come together with the opposite poles from the stator's magnetic field. This coming together of opposing poles will allow the rotor to rotate. When the motor rotates, the brushes will come into contact with many parts of the commutator. A changing magnetic field will be produced inside the motor as a result of a voltage being applied across the brushes. In contrast to brushless DC motors, brushed DC motors do not need a controller to switch the direction of the current. This is due to the fact that it contains brushes and a commutator.

There are some advantages to consider in utilizing a brushed DC motor. For one, the speed of a brushed DC motor is directly correlated to the voltage. Another advantage could be that if only unidirectional rotation is required, and speed and torque do not need to be managed, then no motor controller is needed. Conversely, there are some disadvantages in using a brushed DC motor. For one, the brushes and the commutator are worn out over time. This occurs from the friction when the brushes come into electrical contact with the commutator. For another, the motor is a bit noisy due to the contact between the brushes and the commutator. The noise and brush arcing increases as the motor speed increases. However, it must be noted that the rotational speed is inhibited by the brushes and the commutator. In addition, brushed DC motors have poor acoustic noise and torque ripple.

3.1.7.2 Brushless DC Motor

The main parts of this motor include a stator, a permanent magnet rotor and an electronic controller. This motor is synchronous due to the magnetic field of the stator rotating in equivalent frequency as the magnetic field of the rotor. In contrast to brushed DC motors, brushless DC motors do need a controller to switch the direction of the current. This is due to the fact that it does not contain brushes and a commutator. To attain motor rotation, the stator windings must be supplied with energy in a sequence. The rotor position must be known to know which winding must be supplied with energy. The Hall effect sensors in the stator serve to identify the rotor’s position. From what the Hall sensors identify, the appropriate current is identified to send to the stator to be able to rotate the rotor.

There are some advantages to consider in utilizing a brushless DC motor. This motor does not have the mechanical wear concerns that brushed DC motors have since this motor is brushless. The motor is not noisy thanks to the electronic controller being used for commutation instead of mechanical parts. Unlike brushed DC motors, the rotational speed is not inhibited by brushes. Also, acoustic noise and torque ripple could be decreased by manipulating the winding currents. Conversely, there are some disadvantages in using a brushless DC motor. Due to brushless motors utilizing an electronic controller and possibly using rare earth magnets for the rotor the purchase price is higher than that of a brushed DC motor. However, it must be noted that the purchase price is higher, but over time it could be money better spent due to the motor experiencing a greater life than brushed DC motors.

3.1.7.3 Servo Motor

The main parts of this motor include the actual motor (DC motor in our case), an encoder or some feedback device, and a controller. The encoder produces signals that specify the angle or displacement of the motor shaft for the purpose of giving feedback on the position of the motor to the controller. The controller uses the feedback signal to change the motor's output, accordingly, in an effort to realize the precise movement. The motor's output is changed by giving it a particular speed, position or torque. An amplifier modifies the voltage or current to adjust the position, torque, or speed accordingly. This use of the feedback signal is what makes it a closed-loop system. The driver circuit drives the motor in a closed-loop system to get to the desired position. The driver adjusts the motor's electrical windings to generate magnetic fields that move the shaft. This motor is built to accurately dictate angular or linear position, velocity and acceleration.

In addition, many servo motors have gears on the shaft to manipulate the motor's output torque and rotation speed. Servo motors have three key operating modes: speed control, torque control and position control. Speed control serves to hold a constant speed despite a change in load. Torque control serves to apply a steady torque in cases where a continuous force is needed. In position control, the motor responds to instructions to move a certain distance or angle.

There are some advantages to consider in utilizing a DC servo motor. For one, a servo motor has a high output power with respect to its size and weight. Another advantage could be that it has a high torque to inertia ratio. Also, the motor can reach a high speed at a high torque. They are not noisy at high speeds. They do not suffer from being out-of-step. Conversely, there are some disadvantages in using a DC servo motor. For one, servo motors need to be tuned to stabilize the closed-loop system. Also, safety circuits are needed in the case of a malfunction. In addition, servo motors are worn out by prolonged overload. Servo motors may also have a higher cost than other motors like stepper motors because of the use of more complex components. Servo motors do not precisely control rotation due to the lag when it is rotating with respect to the command pulses. Most importantly, servo motors vibrate when stopped.

3.1.7.4 Stepper Motor

The main parts of this motor include the stator (has teeth on which coils are wired) and the rotor (which can be a permanent magnet or a variable reluctance iron core). The shaft of the stepper motor rotates by moving a specific number of degrees. The angular position of the shaft is known precisely without the use of a sensor by tracking the number of steps executed. When energy is supplied to one or multiple stator phases, a magnetic field is produced from the current moving in the coil and the rotor positions itself with the field. In energizing various phases in sequence, the rotor is able to rotate by a particular amount to achieve the precise position.

It must be noted that there are three distinct rotor types. For the permanent magnet rotor, it positions itself with the magnetic field from the stator. This allows for an adequate torque and stopping torque. The stopping torque comes from the motor holding itself to a change in position even if a coil has energy. This type of rotor has a lower speed and a lower step size than the other rotors. In the variable reluctance rotor, its shape facilitates its ability to position itself with the magnetic field. This rotor is of an iron core. This rotor is better suited to attain higher speeds and higher step sizes. However, this rotor tends to have lower torque, and it does not have a stopping torque. For the hybrid rotor, it is a combination of the permanent magnet rotor and the variable reluctance rotor. It contains two caps that have alternating teeth, and it becomes magnetic around an axis. A high amount of teeth makes it possible for the motor to attain a short step size of around 0.9°. The stator consists of a certain amount of phases, pairs of poles and wire configuration. The typical stepper motor used is the two-phase stepper motor.

Among the various drivers for stepper motors, the three typical drivers are the Step/Direction driver, the Phase/Enable driver, and the pulse width modulation (PWM) driver. Depending on the driver, it could only regulate the voltage of the winding, or it could additionally regulate the current of the winding. In the case of regulating the voltage, the torque and the speed of how the steps are performed rely on motor and load features. Conversely, torque could be manipulated more effectively in the case that the driver regulates the current of the winding. The direction of the current is also dependent on how the stator coils are structured. The stator coils could be structured in a unipolar manner or in a bipolar manner. A disadvantage of the unipolar stepper motor is the fact that only fifty percent of the copper in the motor is used which results in a magnetic field with half the intensity that would be seen if all of the copper were to be used. Conversely, the bipolar stepper motor is able to maximize torque with respect to how much copper is utilized.

The stepper motor has four distinct driving modes that could be implemented. Wave mode operates by having energy supplied to only one phase at a given moment. For full-step mode, energy is supplied to two phases at a given moment. Full-step mode can achieve a greater torque than wave mode due to a greater current flow and magnetic field coming from the additional phase. Half-step mode is the fusion of wave mode and full-step mode. As hinted by the name, the step size is halved in half-step mode. A disadvantage is that the torque is not stable because it alternates when one phase is supplied with energy and when two phases are supplied with energy. Micro-stepping mode is able to have an even shorter step size while also being able to maintain a constant torque. Micro-stepping mode allows for very precise movement with the tradeoff of low torque for a given step. As the steps are shortened, the resulting torque is lower. This could result in missed steps.

There are some advantages to consider in utilizing a stepper motor. For one, a stepper motor does not need a feedback loop system to know the motor's position. The motor's position is ascertained by counting the number of steps executed. Another advantage is the very precise movement that can be attained with micro stepping. Also, the motor is able to have adequate torque at a low speed. Conversely, there are some disadvantages in using a stepper motor. For one, stepper motors could experience missed steps. This would take away the ability to know the motor's position. Also, the max current is drained even when the motor is stationary which results in overheating and is also a detriment to efficiency. Stepper motors are noisy at high speeds. In addition, stepper motors have a low torque-to-inertia ratio and low power density.

3.1.8 Motor Drivers

Motor drivers are devices that work with a microcontroller to control the operation of motors. Motor drivers provide the necessary voltage, current, protection and direction. From the low voltage signal of a microcontroller, motor drivers are able to provide high power to the motor. This feature is possible due to the motor driver functioning as a current amplifier. Motor drivers can be structured differently, but the most common structure is the H-Bridge. An H-bridge is a circuit that makes it possible to manage the direction of a DC motor. The motor is spun forward or backwards by alternating the polarity of the DC motor. The polarity is dependent on which switches are opened or closed in the H-bridge circuit.

By being connected to a microcontroller, the acceleration and deceleration parameters could be easily modified by the pulse-width modulation (PWM) signal of the microcontroller. This is made possible by the microcontroller sending signals to the motor driver. The motor driver will then decipher those signals, and those signals will be stepped up with the reference voltage to drive the motor. The motor driver will then utilize the two voltage input pins of the motor to manipulate the motor output. One pin will turn ON the motor by providing the reference voltage, and the other pin will turn OFF the motor by providing zero volts at the output. When the microcontroller sends a single HIGH input signal to the motor driver, that is when one input is HIGH while the other input is LOW, the motor driver rotates the motor in one direction. When the input signals are reversed, that is the HIGH input is now a LOW input and vice versa, the motor will rotate in the other direction.

3.1.8.1 A4988 Stepper Motor Driver

When it comes to stepper motors, the A4988 is a commonly used and user-friendly motor driver integrated circuit (IC). It is compact with dimensions of 0.6 in. x 0.8 in. (or 15.24 mm x 20.32 mm) and a weight of 1.3 g. It has two board layers, and it is a low-cost stepper motor driver. The driver operates from a minimum operating voltage of 8 V to a maximum operating voltage of 35 V. It can provide a maximum continuous current per phase of 1 A, and it can provide a peak current per phase of 2 A. These ratings make it suitable for small to medium-sized stepper motors. The driver offers micro-stepping from a full step, 1/2 step, 1/4 of a step, 1/8 of a step, and 1/16 of a step. This means that a full step can be broken all the way down to 16 smaller, equivalent micro-steps.

The A4988 contains a built-in translator that makes it easier to control stepper motors. With the translator, only two pins need to be controlled. One pin commands the motor to move a step, and the other pin commands the motor to move in a particular direction. The driver offers many safety features which include short circuit protection, under-voltage protection, thermal shutdown, shoot-through protection, and overcurrent protection. The driver provides 16 total pins. The VDD and GND pins provide power to the internal logic circuitry, The VMOT pin and a different GND pin provide power to the actual stepper motor. The MS1, MS2 and MS3 pins can be set to several HIGH or LOW combinations to achieve one of the five micro-stepping modes. If all of the pins remain disconnected, then the motor will be in full step mode. The STEP and DIR pins are for control. STEP is for the motor to perform steps. DIR dictates the direction of the motor. The EN, RST and SLP pins are for power control. The EN pin enables or disables the driver. The SLP pin places the A4988 into a power-saving sleep mode. The RST pin resets the A4988 when pulled LOW. The 1A, 1B, 2A and 2B pins are for the motor's output. These pins connect the driver to the stepper motor.

Although the A4988 has a maximum current rating of 2 A, the typical current that can be delivered relies on maintaining the chip cool. Absent of any cooling, the driver can operate around 1 A before it overheats. To operate safely above 1 A, a heatsink or other cooling medium must be used. Stepper motor performance can be enhanced by providing the stepper motor a higher voltage than what it is rated for. Being able to safely operate the motor with a higher voltage than what it is rated for is made possible by limiting the current flowing through the coils of the motor. This can be done by manipulating the current limiting potentiometer on the A4988.

3.1.8.2 TMC2209 Stepper Motor Driver

The TMC2209 is a very silent stepper motor driver built for two phase stepper motors. The driver operates from a minimum operating voltage of 4.75 V to a maximum operating voltage of 29 V. It can provide a maximum continuous current of 2 A RMS, and it can provide a peak current of 2.8 A. The driver contains pins that offer micro-stepping from 1/8 of a step, 1/16 of a step, 1/32 of a step, and 1/64 of a step. Beyond the micro-stepping offered by the pins, micro-stepping from full step all the way down to 1/256 of a step is possible by implementing the MicroPlyer™ interpolation feature using the UART interface. The StealthChop2™ feature allows for complete silence of the motor when in operation and when it is idle. The StallGuard4™ feature can warn of motor overload. The CoolStep™ feature allows for current control to save energy up to 75%. The driver offers many safety features which include overcurrent protection, undervoltage detection, thermal shutdown, short circuit protection, and under-voltage detection.

3.1.8.3 TB67S581FNG Stepper Motor Driver

The TB67S581FNG is a two-phase bipolar stepper motor driver IC manufactured by Toshiba. The driver has dimensions of 0.6 in. x 0.8 in. (or 15.24 mm x 20.32 mm) and has a weight of 1.6 g. It comes with four board layers, and it is a low-cost stepper motor driver. The driver operates from a minimum operating voltage of 8.2 V to a maximum operating voltage of 44 V. It can provide a maximum continuous current per phase of 1.5 A, and it can provide a peak current per phase of 2.2 A. The ability to operate under the continuous current of 1.5 A is when a heatsink or some other cooling medium is not used. However, if the necessary cooling medium is implemented then the TB67S581FNG can operate up to the peak current of 2.2 A. The driver offers micro-stepping from a full step, 1/2 step, 1/4 of a step, 1/8 of a step, 1/16 of a step, and 1/32 of a step.

The driver offers many safety features which include under voltage lockout detection, thermal shutdown detection, short-to-ground and shorted-load protection, and overcurrent detection. Several decay modes are provided such as mixed decay, slow decay and fast decay. It also includes a sleep mode which serves to save power. Higher step rates can be achieved by providing the stepper motor with a higher voltage than what it is rated for. This is made possible by limiting the current flowing through the coils of the motor. This can be done by manipulating the current limiting potentiometer on the TB67S581FNG.

3.1.8.4 DRV8825 Stepper Motor Driver

The DRV8825 is a commonly used and user-friendly motor driver integrated circuit (IC) manufactured by Texas Instruments. It has four board layers, and a compact size of 0.6 in. x 0.8 in. (or 15.24 mm x 20.32 mm) and a weight of 1.6 g. The DRV8825 is the most expensive when compared to all of the aforementioned stepper motor drivers but it is still affordable. The driver operates from a minimum operating voltage of 8.2 V to a maximum operating voltage of 45 V. It can provide a maximum continuous current per phase of 1.5 A, and it can provide a peak current per phase of 2.2 A. Being able to operate under the continuous current of 1.5 A is when a heatsink or some other cooling medium is not used. However, if the necessary cooling medium is implemented then the DRV8825 can operate up to the peak current of 2.2 A. The driver offers micro-stepping from a full step, 1/2 step, 1/4 of a step, 1/8 of a step, 1/16 of a step, and 1/32 of a step. This means that a full step can be broken all the way down to 32 smaller, equivalent micro-steps.

The DRV8825 utilizes a simple step and direction interface which works by the motor executing a step and moving the motor in a particular direction, respectfully. The driver offers many safety features which include short-to-ground and shorted-load protection, under-voltage lockout, over-temperature thermal shutdown, and overcurrent shutdown. Higher step rates can be reached by providing the stepper motor with a higher voltage than what it is rated for. This is made possible by limiting the current flowing through the coils of the motor. This can be done by manipulating the current limiting trimmer potentiometer on the DRV8825.

The driver contains 16 total pins. The VMOT and GND pins provide power to the driver itself and the actual stepper motor. The M0, M1 and M2 pins can be set to several HIGH or LOW combinations to achieve one of the six micro-stepping modes. If all of the pins remain disconnected, then the motor will be in full step mode. The STEP and DIR pins are for control. STEP is for the motor to perform steps while DIR dictates the direction of the motor. The EN, RST and SLP pins are for power control. The EN pin enables or disables the driver. The SLP pin places the DRV8825 into a power-saving sleep mode. The RST pin resets the DRV8825 when pulled LOW. The FAULT output pin goes LOW after the DRV8825 is triggered by one of the many safety features. When this pin is activated, the driver is disabled for protection. The driver is able to return to normal upon activating the RST pin or by disconnecting and reconnecting the VMOT pin. The A1, A2, B1 and B2 pins are for the motor’s output. These pins connect the driver to the stepper motor. The A1 and A2 pins connect to one coil while the B1 and B2 pins connect to another coil.

3.1.9 Laser Diode Drivers

The laser diode driver works with the microcontroller to control the operation of the laser diode. The main emphasis of the laser diode driver is to provide the appropriate constant current that the laser diode typically operates in. The current that the driver provides directly impacts the laser diode's wavelength and output power. Any discrepancy in the current flow like noise or induced transients will render undesirable laser diode results. It is important to note that if the laser diode receives a forward or reverse voltage outside of its ratings, then the laser diode can be damaged. It is important to think about the protection offered by a laser diode driver so that nothing gets damaged by a sudden discrepancy. Such protections could include slow-start circuits, over-voltage protection, over-current protection, and plug power and AC transient surge protection.

When selecting a laser diode driver, there is a distinction between low power laser diode drivers and high-power laser diode drivers. Low power laser diode drivers output current between 1 mA to 5 A. High power laser diode drivers output current between 5 A and 100 A. When it comes to laser diode drivers in an integrated circuit (IC) form, they typically only provide up to 500 mA of current. Laser diode driver offered as a board module will be able to provide current from 50 mA to 100 A. Of course, laser diode driver board modules will come out much more expensive compared to in an IC form. The laser diode that will be used for this project is the GH04C03A9G which needs an operating current between 2 A and 2.4 A. This current rating clearly rules out the possibility of utilizing a laser diode driver IC.

3.1.9.1 WLD33ND Laser Diode Driver

The absolute maximum rating for the operating current of the laser diode, GH04C03A9G, is 3 A. A simple internet search for laser diode drivers that provide 3 A of constant current yielded this diode driver from Wavelength Electronics as a top result. It has quite a compact size with dimensions of 1.3 in. x 1.26 in. x 0.3 in. (or 33.02 mm x 32.004 mm x 7.62 mm) and a weight of 17 grams. It provides a constant current up to 3 A from a 5 V to 12 V power supply. It has a power dissipation of 10 W with an operating temperature range between -40 ºC to 45 ºC. The laser diode driver offers safety features such as slow-start diode protection and over-temperature shutdown. It also has a bandwidth of 2 MHz and an adjustable laser diode current limit. What is neat is the fact that it is supposedly compatible with any type of laser diode. Overall, this laser diode driver will suit the project’s needs very well, but the high price of 137 USD must be kept in mind.

3.1.9.2 LMH13000 Laser Diode Driver

The LMH13000 is an integrated circuit (IC) from Texas Instruments that can provide up to 1 A of continuous current or a maximum Iout of 5 A. It needs a power supply voltage between 3 V to 5.5 V. Based on these ratings it would appear that this laser diode driver IC would meet the needs of the GH04C03A9G laser diode. A question was posed to a Texas Instruments engineer via the Texas Instruments “Design support” whether this laser diode driver will meet the needs of the GH04C03A9G laser diode. Someone from Texas Instruments Customer Support replied via email that “I believe it can be able to handle GH04C03A9G.” Before making the move on purchasing that driver, the data sheet was at least briefly read to make sure that everything will check out. Upon reading, it was noted that the driver provides a maximum continuous current of 1 A and a maximum pulsed current of 5 A. This nuance between continuous current and pulsed current was further examined. It was ultimately realized that the GH04C03A9G laser diode operates off of continuous current, and its data sheet mentions nothing about pulsed current.

3.2 Software Research

3.2.1 Operating System and Language (Nick)

Table 9: Operating System and Language Table

Layer	Option	Pros	Cons	Fit for Project
OS	Raspberry Pi OS	First-party support for Touch Display 2 Easy Kiosk setup	Not hard real time Potential jitter under load when it comes to timing	Chosen, best balance for UI support and stability
	Ubuntu	Long term stability and security support Support snap containers	More resource intensive Slower boot Requires manual configuration for the touch display	Not needed for what its offering compared to the Raspberry Pi OS that offers better integration
Language	Python	Faster Iteration and good critical timing Simple/Large Library Support	Slower as python is interpreted and not compiled	Chosen, ideal for UI logic and serial communication to MCU
	C/C++	Compiled language with timing that is	More complex syntax and manual	May be used on microcontroller side for real time

		more predictable Minimal memory use; efficient for embedded environments	memory management Prone to low level bugs	PWM, interlocks, and safety control

Our project uses a Raspberry Pi 4B running Raspberry Pi OS (a Linux-based system) as the primary operating system, chosen for its strong community support, open-source libraries, and great compatibility with embedded peripherals; especially with our chosen touchscreen. The Pi will operate in kiosk mode, ensuring that the only visible and running application is our system's graphical interface. This approach simplifies operation and reduces the chance of user error, and implementation is straightforward thanks to official Raspberry documentation serving as a guide.

However, the project also demands precise timing and deterministic control, which are difficult to guarantee when the HMI runs on a general-purpose multitasking OS like Linux. Since Linux schedules tasks dynamically (meaning the operating system continuously decides which process gets CPU time based on priority, load, and background activity), timing can vary slightly from one event to another. These small variations, or Jitters, are negligible for normal operations like updating the screen or reading user input, but they might become a problem when trying to use precise control signals when it comes to laser control and safety concerns. Even with PREEMPT_RT real-time patch, which improves kernel preemption and significantly lowers average scheduling latency, the system remains "soft real-time" rather than "hard real-time." Researchers at the Max Planck institute for Software Systems measured latencies under load reaching several hundred microseconds to a few milliseconds in PREEMPT-RT Linux[20]. Such jitter is unacceptable for microsecond-sensitive operations like laser PWM gating or safety interlocks, which require strict and repeatable response times.

To resolve this, real-time control will be delegated to a dedicated microcontroller running compiled C/C++ firmware. This division allows the Raspberry Pi to handle high-level tasks such as the user interface, job management, and file transfers, while the microcontroller executes timing-critical operations with deterministic precision. This hybrid structure combines the Pi's flexibility with the microcontroller's reliability, ensuring both a robust HMI with a safe and accurate laser control.

3.3 Optical Design

3.3.0 Laser Source Considerations (Jacqui)

When comparing laser sources, we considered fiber, CO2, solid-state, and semiconductor lasers. These were the main types used in different types of laser cutting, including cutting metal and non-metal objects. These of course are within the visible wavelength spectrum since an infrared wavelength would be hard to align without an infrared viewing card. The most common type of laser used for non-metallic objects are CO2 lasers, while fiber lasers will work with most materials although they are limited in the material thickness they can cut.

The basics components of a laser are the gain medium, pump mechanism, optical resonator or cavity, and the output coupler. The pump mechanism supplies energy to the gain medium, inciting a population inversion and causing stimulated emission of photons. This emission of photons is reflected by the optical cavity mirrors and passes through the gain medium inside, causing amplification before exiting through the output coupler shown as R2. This output coupler can be a partially transparent mirror or a pulsed shutter that allows for a fraction of the beam to exit the cavity [13].

CO2 lasers are gas-discharge lasers that use electricity to vibrate CO2, or carbon dioxide, molecules. This involves inducing an electric field over a gas tube full of a specific ratio of N2 to CO2 gas with hydrogen, xenon, and helium. The ends of the laser tube have Brewster mirrors, one half silver and the other fully silver. With powers ranging from watts to kilowatts and a wavelength of either 10.6 or 9.6 micrometers, this laser type can be very useful for industry applications when cutting materials more than 20 millimeters thick [12]. We chose to forgo pursuing this option because it would be difficult for us to ensure the correct gas ratios in the gas chamber/tube when building this laser.

Fiber lasers use a doped fiber optic strand as the gain medium, coupled between the laser cavity mirrors to create stimulated emission of photons. The wavelength emitting from these lasers is dependent on the doping of the fiber. For example, ytterbium doped fibers emit a wavelength of around 1060 nanometers, and these are a typical doping choice for the fiber. These are compact and low maintenance and are commonly used for laser cutting metals because their wavelength is more effective than other types of lasers. The main reason for not pursuing this type of laser was inexperience with fiber lasers and the possibility of too much power incident on the fabric while cutting.

The laser that most people imagine are typically the Nd:YaG lasers that use an Nd:YaG crystal as the gain medium. This is a solid-state laser due to its use of a crystal as the gain medium. The wavelength of a solid-state laser is dependent on the crystal used, and the wavelength from Nd:YaG is 1064 nanometers. An Nd:YaG laser is suitable for laser cutting of both metals and non-metals but requires active cooling and potential maintenance of the crystal.

Laser diodes are semiconductor lasers due to the use of a semiconductor PN junction as the gain medium. Our specific laser diode uses InAlGaN as the chip, giving us the low wavelength of 445-465 nanometers and laser diodes can produce wavelengths from 375 to 2000 nanometers depending on the chosen semiconductor. The resonator cavity needed to pump the laser is already built into our diode, negating the need for a pair of mirrors to form the optical cavity around the laser like those needed in CO2 lasers.

Considerations were given into the power needed to cut through different types of fabrics. However studies revolving these topics focus on the power of the laser, not the actual incident power from the beam. Because of this it is not valid to correlate wattage of lasers to actual power going into the material, in our case fabric. This is why the previous senior design group was able to use a 3-5 watt laser to safely engrave paper without cutting completely through it. With any laser cutting project, there must be significant consideration into the cutting speed to ensure there is not a high-powered laser resting on the cutting material for too long, potentially igniting the material. Because of this concern, we knew a laser diode would be our best option as it has the lowest power when compared to the other types of lasers.

3.3.0.1 Fabric/Textile Considerations (Jacqui)

Laser–textile interaction is governed primarily by how different fibers absorb energy, the thermal mechanisms through which they degrade or melt, and the rate at which the laser delivers energy to the material. We were able to find multiple articles where these rates were investigated for differing fabrics such as non-woven polyester, wool, and even buffalo leather. These articles collectively illustrate how fiber type, laser power, and scanning speed dictate whether a fabric is cleanly cut, partially melted, or thermally damaged.

Natural fibers such as cotton undergo thermal decomposition rather than melting. As laser intensity increases, cotton shows grooves, cracks, mass loss, and progressive surface damage. Hung et al. report that cotton experiences structural deterioration as energy density rises, confirming that cellulose-based fibers burn, char, or carbonize rather than forming a melt layer [33]. Similarly, studies on cotton/polyester blends show that the cotton fraction chars while the polyester fraction melts, producing hybrid thermal behavior. This mixture makes cut quality highly sensitive to power levels: excess power leads to carbonization and edge darkening, while insufficient power results in incomplete separation.

In contrast, synthetic thermoplastics such as polyester (PET) primarily melt and resolidify during laser cutting. The UV nanosecond laser study shows that increasing laser fluence widens the kerf and produces characteristic spherical melt droplets along the edge, confirming that the dominant mechanism is localized melting followed by ablation. Chemical analysis (EDS and XPS) reveals increased oxidation at moderate speeds but heavy carbonization when scanning speeds are too low, indicating excessive heat accumulation. At very high speeds (>600 mm/s), the laser does not deliver enough energy per unit length, and the fabric fails to cut through, demonstrating that both under- and over-exposure degrade cutting quality [33].

The relationship between laser power, cutting speed, and cutting time is illustrated clearly in the non-woven PET results. Clean cutting is achieved with a pulsed laser at 30 kHz with a scanning speed of 500 mm/s, producing a narrow kerf (~0.214 mm) with minimal thermal damage. At this speed, the effective time required to cut along a line can be directly derived: the laser advances 500 mm each second, meaning it cuts 1 cm in 0.02 seconds. Lower scanning speeds (300–400 mm/s) increase thermal exposure, producing wider kerfs and more discoloration, while higher speeds (>600 mm/s) reduce the delivered energy density below the threshold required for through-cutting [33]. Thus, cutting time is not simply a function of how fast the gantry moves—it is constrained by the minimum laser energy needed per unit area to remove material.

Zoghi's article investigated these trends, primarily focusing on continuous wave and pulsed 1064 nanometer CO2 laser cutting and regarding wool and polyester. This data shows that cut depth is power-dependent, with higher laser power producing deeper penetration but also greater risk of discoloration, melting, or burning. Higher powers can shorten cutting time by enabling higher scanning speeds, but only within the window in which heat-affected zones remain acceptable. Excessive power or too slow a speed results in charring (cotton), heavy melting (polyester), and degraded edge quality across fiber types. They also found that the addition of synthetic materials makes a fabric easier to cut. However in their investigation they found that materials of 45% wool and 55% polyester with a thickness of .5 millimeters were not cut until 8 watts of power was used and did not start to catch fire until about 48 watts of laser power was used [34].

Overall, these two articles show that the optimal cutting condition for any textile lies in a balance: enough power to achieve complete through-cutting at practical speeds, but not so much that thermal damage widens the kerf or degrades the fiber structure. Cotton and natural fibers tend to burn and crack under high power, while polyester melts and forms beads. Non-wovens require sufficient pulse energy to overcome low density and porosity. Cutting time, determined by scanning speed, is ultimately limited by the minimum energy per unit length required for the beam to vaporize or melt through the fabric. The combined results from both papers therefore demonstrate how laser power and interaction time jointly control both the quality of the cut and the practical throughput of laser-based textile processing.

In Khalaf's article, he and several other writers investigate how different diode laser powers affect the quality of laser cutting on buffalo leather. This source was the only source we could find that uses a differing laser diode power to cut textiles, which in this case was leather. Using three power levels- 2.5,5.5, and 20 watts- to assess which is more likely to carbonize the material, meaning to form burnt or blackened edges, as well as assess the kerf width corresponding to the material. They investigate these, as well as material removal rate, as a function of the laser diode power. The 20 watt laser diode was found to be optimal, not just for its higher power but also for their ability to correct the beam shape using this diode in comparison to the other two diodes. They determined minimizing the beam size by focusing the beam tightly enables higher power density. This contributes to less carbonization due to reducing the required interaction time between the material and the laser beam. They note an optimal distance from the laser to the leather being 18mm but note that this can be adjusted to compensate for differing cutting speeds [35]. This paper's information was helpful, despite using thicker material, because it confirms that we will be able to cut fabric using our 3.5-watt diode without reaching the maximum power.

3.3.0.2 Heat Sink Considerations (Jacqui)

Table 9: Heat Sink Comparison Table

Material	Stainless Steel	Aluminum	Copper
Thermal Conductivity (W/m*K)	14-20	150-205	385-400
Comparative Weight	Heavy	Light	Heavy
Machinability	Difficult	Easy	Medium
Cost	Medium	Cheapest	Most Expensive
Electrical Conductivity	Poor	Good	Excellent (May need isolation)

The machinability comparisons are based on the capabilities of the UCF machining lab or the students themselves. After reviewing these materials, we prioritized creating an aluminum heatsink, however we were given a copper heatsink that we can cut into to fit our diode. In addition to the heatsink, we will use a TO-220 Mica insulating sheet with thermal paste to ensure the copper heatsink does not conduct unwanted electricity.

3.3.1 Laser Diode Comparison Table & Description (Jacqui)

Table 100: Laser Diode Comparison Table

Laser Diode			
Name/Product (Brand)	455nm 5500mW Laser Diode (LaserTree)	455nm 3500mW Laser Diode (LaserTree)	405nm 3.3W Laser Diode (LaserTree)
Threshold Current (Amps)	.24-.44	.25-.33	.43-.53
Operating Current (Amps)	3.5	2.1-2.4	1.6-2.2
Operating Voltage (Volts)	3.5-4.7	4.4-5.2	4.7-5.5
Typical Wavelength and Range (Nanometers)	455 445-465	455 445-465	405 400-415
Output Power (Watts)	5.5	3.5	3.3
Cost (USD)	55	25	285

For F.L.C.S we decided to go with a laser diode system because of its compact size and due to our inexperience with CO2 lasers, a common method for cutting textiles. Using laser diode for our beam source allows us to adjust the power of the laser for varying fabric thicknesses, due to the linear relationship between threshold current and output power or light [13]. Prior to hitting the threshold current, the laser diode operates like an LED, yet afterwards it operates as a laser with increasing output light as current increases. A previous senior design project at our university successfully designed an engraving system using a 405 nm, 500-milliwatt laser diode [5].

When choosing the specific laser diode for our system the first concern was the amount of power and absorbance of wavelengths that allow for burning through fabric. El Sherif provides information regarding the typical absorption found in polyester between wavelengths 400 and 460 nm, we know that the absorption will be higher around 400 nm than 450 nm. However when accounting for varying red, yellow, and blue dye concentrations, 450 nm is a wavelength that will have more uniform absorption across different colors [14]. Because of this in tandem with the previous senior design groups' performance, I believe we should be able to cut through fabrics with our 455 nm 3W laser diode. The graph to the right represents a pseudo-absorption diagram for yellow fabric dyes using measured reflectance, R [15]. As you can see on the right, throughout the visible spectrum, 380-750 nm, wavelengths less than 500nm are absorbed better into textiles or fabric, allowing the fabric to burn easier and with less power or passes needed by the laser. Gathering this data regarding yellow fabric dyes was essential since would be the lightest dye used in fabric, corresponding with the most reflectance in the lower wavelengths. With our financial constraints, we were unable to find 400 nm laser diodes with the minimum of 3 watts needed to burn through the fabric.

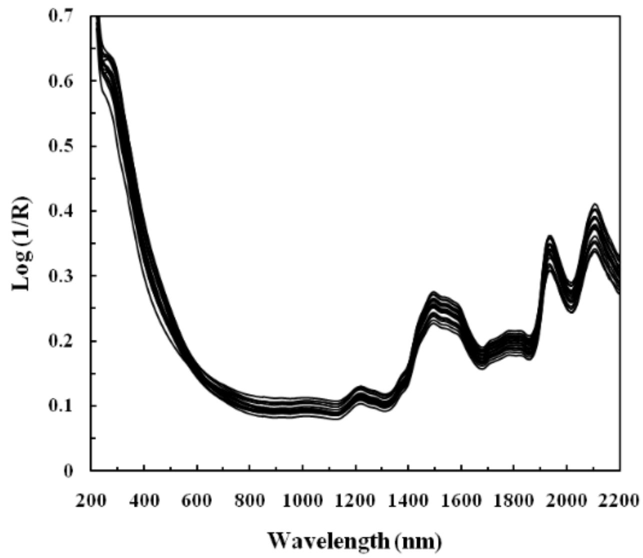

Figure 10: Absorption v. Wavelength Graph for Cotton Fabrics with Heavy Concentrations of Yellow Dye [15]

3.3.2 Lens Comparison Tables & Descriptions (Jacqui)

Table 111: Aspheric Lens Comparison Table

Beam Shaping Optics			
Name/Product (Brand)	**C710TMD-A Aspheric Lens (Thorlabs)**	**C140TMD-A Aspheric Lens (Thorlabs)**	**PS873-A Anamorphic Prism Pair (Thorlabs)**

Focal Length (mm)	1.5	1.5	N/A
Design Wavelength (nm)	1550	780	405
Cost (USD)	111.17	104.03	203

To start our lens system, we will first correct our elliptical beam shape from our laser diode into a circular beam. This can be done in a few different ways. A baseline to help shape the beam is by using circular cylinder lenses throughout our system, but we must first collect the beam from the laser diode and use either an aspheric lens or anamorphic prism pair to force the beam shape. If a circular cylinder lens was used directly after the laser diode, the excess light in the vertical direction could pass over the edge of the lens, introducing stray beams into our enclosure. We focus on expanding the beam because expanding the beam prior to focusing ensures we will have a small spot size incident on the fabric [16].

Using an anamorphic prism pair as our main beam shaping optic allows us to correct the aspect ratio of the beam, as opposed to using multiple spherical lenses that would shape the beam but would change the polarization. Because the anamorphic prism pair is unmounted due to financial constraints, we will be utilizing 3D printing to mount the lens in the required position to effectively reshape the beam. Since light diverges as it travels, we prioritized having a shorter lens system to minimize divergence and to best suit the size of our enclosure. Although our chosen aspheric lens has a design wavelength of 780 nm, this will not have an impact on the lens system due the focal length varying slightly for different wavelengths. Because of this we will be adjusting the distance between this lens and other optical components prior to our demo to ensure the distance is correct even if the focal length is slightly different.

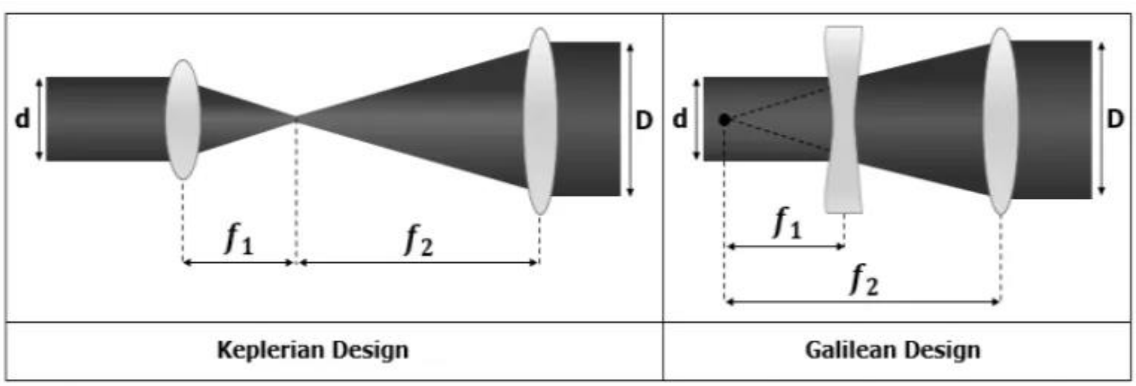

Figure 11: Keplerian and Galilean Lens Systems [17]

For beam expansion there are a couple of systems we can utilize to best expand the beam before it reaches the focusing lens. These systems are called Keplerian and Galilean. For our system we choose to utilize a Galilean beam expander because it does not focus the light into a singular spot, like the Keplerian system shown in Figure 11 above. Using a Keplerian system would create a hot spot in our system prior to contact with the fabric. Additionally, using a Galilean system enables us to have a smaller length lens system than the Keplerian counterpart. Expanding our beam prior to contact with the focusing lens decreases divergence and ensures a smaller spot size incident on the fabric [12].

Table 12: Beam Expander Lenses Comparison Table

Lenses for Beam Expander			
Plano-Concave Lenses			
Name/Product (Brand)	**LA6002 (Thorlabs)**	**LA8126-E (Thorlabs)**	**LC1975 (Thorlabs)**
Back Focal Length (mm)	45	19.3	-25.4
Reflective Coating Range (nm)	N/A	1000-6000	N/A
Design Wavelength (nm)	465	4000	587.6
Material	Magnesium Fluoride	Silicon	NBK-7
Diameter (mm)	25.4	12.7	6
Cost (USD)	387.66	286	28.72
Convex Lenses			
Name/Product (Brand)	**Bi-Convex Lens LB1945-AB (Thorlabs)**	**Plano-Convex LA1613 (Thorlabs)**	**Bi-Convex Lens LB4265-A (Thorlabs)**
Back Focal Length (mm)	198.4	125	149.4
Diameter (mm)	25.4	12.7	25.4
Cost (USD)	45	28.7	132.68

When designing the beam expander expansion system we focus on plano-concave and plano-convex lenses because combining these will help us expand our beam. The laser diode beam will diverge, or spread, after the plano-concave lens and converge after the convex lens. Utilizing a biconvex at the end of this lens system enables the beam's size to be almost constant as the distance from the lens increases, making it a nearly collimated beam when placed at the correct distance from the plano-concave lens. Whereas when using a plano-convex lens, like we originally accounted for, the beam can expand until it reaches the maximum allowed by the size of the previous lens.

We focused our attention on the back focal length of these lenses due to its involvement in the magnification formula of a Galilean beam expander. Having a large back focal length would result in less beam expansion, and using a pair of lenses with positive back focal lengths would ensure our system magnifies the beam instead of expanding it.

Most of our lenses have an anti-reflectance (AR) coating that minimizes loss. An increase in loss corresponds to lower power incident on the fabric. We avoided lenses such as the LA3803-E due to their reflectance coating being in the range of 2-6 micrometers, which would not minimize loss for our diode's typical wavelength of 455 nanometers. The AR coating covering the aspheric lens and anamorphic prism pair works for wavelengths 350-700 nm, whereas the bi-convex has a range of 400-1100 nm. Additionally, we prioritized looking at cheaper lenses, mainly those made of NBK-7, a common glass type that doesn't fracture easily and is relatively easy to manufacture. The only concern with NBK-7 is the heat tolerance but with our low laser power and short run times we do not need to be concerned.

3.3.3 Optical Design Calculations (Jacqui)

When combining our lens into a system we can utilize Zemax OpticStudio to get an idea of our beam behavior due to our lenses and subsequent coatings. This software does not allow us to account for the initial beam shape due to the use of a laser diode or account for the addition of the anamorphic prism pair. Our beam expansion system gives us a magnification of -7.8 shown below, resulting in a diverging beam 7.8 times its initial size. High magnification was desired due to the assumption that the initial beam size will be in micrometers.

$$Magnification = M = \frac{Back\ Focal\ Length\ (Bi - Convex)}{Back\ Focal\ Length\ (Plano - Concave)} = \frac{198.4}{-25.4} = -7.8$$

With Zemax software we can find the amount of power incident on the mirrors using the physical optics propagation function. The following calculations account for the loss of our singular lens that is not coated. Using the irradiance formula below and the information provided by our Zemax shown in Figure 24, we can find a max power of 5.45 milliwatts per pixel, with each pixel corresponding to 0.76 millimeters due to the graph having 5 pixels per 3.8 millimeters. Using this ratio, we get 9.43 milliwatts per mm^2. It is very likely our maximum power in watts will increase compared to our calculated numbers due to the inclusion of our laser diode in testing.

$$I_0 = Peak\ Irradiance, w = Beam\ radius, P = Power$$

$$I_0 = \frac{2P}{\pi w^2} => 7.96 * 10^{-3} = \frac{2P}{\pi\left(\frac{1.32}{2}\right)^2} => P = .00545\ Watts$$

$$\frac{5.45}{(.76mm)^2} => 9.43\frac{mW}{mm^2}$$

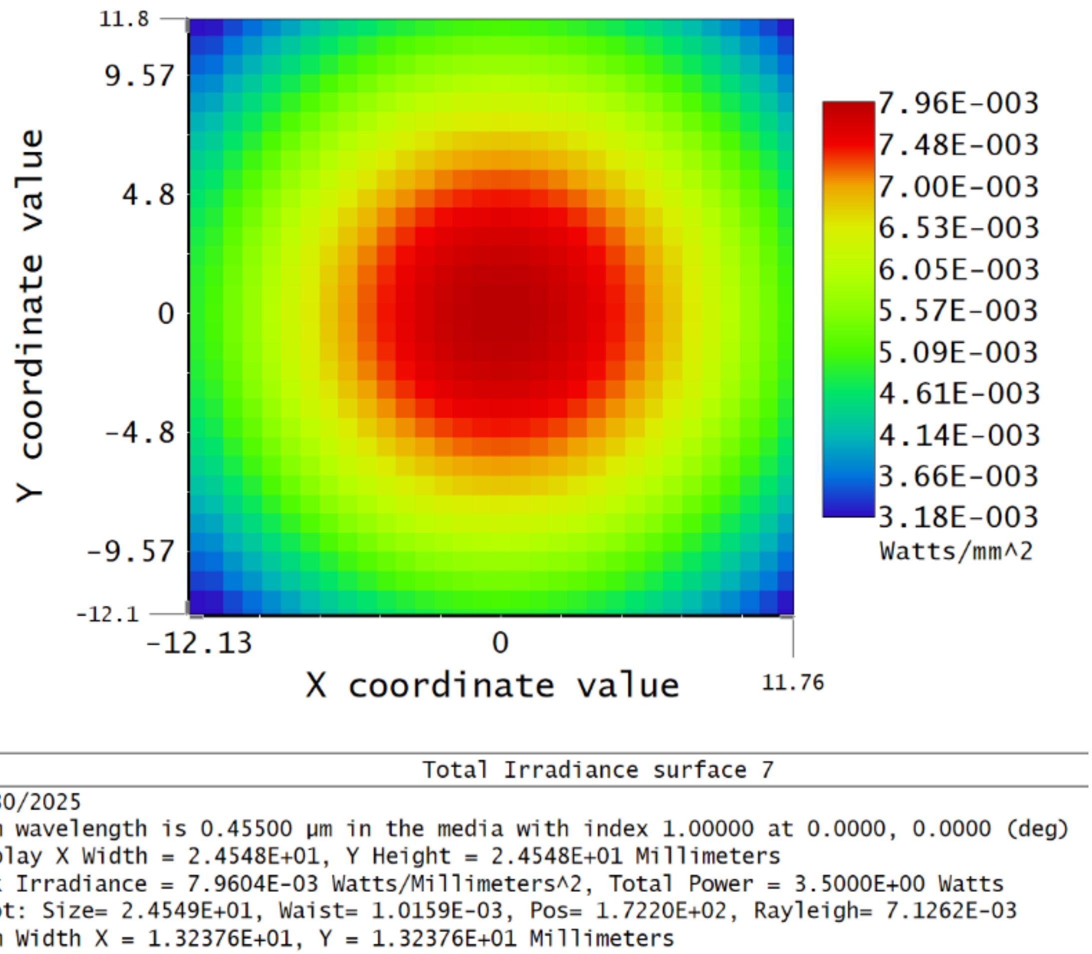

Figure 12: Beam Profile via Zemax

3.3.4 Mirrors Comparison Tables & Descriptions (Mike)

Table 13: Mirrors Comparison Table

Mirrors			
Specifications	**Fused Silica Broadband Dielectric (E02)**	**Protected Silver**	**Protected Aluminum**
Reflectivity (455 nm)	>99%	>97%	>90%
Bandwidth	Moderately broad 400nm - 750nm	Very broad 450 nm - 2 µm	Very broad 450 nm - 2 µm
Absorption	<1%	<3%	<10%
Laser Damage Threshold	High threshold (470 W/cm)	Moderate threshold (213 W/cm)	Low threshold, lot of power absorbed (43 W/cm)

Surface Quality	High quality, laser-grade, low scatter (10-5 Scratch-Dig)	Good quality, good for optics (40-20 Scratch-Dig)	Good quality, good for optics (40-20 Scratch-Dig)
Cost	Most expensive $50-$60	Least expensive ~$30	Moderately expensive ~$40

When considering how to best direct the laser beam onto the fabric, some different properties of the mirrors were taken into account such as reflectivity and overall quality. Based on the different options from the table, it seems like using dielectric mirrors would work the best for this system. Compared to the other materials, it is the highest quality and absorbs the least amount of light from the beam. The only downside to having dielectric mirrors over a moderately good mirror like protected silver is that it is a more expensive option.

For dielectric mirrors, they are available with different coatings which reflect best at different ranges of wavelengths, shown on the graph below (Thorlabs). Using the information displayed, it can be determined that both E01 and E02 coatings could work sufficiently for the beam wavelength being used, but E02 has slightly more reflectance over E01.

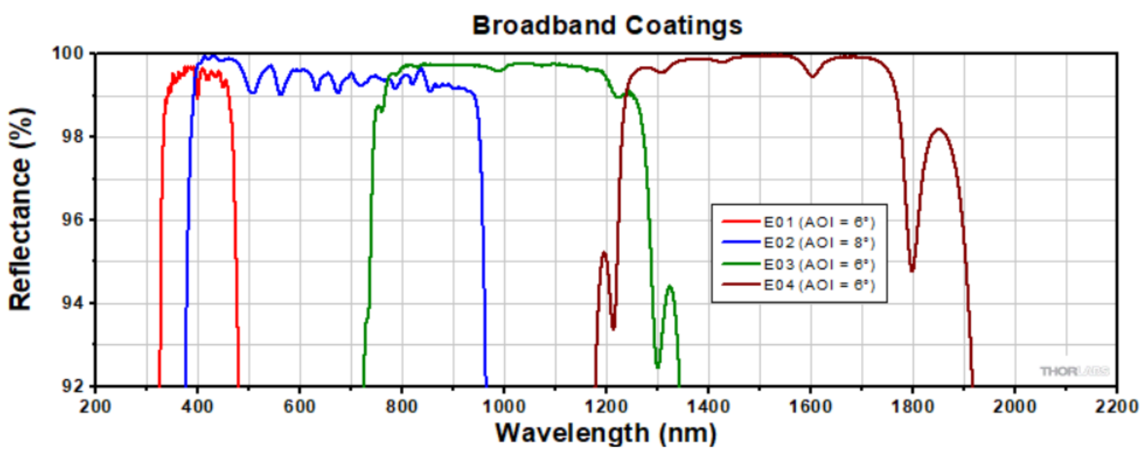

Figure 13: Reflectance of dielectric mirrors with each of the different coatings available from E01 to E04 on Thorlabs. [21]

3.3.5 Focusing Lens Comparison Tables & Descriptions

After the mirrors, a focusing lens is used to increase the on-sample peak irradiance. Because some fabrics are thick or may require multiple passes, a longer focal length is often preferred to provide sufficient working distance between the lens and the fabric.

3.3.5.1 Spheric and Aspheric Lens Comparison

Common economical lens types are plano-convex, bi-convex and aspheric lenses. Plano-convex and bi-convex lenses are widely available in many sizes and focal lengths, but spherical lenses introduce spherical aberration that enlarges the focused spot and reduces the achievable peak intensity. Aspheric lenses correct much of the spherical aberration and can produce a smaller, closer-to-diffraction-limited spot, but they are typically more expensive.

To simulate the magnitude of the spherical aberration produced by spherical lenses compared to aspheric lenses, Zemax can be used to show the final spot size aberrations at the focal point of each type of lens at 455nm wavelength. They all also show the airy disk, the smallest spot size attainable due to diffraction. Ideally, the aberrated spot size should be close to or smaller than the airy disk.

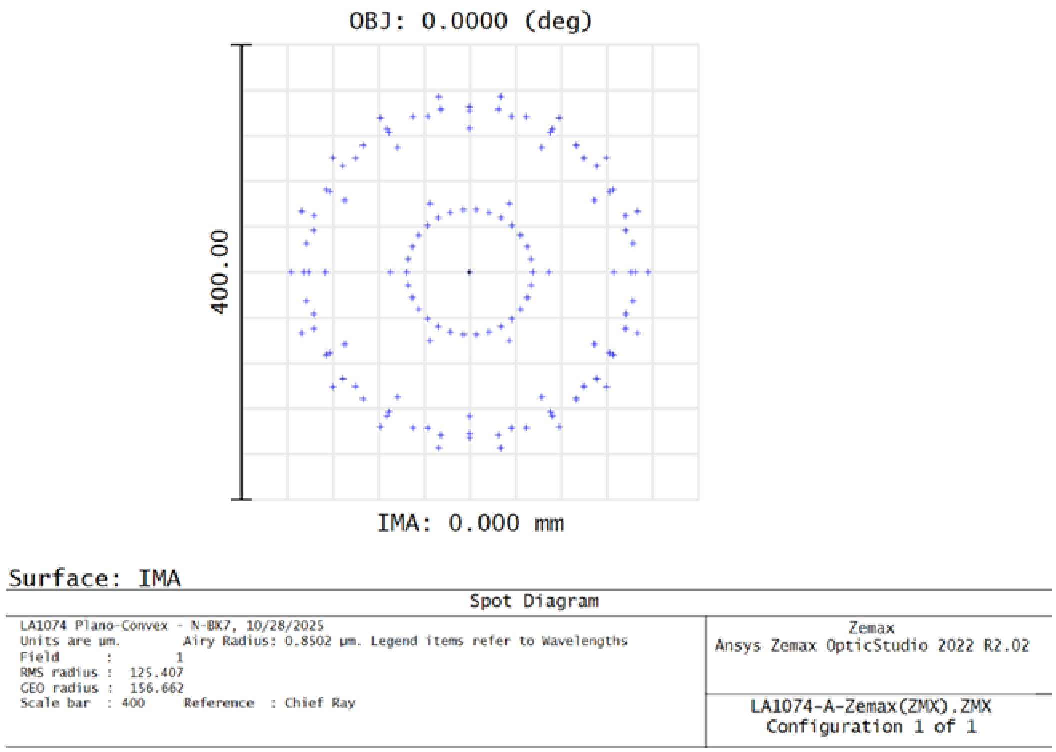

Figure 14: (LA1074-A) Plano-convex 19.6 mm focal length lens, minimum spot size 313.324 µm (Zemax)

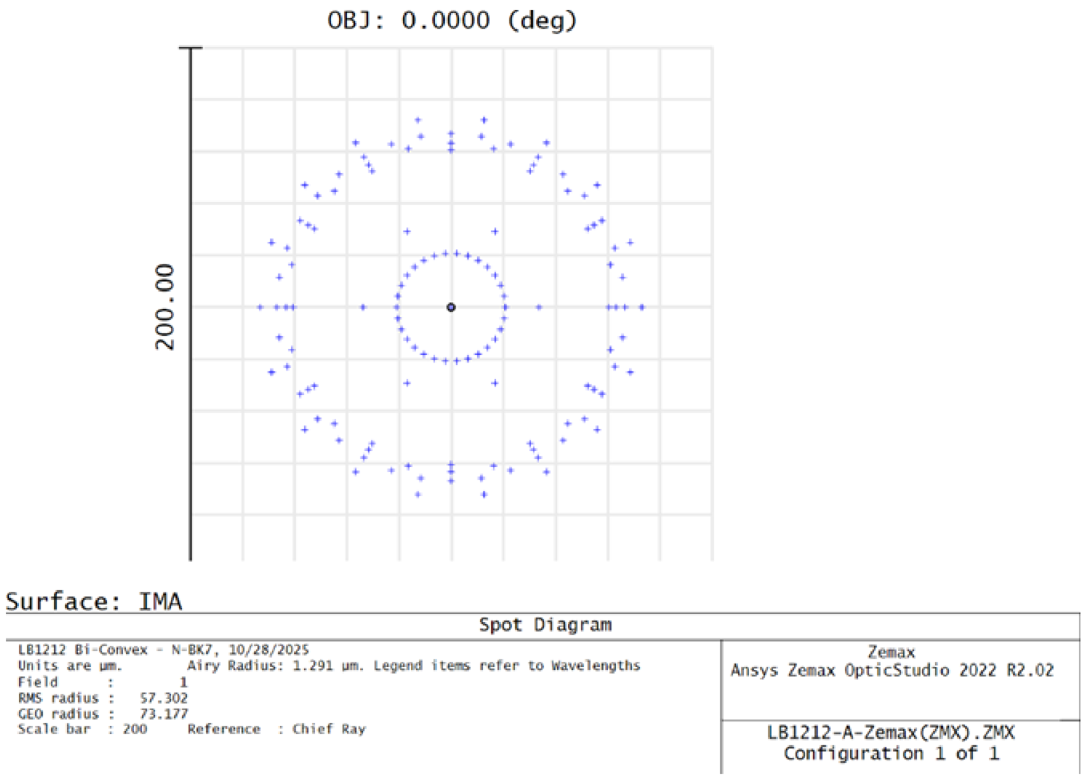

Figure 15: (LB1212-A) Bi-convex 19.6 mm focal length lens, minimum spot size 146.354 µm (Zemax)

In both figures, the airy disk is so small that it is barely visible or not visible at all. Compare the size of the airy disk and the overall aberrated size of the spot produced by the aspheric lens to the above spheric lenses.

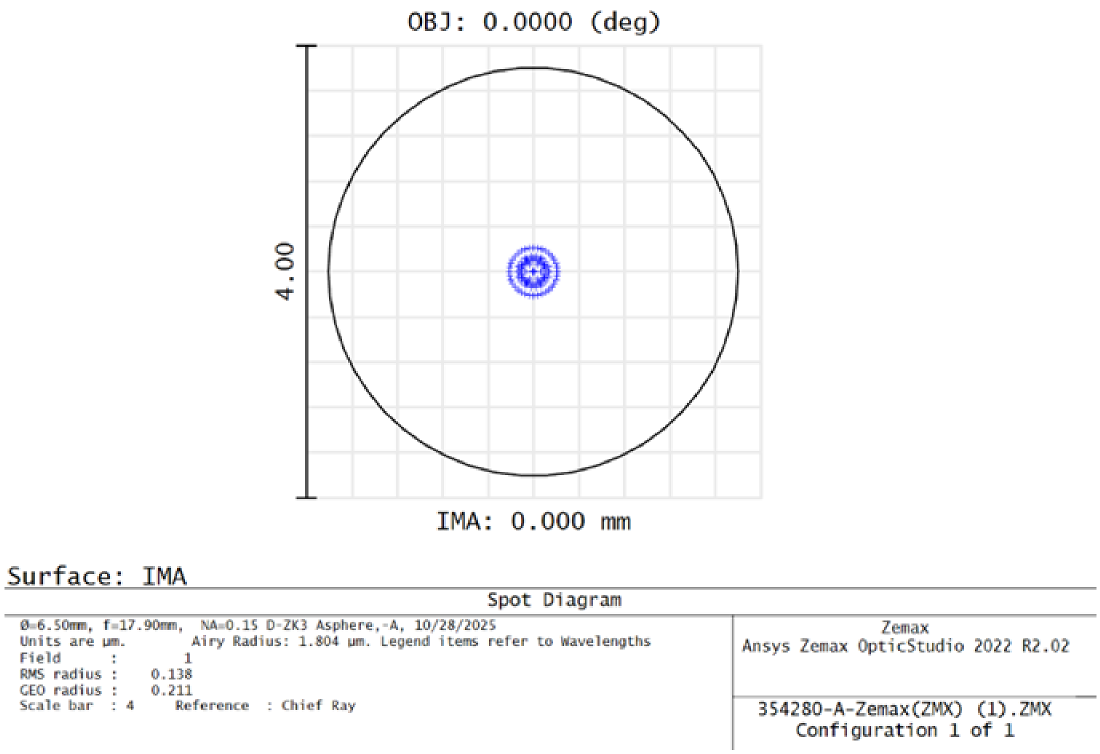

Figure 16: 354280-A: Aspherical 17.9 mm focal length lens, minimum spot diameter of 0.422 µm. Due to diffraction, the actual spot diameter is 3.608 µm. (Zemax)

As can be seen in the figures above, the aspherical lens is far superior to the plano and bi convex lenses when it comes to focusing the laser to a small spot, with the smallest spot size achieved by the aspherical lens being three magnitudes smaller than the other lenses.

3.3.5.2 Deciding an Aspheric Lens

When searching for aspheric lenses, as much optical power should traverse through the lens as possible, so an aspheric lens with an AR coating would be desirable.

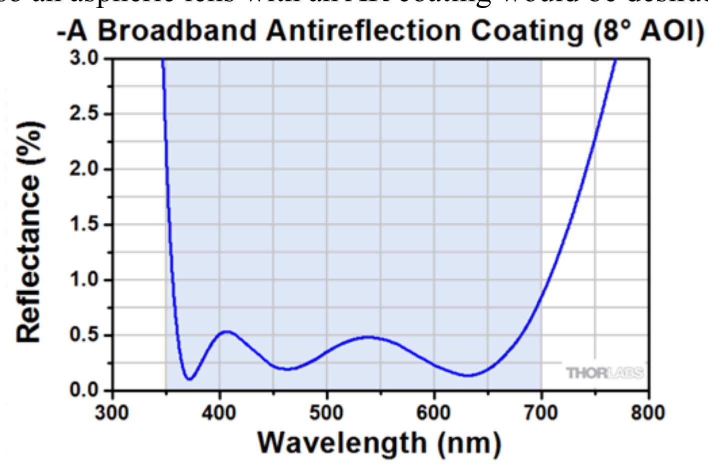

Figure 17: Graph of the AR coating's reflectivity against the incident wavelength. The coating appears to have a reflectance of about 0.25% at 455 nm. [22]

The effective focal length is only accurate for a specific wavelength, noted as the "design wavelength". Most of the wavelengths the specifications are designed around are between 600 nm to 800 nm. Due to chromatic dispersion, those specifications listed would not be accurate, since the focal length would be a shorter distance for 455 nm. For example, the lens 354280-A was designed at 780 nm and had a recorded effective focal length of 18.4 mm. When 455 nm was sent through the lens instead, the actual effective focal length of the lens shortened to 17.9 mm. [22]

Table 14:Focusing Lens Comparison Table

Aspheric Focusing Lens		
Specifications	A280-A https://www.thorlabs.com/thorproduct.cfm?partnumber=A280-A	354280-A https://www.thorlabs.com/thorproduct.cfm?partnumber=354280-A
Effective Focal Length (455 nm)	17.8 mm, slightly shorter	17.9 mm, farthest
Coating	AR (350 nm – 700 nm)	AR (350 nm – 700 nm)
Spot Diameter at Focal Point (455 nm)	11.256 µm aberrated spot size, not diffraction limited by airy disk, good quality	0.422 µm aberrated spot size, diffraction limited by airy disk with 3.608 µm diameter, best quality
Lens Diameter	6.5 mm	6.5 mm
Cost	$98.83	$83.90

From Thorlabs, there were really only two unmounted aspherical lenses which seemed like appropriate options, especially since these lenses had the longest effective focal length out of any of the other aspheric lenses available on the website.

3.3.5.3 Focusing Lens Calculations

In the setup for the laser system being used, the collimated input beam diameter is significantly smaller than the focusing lens aperture. In this case, using the Gaussian equations for calculating the intensity of the final spot would be the most accurate. To find the peak on-axis intensity of the spot, the spot radius at the waist with intensity at least $\frac{1}{e^2}$ of the maximum (ω_0) must be found along with the oncoming power of the collimated beam onto the lens.

$$\omega_0 = \frac{f\lambda}{\pi\omega_i}$$

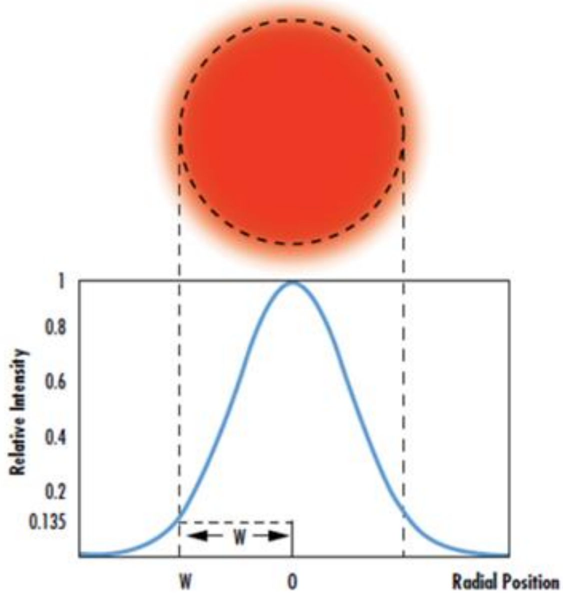

Figure 18: Visualization of the radius (W) of the waist which has $\frac{1}{e^2}$ of the maximum intensity. [27]

The desired wavelength of the light is 455 nm (λ) and the focal length at this wavelength is 17.9 mm (f). At this moment, the exact expected beam radius incident onto the lens is not certain, only that it is significantly smaller than the lens radius (3.25mm), so for simplicity it will be assumed that the incident beam radius is 1mm (ω_i). With these parameters, the spot radius at the waist is calculated to be 2.59 µm. Though, if the incident beam radius which could be achieved could be expanded into an area with an even larger radius, then the focused spot size could be reduced even further.

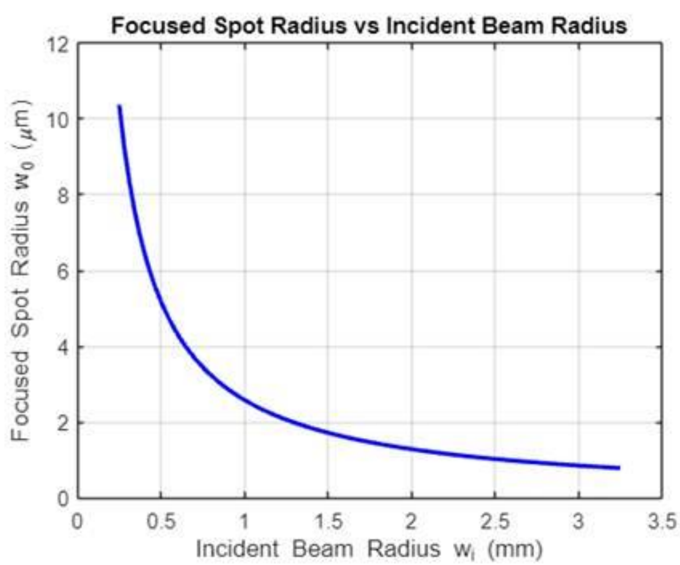

Figure 19: Graph illustrates the relationship between the incident beam size and the final spot size. (MATLAB)

The output power (P) of the laser system will be roughly 3W. This amount of power is extremely high for a laser beam and will result in a very high intensity spot for cutting.

$$I_0 = \frac{2P}{\pi {\omega_0}^2}$$

Since, again, the oncoming collimated beam will have an assumed radius of 1 mm, the peak intensity of the spot with these parameters is $2.84 * 10^5\ W/mm^2$. If the spot size into the lens could be increased, the intensity onto the fabric could increase significantly, as can be seen in the graph below.

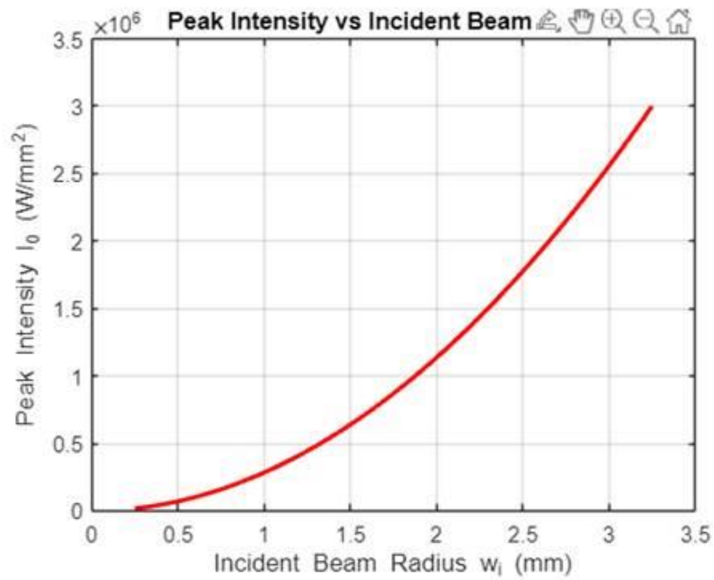

Figure 20: Relationship between the incident beam size and the spot peak intensity. (MATLAB)

Using the peak intensity of the spot, the Gaussian intensity profile of the final spot can be graphed to accurately predict what the spot will look like incident onto the fabric, given that it is smooth and flat on the canvas with minimal wrinkles.

$$I(r) = I_0 e^{-2(\frac{r}{\omega_0})^2}$$

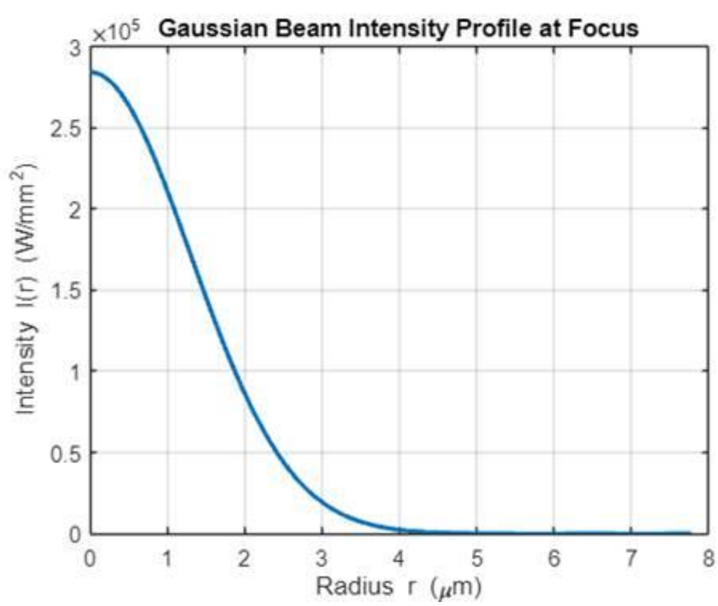

Figure 21: Focus spot intensity profile at input radius at 1mm (MATLAB)

This intensity profile is only attainable if the distance between the focusing lens and the fabric are at a very specific distance from each other due to the small Rayleigh range of the focus spot. The Rayleigh range is the distance from the beam waist where the spot radius increases by a factor of square root 2.

$$z_R = \frac{\pi {\omega_0}^2}{\lambda}$$

Using the equation above to find the Rayleigh range, it is $46.4\ \mu m$, which is incredibly small. This means, depending on the roughness of the fabric and the smoothness of the overall operation of the gantry system, that the likelihood of the spot on the fabric is not very likely to be within the Rayleigh range most of the time.

$$\omega(z) = \omega_0 \sqrt{1 + \left(\frac{z}{z_R}\right)^2}$$

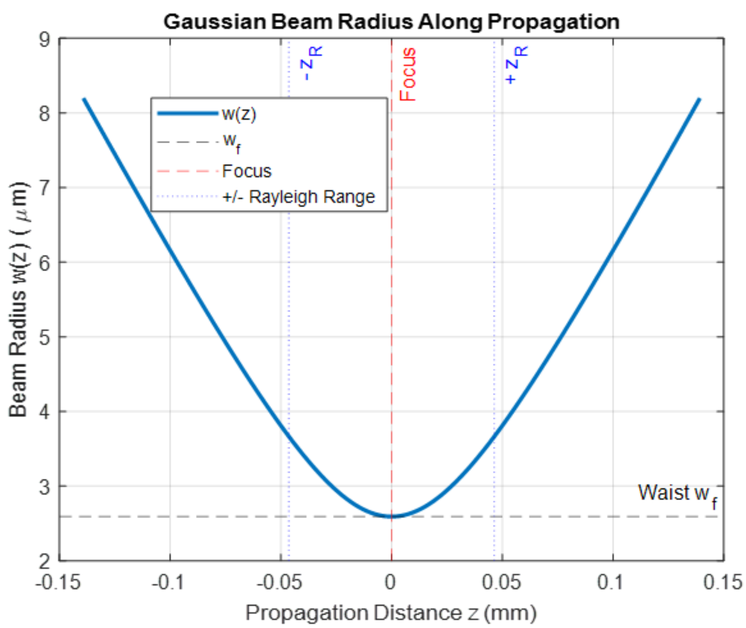

Figure 22: The Gaussian beam propagated near the focal point of the focusing lens (ω_i = 1 mm). The positive and negative Rayleigh ranges are labeled $-z_R$ and $+z_R$. The range between $-z_R$ and $+z_R$ is the depth of focus. (MATLAB)

Using the above equation, the Gaussian beam radius of the spot can be visualized with respect to the distance from the focusing distance. If the radius of the beam into the lens expands larger than the default 1mm, the Rayleigh range would be even smaller and hence the likelihood of the spot being within the Rayleigh range becomes even smaller.

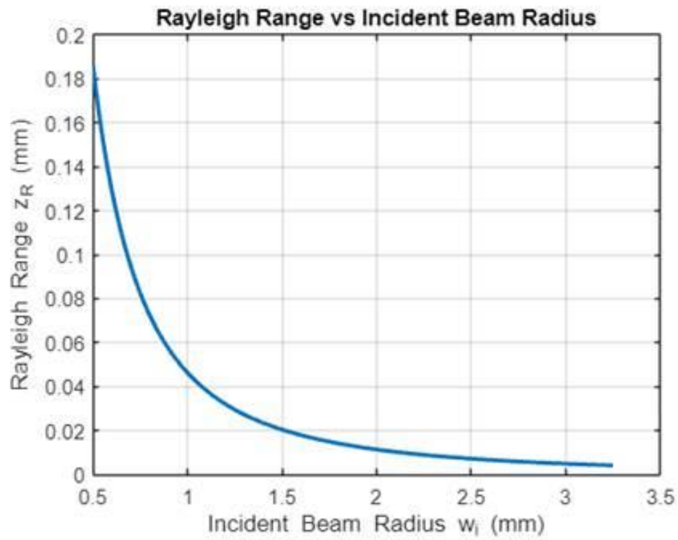

Figure 23:The relationship between the incident beam radius and the Rayleigh range. (MATLAB)

3.3.5.4 Effects of Spot Characteristics and Cutting Speed

The final spot size plays a critical role in how clean and efficient the cut will be. Although articles on laser cutting fabrics are scarce, much more is known about cutting other materials. Though they are not fabric, many of the same characteristics can be applied to them.

When the spot size is small, the intensity is maximized, meaning finer details can be cut more quickly. Since the beam energy is concentrated into a smaller area, the required exposure time in an area to cut through the material is decreased. In this case, the gantry head can move faster and finish a cut quicker. However, as the spot size decreases, the depth of focus shrinks. For thick or uneven fabrics, a shallow depth of focus can degrade cut quality. If the surface of the fabric is outside of the depth of focus, the beam area expands, intensity drops, and the cut may not penetrate cleanly. [28, 29]

Alternatively, if the spot size is too large, then the intensity of the spot is much lower, meaning more time is required to achieve the same cut depth. A larger spot tends to reduce precision, increases the cut width, and can lead to rougher, less defined edges. The material removal is less efficient because the energy is spread over a larger area. The sensitivity to focus and fabric height variation is reduced, but at the cost of cut quality and speed. [30] If the power is being adjusted instead of spot size, the effect on the final spot intensity of the power being excessively high is equivalent to the spot size being excessively small, and vice versa.

Intensity may need to be adjusted when changing the fabric material, changing the final size of the shape, or when the material surface is uneven. For instance, a thicker fabric may cut more effectively with a larger spot size and higher power so that the beam remains effective across variations in height and ensures it is cut all the way through, given the case it is set to be cut in a single pass. Meanwhile a delicate fabric may necessitate reducing power to avoid unwanted damage.

To adjust the final spot on the fabric, both the spot size and the source laser power are valid for adjustment, but they both have trade-offs. Adjusting laser power, with constant spot size, increases intensity directly and can speed up processing or enable thicker cut-through, but it also increases thermal load and risk of damage. Adjusting spot size, with laser power held constant, changes the intensity by concentrating or spreading the beam. Reducing spot size increases the intensity but reduces depth of focus, requiring better alignment and smooth gantry translation. Increasing spot size reduces intensity but reduces sensitivity to height variations and works for thicker materials. Practically, both should be optimized. First, a spot size should be chosen which is appropriate for the fabric and resolution, then set the power and traverse speed to achieve the required intensity and cut time with minimal to no damage to the fabric.

Cutting speed, meaning the speed at which the gantry head traverses over the fabric, has as much impact on cutting quality as spot size and intensity. When the cutting speed is too slow, this leads to excessive thermal input onto the fabric, which may cause burning, melting, or distortion of textile edge. The result of those effects is large kerf width, meaning wider cuts, and overall low accuracy cutting.

On the other hand, if the cutting speed is too fast, the beam does not deposit enough energy per unit length to fully sever the fabric. This may result in incomplete cuts and uncut fibers at the bottom of the cut. This means that either the laser power should be increased, the spot size should be decreased, or the cutting speed should be reduced. [31]

3.3.6 Image Acquisition and Processing

The imaging system is designed to operate with a camera mounted overhead, facing directly down toward the working field. During operation, the fabric will be laid flat within this field, ensuring that the entire working area is captured in a single image. The gantry system will be positioned completely outside the camera's field of view during image capture to ensure the entire fabric canvas is unobstructed to the camera.

Over the imaging area, ambient lighting will be carefully controlled and sufficiently bright to provide uniform illumination across the entire surface of the fabric. Proper lighting ensures that fabric details, textures, and marker sketches are clearly visible, minimizing shadows or glare that could interfere with image analysis down the line. The contrast between the fabric and the marker lines is especially critical for accurate sketch detection. For initial testing and algorithm development, only black and white markers will be used, as their contrast against most fabrics simplifies image segmentation. As the system's reliability improves, additional marker colors may be introduced, including UV fluorescent markers. Using UV illumination, these inks allow for cuts with invisible sketches, meaning the final product would not have any visible marker residue and resulting in an overall cleaner appearance.

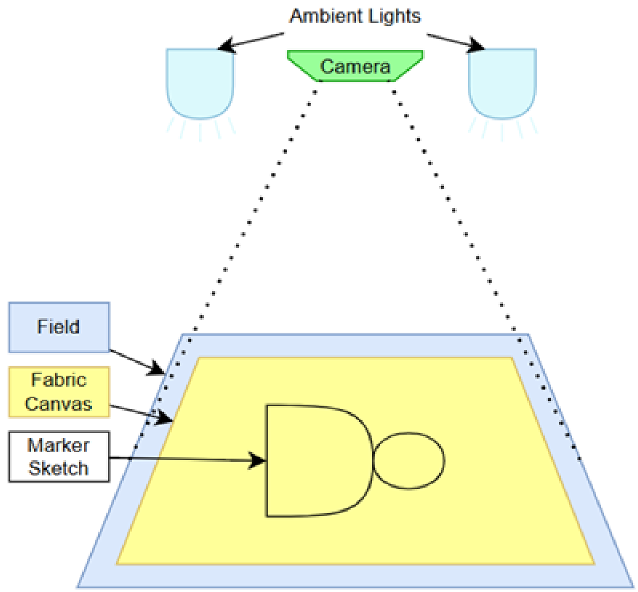

Figure 24: Schematic of the camera setup (not to scale and gantry out of frame)

Once the overhead image is captured, it will be transmitted to the Raspberry Pi for processing. The Raspberry Pi will execute a color-detection algorithm that identifies and stores the pixel coordinates of pixels which fall within the color threshold defined by the user. This information represents the approximate path of the user's sketch on the fabric.

Next, a path-generation algorithm will process the detected pixel data to compute a continuous path running along the center of the marker lines. This path extraction step effectively converts the sketch data into a vectorized format suitable for motion control. The resulting path coordinates can then be passed to the gantry system, which will trace and cut along these lines in a predefined sequence.

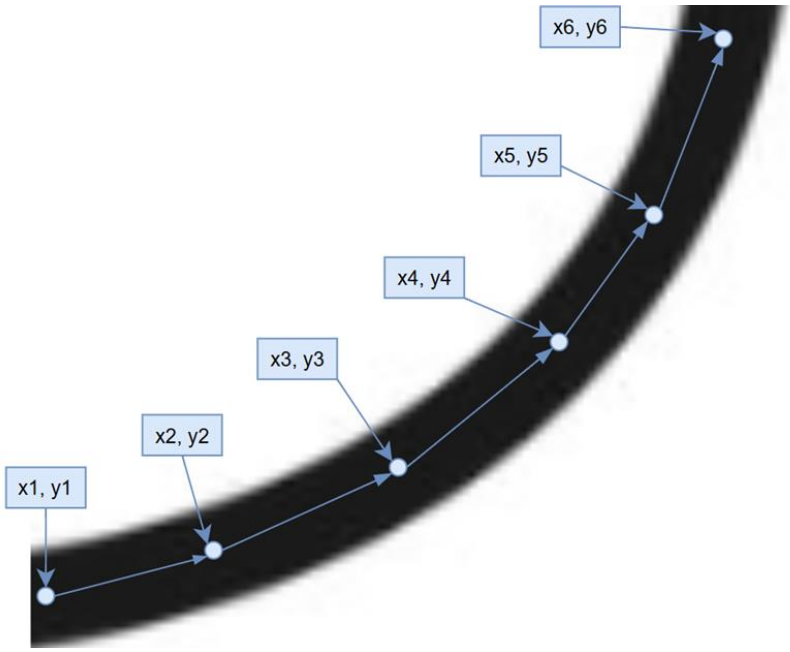

Figure 25: Simplified visualization of the ideal gantry path being generated along a simulated marker sketch.

3.3.6.1 Camera Selection

Since the project is using a Raspberry Pi Model 4B as the control board, the cameras that can be used are limited to the ones which are compatible with that type of board. Most of the other cameras listed on their website are not practical, such as the HQ Camera which requires extra lenses, though it would give the best quality images given proper lenses. The two main contenders are Camera Module 3 and Camera Module 3 Wide.[36]

Table 15: Pi Camera Selection Comparison Table

Raspberry Pi Cameras		
Specifications	**Camera Module 3**	**Camera Module 3 Wide**
Sensor Resolution	4608 × 2592 pixels	4608 × 2592 pixels
Focus	Motorized	Motorized
Weight	4g	4g
Depth of Field	10 cm+, larger range of focus	5 cm+, shorter range of focus
Horizontal Field of View	66 degrees	102 degrees, image distorted at the edges

Vertical Field of View	48.8 degrees	67 degrees, image distorted at the edges
Price	$25	$35

Based off the table above, Camera Module 3 is the best option for the overhead camera. Also, given the height of the enclosure (600 mm), this is more than sufficient height for the camera to capture the entire field. In fact, if the field is 350 mm x 350 mm, the camera would have to be approximately 390 mm minimum above the field to capture the entire area.

$$\frac{350\ mm}{2\tan\left(\frac{48.8^\circ}{2}\right)} = 385.79\ mm$$

This leaves sufficient room above the camera or below the field where components could be located.

After the camera captures the image, it will undergo image processing and path generation, which will direct the movement of the gantry system. As this system transfers from optics to software, image processing is expanded upon in Chapter 7.

3.3.7 Reflected Scattered Light Detection

Since different colors or types of fabrics, or marker sketches may reflect different amounts of the laser wavelength, there should be a way to detect how much of the light is not being absorbed and instead being reflected from the surface. To detect this light, on the same module which the focus lens will be mounted on, there will be photodiodes facing downwards and angled towards the focus spot to capture the scattered light. If a significant amount of light is being reflected, the output power of the laser would have to scale up to counteract the light being reflected or vice versa.

For photodiodes, there are many options available. At first, since the reflected light is blue, it would have seemed like I would need a blue-sensitive photodiode, but due the sheer intensity of the light, the amount that will be reflected off, and the limited amount of exterior lighting from the tinted enclosure glass, the blue light would saturate the photodiodes even is 455 nm is not the peak wavelength. This widens the options available for the photodiode selection.

One of the most popular and cheapest photodiodes which could work is BPW34. Though the photodiode works best at 900 nm, it is still responsive with a sensitivity of about 0.15 at 455 nm. If this photodiode could be connected to a transimpedance amplifier circuit, the output from the photodiode could be significantly increased.

3.4 Part Selection

Upon carefully researching and evaluating the project’s needs and what is out there in the market, particular parts were identified to meet those needs. There was an emphasis on the project’s design requirements and how well all of the parts would be able to integrate properly.

3.4.1 Motor Selection

Among the key features that were analyzed include movement precision, affordability, torque, current, and ease of use. Brushed and brushless motors were identified as not being able to meet the necessary position control necessary for the project. Servo motors and stepper motors were identified to provide desirable movement precision and control. Although servo motors do have some features that are superior to those of stepper motors, ultimately bipolar stepper motors with a hybrid rotor were chosen for the performance they provide with respect to their cost. It was also determined that certain components of the servo motor may not be necessary such as the use of an encoder.

A key feature of the stepper motor that stood out was the simple design of being able to count the short, incremental steps of the stepper motor to determine its position. Several stepper motors were analyzed to see which would best integrate into our project design. The project design will incorporate three stepper motors. One stepper motor for X-axis movement, one stepper motor for Y-axis movement, and finally one stepper motor for Z-axis movement. Being able to control three different axes is crucial to the effectiveness of the laser cutting through different materials.

When looking into the hybrid stepper motors available in the market, a variety of frame sizes are available. The most common that appeared in an internet search included NEMA 14, NEMA 17 and NEMA 23 stepper motors. The number "17" in NEMA 17 represents the faceplate dimensions of 1.7 inches by 1.7 inches or 57 mm by 57 mm. Of all the frame sizes available, the NEMA 17 was the most attractive as it offers a suitable size with respect to the desired size of the gantry system.

Table 16: NEMA 17 Stepper Motor Comparison

Stepper Motor Comparison			
Motor	17HE24-2104S	**17HS15-1504S1**	17HS08-1004S
Rated Current (A)	2.1	1.5	1.0
Step Angle (°)	1.8	1.8	1.8
Holding Torque (N*cm)	60.0	45.0	16.0
Dimensions (mm)	42x42x60	42x42x39	42x42x20
Weight (kg)	0.476	0.28	0.14
Cost (USD)	8.97	9.13	6.68

From the table above, several NEMA 17 stepper motors were compared. The key specifications that were closely analyzed included the rated current, the holding torque, and the dimensions. From these specifications, the last deciding factor was the cost effectiveness relative to what the motor offers. A key observation is that as the holding torque increases, the dimensions and weight also increase. The 17HS15-1504S1 bipolar stepper motor was chosen as it provided the ideal holding torque for the project design while also offering decent dimensions and weight.

3.4.2 Motor Driver Selection

Among the key features that were analyzed include operating voltage, continuous current, affordability and ease of use. Micro-stepping is important for precise movement control of the stepper motors, but many of the motors looked into had similar micro-stepping capabilities. Also, many of the motor drivers looked into also provide similar protection features. It is important to note that out of the four motor drivers that were looked into, the A4988 and the DRV8825 had the most internet resources because they are the most widely used for NEMA 17 stepper motors.

A key requirement for the NEMA 17 stepper motors to work is that the motor driver would have to operate at or close to 1.5 A. For this reason, the A4988 was the least favorable for the project design due to the simple fact that in order to operate at a continuous current of 1.5 A, the motor driver would need to incorporate a heatsink or some other cooling medium to efficiently operate at that current.

Although the DRV8825 is the most expensive, the fact that it has many detailed resources easily available on the internet seemed quite desirable. So, from that assessment, the goal was to see if the TMC2209 or the TB67S581FNG were similar to the functionality of the DRV8825. From closely analyzing the TB67S581FNG, it was determined that it had the equivalent sort of pin layout and functionality as the DRV8825. Basically, the TB67S581FNG would be able to be used similar to the DRV8825 and provide similar performance while also coming at a much lower cost. In analyzing the TMC2209, it was determined that certain features may not be necessary. Since the project design will incorporate three stepper motors, three TB67S581FNG motor drivers will be implemented.

Table 17: Motor Driver Comparison

Motor Driver Comparison				
Motor	A4988	TMC2209	**TB67S581FNG**	DRV8825
Operating Voltage (V)	8 - 35	4.75 - 29	8.2 - 44	8.2 - 45
Max. Continuous Current (A)	1.0	2.0	1.5	1.5
Peak Current (A)	2.0	2.8	2.2	2.2
Micro-stepping	Down to	Down to	Down to	Down to

Resolution	1/16	1/256	1/32	1/32
Dimensions (mm)	15.24x20.32	15.24x20.32	15.24x20.32	15.24x20.32
Cost (USD)	8.95	8.95	6.95	15.95

3.4.3 Laser Diode Driver Selection (Tony)

With the project's budget in mind, the best option for the laser diode driver is to design a laser diode driver circuit. For one, no laser diode driver integrated circuit met the operating current needs for the GH04C03A9G laser diode. It needs an operating current between 2 A and 2.4 A. For another, the laser diode driver board modules available that do offer the necessary operating current are all very expensive. The design in mind is an op-amp voltage-controlled current sink which facilitates current regulation. The circuit design will include components such as a transistor, an op-amp, resistors and capacitors. More details on the laser diode driver circuit design will be in chapter 6 of Hardware Design.

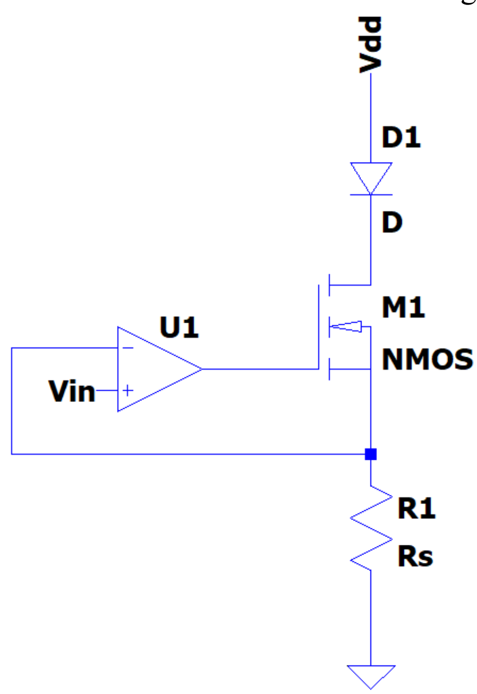

Figure 25: Laser Diode Driver Basic Circuit Design using LTspice.

3.4.4 Lens System Selection (Jacqui)

The optical components selected for F.L.C.S. were chosen deliberately to balance precision, safety, manufacturability, and cost while meeting the performance requirements for fabric cutting with a 3.5-watt laser diode. We chose a 445–465 nm laser diode because visible-wavelength diodes are compact, inexpensive, and offer strong absorption across most common fabrics, enabling efficient cutting at lower power compared to CO_2 or fiber lasers. The aspheric lens was selected to efficiently collimate the highly divergent output of the diode, maximizing usable optical power and minimizing stray light inside the enclosure. To correct the diode's inherently elliptical beam shape, an anamorphic prism pair was chosen over cylindrical lenses because it preserves polarization and allows reliable aspect-ratio correction within a compact footprint suitable for the enclosure. The Galilean beam expander, built from a plano-concave and bi-convex lens, was selected because it enlarges the beam without creating an internal focal point, preventing hazardous hotspots and reducing divergence before the focusing stage. Anti-reflective coatings and NBK-7 glass were prioritized to minimize optical loss while staying within budget, and all components were chosen to integrate easily with custom 3D-printed mounts. Together, this optical lens system ensures that the beam remains well-shaped, expanded, and controlled before reaching the mirror system, enabling a consistently small, focused spot on fabric and reliable cutting performance across different textile types.

3.4.5 Optical Components Selection (Mike)

Table 18: Mirror Selection (Highlighted)

To reliably redirect the 455 nm beam, the optical surface must be capable of reflecting as much power as possible while minimizing absorption. Common metallic mirrors such as silver and aluminum have a higher absorption and lower damage thresholds. These shortcomings can lead to reduced beam intensity, heating of the mirror, and potential degradation.

Dielectric mirrors, on the other hand, are engineered to achieve reflectivity over 99% across the visible spectrum, dramatically reducing power loss and power absorption. Additionally, dielectric coatings are more durable compared to metal coatings, making them far more suitable for handling concentrated high-power beams without risking damage.

Mirrors			
Specifications	**Fused Silica Broadband Dielectric (E02)**	**Protected Silver**	**Protected Aluminum**
Reflectivity (455 nm)	>99%	>97%	>90%
Bandwidth	Moderately broad 400nm - 750nm	Very broad 450 nm - 2 µm	Very broad 450 nm - 2 µm
Absorption	<1%	<3%	<10%
Laser Damage Threshold	High threshold (470 W/cm)	Moderate threshold (213 W/cm)	Low threshold, lot of power absorbed (43 W/cm)

Surface Quality	High quality, laser-grade, low scatter (10-5 Scratch-Dig)	Good quality, good for optics (40-20 Scratch-Dig)	Good quality, good for optics (40-20 Scratch-Dig)
Cost	Most expensive ~$50	Least expensive ~$30	Moderately expensive ~$40

When choosing the focusing lens, aspherical lens have been shown to produce the best quality spot and hence create the best quality cut. From the available aspheric lens, the lens with the longest possible focal length is desired so that the lens does not bump into the fabric accidentally.

Table 19: Focus Lens Selection (Highlighted)

Aspheric Focusing Lens		
Specifications	**A280-A**	**354280-A**
Effective Focal Length (455 nm)	17.8 mm, slightly shorter	17.9 mm, farthest
Coating	AR (350 nm – 700 nm)	AR (350 nm – 700 nm)
Spot Diameter at Focal Point (455 nm)	11.256 µm aberrated spot size, not diffraction limited by airy disk, good quality	0.422 µm aberrated spot size, diffraction limited by airy disk with 3.608 µm diameter, best quality
Lens Diameter	6.5 mm	6.5 mm
Cost	$98.83	$83.90

From the choices in the Raspberry Pi website, the best option seemed to be the Camera Module 3 since it had had the best specifications for the best price. A Wide camera module is not needed since the edges of the image would be distorted.

Table 20: Camera Selection (Highlighted)

Best Raspberry Pi Cameras		
Specifications	**Camera Module 3**	**Camera Module 3 Wide**
Sensor Resolution	4608 × 2592 pixels	4608 × 2592 pixels

Focus	Motorized	Motorized
Weight	4g	4g
Depth of Field	10 cm+, larger range of focus	5 cm+, shorter range of focus
Horizontal Field of View	66 degrees	102 degrees, image distorted at the edges
Vertical Field of View	48.8 degrees	67 degrees, image distorted at the edges
Price	$25	$35

Chapter 4: Real World Design Constraints and Related Standards

4.1 Standards

4.1.1 Laser Safety Standards (Jacqui)

When it comes to operating a laser many safety precautions should be taken to ensure safe operation. Laser classes and standards help us identify how we should be using and behaving around our lasers to ensure no one is harmed while making this fabric laser cutter system. We included considerations of the American National Standards Institute as well as Florida Administrative codes. For the laser safety classes, the potential hazard of the laser increases as the number increases. These hazards are considered in terms of harmful impacts towards our skin and eyes. Products including lasers must have a label listing the classification of the laser.

Lasers labeled Class 1 do not pose a threat of biological damage. This means it is not an eye, skin, or burn hazard. Class 1M contains lasers that do not produce hazardous conditions during normal operations, unless the laser is being viewed by an optical instrument. Class 2 lasers are within the visible spectrum of 400-700 nm and do not exceed 1mW in power. This class includes both continuous wave and pulsed lasers. The maximum duration for eye exposure during use of these lasers is .25 seconds, equal to human aversion responses, meaning you should not attempt to look at them. These lasers should not be viewed directly with optical instruments. 2M lasers are still in the visible spectrum and the human aversion response normally protects the eye for unaided viewing. These lasers are potentially hazardous if viewed with certain optic instruments [18].

Class 3 is split into 3B and 3R lasers that include lasers within the visible spectrum. 3R corresponds to lasers with a beam between 1 milliwatt and 4.99 milliwatts of power, so direct eye exposure should be avoided. Whereas class 3B lasers have a beam power of 5 milliwatts to 500 milliwatts, or half a watt, and any exposure to this beam should be avoided. This includes lasers that can harm your skin and materials if held long enough at close range. When considering exposure to beams from any class of laser, include considerations of stray or reflected beams.

Class 4 lasers are the biggest concern, as these need-controlled measures to prevent exposure from the direct beam or a reflected beam. These lasers have the potential to ignite and create fire, causing airborne byproducts or materials. These lasers are greater than a half of watt of power and pose a threat to your skin and materials from burns. Do not stare at these lasers even when the laser dot is on another surface, and the light can be bright enough to cause a sustained afterimage lasting longer than 10 seconds. If this sustained afterimage occurs, laser light is too bright [19]. When operating any laser, it can be useful to have a laser safety officer contact to ask questions regarding your specific setup or design.

Since the laser output of our laser diode will be variable it can range from a class 3 to a class 4 laser. This is why we have taken the precautions to have an enclosure system that includes a HEPA filter as well as OD6+ laser safety windows.

4.1.2 Software Development Standards (Nick)

Software reliability is important since incorrect logic or latency can directly impact laser safety. The firmware running on the ESP32-based board controller is developed in C/C++ and follows widely accepted embedded systems practices, including minimizing dynamic memory allocation, enforcing type safety, and maintaining deterministic execution where possible.

These practices align with principles outlined in standards such as MISRA-C:2012, which aim to reduce undefined behavior and improve code reliability in safety relevant systems. On the supervisory side, the Raspberry Pi software is developed in Python using structured programming techniques, input validation, and controlled hardware interaction to ensure safe and predictable operation.

Together, these software practices promote system stability, maintainability, and safe operation in mixed real-time and high level computing environments.

4.1.3 Communication and Interface Standards (Nick)

The system utilizes standardized serial communication protocols to enable reliable data exchange between the Raspberry Pi 4B and the laser engraver controller. Communication is implemented over USB 2.0, which provides a virtual serial (CDC) interface compliant with USB-IF specifications for device enumeration, data transfer, and power management.

At the data level, communication follows standard asynchronous serial transmission principles derived from EIA/TIA-232 conventions, including start and stop bit framing and byte-orientated data exchange. This ensures compatibility with widely supported serial communication tools and libraries.

The command structure transmitted over this interface is based on standard G-code, a wildly CNC control language used for motion control systems. The GRBL firmware running on the controller interprets these commands and executes them with precise timing, ensuring coordinated motion and laser control.

Chapter 5: Application of LLMs

5.1 ChatGPT

5.1.1 Assistance (Nick)

ChatGPT has emerged as a transformative modern tool, reshaping research and development workflows in a manner reminiscent of the handheld calculator's impact on engineering education decades ago. With the introduction of Model 5, its capacity for technical reasoning, data organization, and natural-language coding assistance has made it especially valuable for multidisciplinary engineering projects such as ours. Throughout this project, ChatGPT was used not merely as a conversational assistant but as a codesign partner supporting decision-making, code generation, literature review, and design choices such as name selection and logo design.

5.1.2 Summarizing Assistance (Jacqui)

After the majority of Senior Design 1 was completed, we realized we had to write an executive summary of the project. This executive summary is needed to capture the potential impact our project has, or value, as well as its overall purpose and main goal. We used ChatGPT to gather ideas of how to correctly communicate this impact and the historical significance of fabric/textile cutting. The inquiries were "Please write a paragraph of the importance/impact of fabric/textiles on human culture and the way we express ourselves" as well as "write a paragraph about making fabric cutting more accessible by allowing it to be done via fabric laser cutting, and how this will have an important impact". This gave us a chance to edit and add text needed to highlight the importance and impact of our project, which we then used to start the executive summary. We then added project specific features and explained the purpose of our project in a concise way to flow with what was provided via ChatGPT.

5.1.3 Part Selection Assistance (Nick)

In the early phases, ChatGPT assisted in comparing potential system architectures for the Fabric Laser Cutter System (F.L.C.S), evaluating platforms such as the Raspberry Pi 4B, Pi 5, Jetson Nano, ESP32, and Arduino Mega 2560. The comparison data it provided included numerous technical specifications such as processor speeds, connectivity, and power requirements which offered a solid baseline for evaluation. However, it quickly became clear that these numbers could not be accepted at face value. As accurate as Model 5 often is, it remains susceptible to occasional errors.

To ensure reliability, we conducted independent verifications of the specifications that ChatGPT provided, consulting official datasheets, manufacturer documentation, and vendor product listings. Most of the values aligned closely with ChatGPT's output, confirming its usefulness as a research accelerator. Yet, certain parameters such as latency performance, real-time responsiveness, and power draw under load were difficult to confirm since they were either not specified in the datasheets or varied by testing environment. These cases required additional investigation.

This process underscored a critical lesson about using AI tools in engineering research: while ChatGPT can rapidly synthesize complex technical data, human validation remains essential. The model's role is best seen as a guide, not an absolute authority. By cross-checking every specification and reconciling inconsistencies, the team ensured that each design decision was grounded in verifiable data rather than unverified model output.

5.1.4 Assistance in Code Generation and Web Development (Nick)

During the implementation phase, ChatGPT played an important role in the development of the project's website, which serves as a digital interface for documentation and demonstration. Initially, we began constructing the website using basic HTML and CSS, relying on the guide provided in order to understand page structure and styling. However, these early attempts lacked organization and consistency, often requiring time to adjust the layout of the website.

ChatGPT streamlined this process by providing step-by-step guidance and example code structures that aligned with modern web-development standards. It explained how to properly format HTML documents, apply CSS for layout control, and organize content sections for clarity.

The biggest help yet was how to integrate our project documents into the website. As of right now the website is in its infancy with not much to look at. However, it provides an easy-to-access hub for all our documents as we work toward our final submission and presentation. By creating a single, centralized platform, ChatGPT made it easier to host progress updates, link technical files, and maintain version control throughout the development process.

As the project continues to grow, the foundation built through ChatGPT's guidance will allow for smoother expansion into interactive elements, and visual media integration. This early groundwork not only improved efficiency but also ensured that the website remains structured, scalable, and reflective of the team's professional standards.

5.1.5 Assistance in Literature Review and Research (Nick)

Beyond technical implementation, ChatGPT also served as an effective tool for conducting and organizing literature obtained from google scholar or its own recommendation. During the research phase, it was used to identify credible sources, summarize technical papers, and clarify complex topics relevant to our system's design such as display latency, and real-time processing on embedded Linux. By providing a link from google scholar and prompting the model with targeted questions, it was possible to generate clear explanations and summaries of engineering concepts that would otherwise require extensive manual searching.

Additionally, ChatGPT aided in the citation and documentation process by suggesting how to reference online articles, technical datasheets, and manufacturer documentation. Whether the task involved citing a paper within a paragraph or determining what information could be appropriately referenced, ChatGPT provided accurate guidance that helped maintain consistency while avoiding legal trouble that could be present when reference another's work.

In summary, ChatGPT's contribution to the literature analysis lay in its ability to synthesize information, improve organization, and accelerate understanding. It functioned as a research assistant capable of guiding exploration without substituting critical analysis. This integration of AI into the research workflow not only enhanced productivity but also strengthened the depth and quality of the project's foundation.

5.1.6 Assistance in Design Choices (Nick)

ChatGPT also played a role in the creative design process, particularly selecting the project's name and developing a logo. Early in the project, several names were proposed, but many lacked technical relevance or did not reflect the system's function. Eventually we landed on Cutting Laser for Optimized Textile Handling (C.L.O.T.H); but that too did not truly reflect our project as it lacked the clarity needed for an outside reviewer to get a sense of what the project is about. As a replacement, ChatGPT generated ideas such as the friendly name "Draw2Cut" and the attractive name "VisionCut"; eventually the final acronym F.L.C.S (Fabric Laser Cutter System) was chosen to represent us as it best captured the project's focus and professional tone.

In addition to name exploration, ChatGPT contributed to the logo design process by generating potential designs that could represent our system. This was one of the most impressive aspects of ChatGPT as the generated designs were clean, simple, and functional. With additional prompts regarding color, depth, and style, ChatGPT was able to present the final logo concept that now represents the entire project.

Overall, ChatGPT's involvement in these design choices simplified the brainstorming phase and provided quick, clear feedback on visual and conceptual direction. While the final designs were adjusted by hand, the model's input helped narrow down options and maintain our identity.

5.1.7 Conclusion (Nick)

Throughout the development of the Fabric Laser Cutter System (F.L.C.S.), ChatGPT proved to be a versatile, reliable, and valuable tool that supported the team in multiple aspects of the project. From assisting in part selection and website development to organizing papers and refining the project's identity, it enhanced both technical efficiency and creative direction.

Despite its strengths, ChatGPT was not without limitations. Some of the information it produced required verification, and certain outputs needed refinement to align with the project's real-world constraints. Nevertheless, its integration into the workflow demonstrated how AI can act as a capable partner that amplifies human effort rather than replacing it.

Overall, ChatGPT's inclusion in this project not only improved productivity and organization but also offered a peek at the future use of large language models with engineering design, research, and documentation.

Chapter 6: Hardware Design

6.1 Optical Design

6.1.1 Optical Design Prior to Mirrors (Jacqui)

Below is an optical schematic of the lens system without the anamorphic prism pair demonstrating the expansion of the beam after the bi-convex lens. Although the beam initially expands, it become nearly collimated after around 200 millimeters or 7.8 inches. This was intentional as it allows us the needed space to build the mirror system such that it does not impact our laser lens system and has enough room to move and change position before the beam reaches the focusing lens. To compensate for the anamorphic prism pair, a blank space of around 30mm was placed between the aspheric and plano-concave lens.

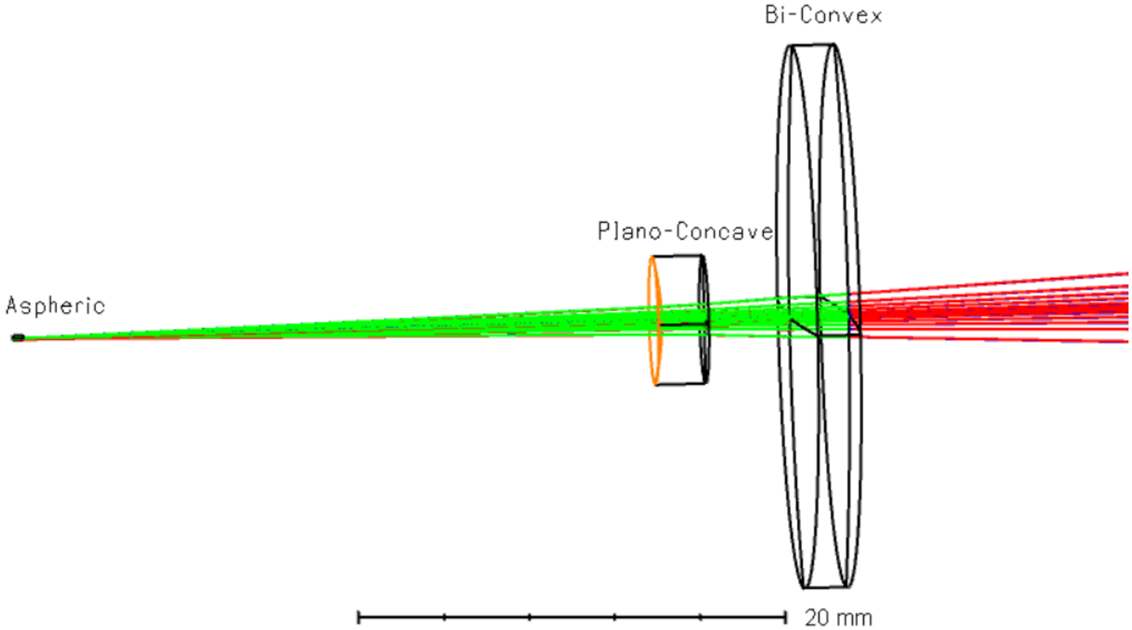

Figure 26: Lens Diagram via Zemax

Our PSE students performed two optical demos throughout senior design 1. To prepare for these demos, I prepared 3D printed mounts to secure the lenses in place. Each of these lens mounts had to incorporate hexagonal shaped nuts to allow for them to be mounted using set screws with optical posts. The figure on the right demonstrates a snap mount designed by Kiva [32] which I used as a starting point for our lens mounts. By creating a copy of Kiva's files we can adjust them as needed to fit our lenses. When using these snap mounts we were able to make mounts for each of our lenses. Even for our smallest lens, the LC1975 with a 6-millimeter diameter, where we were able to print an adapter type piece that holds the lens perfectly in place in the snap mount.

Figure 27: Snap Lens Mount for LB1945-A

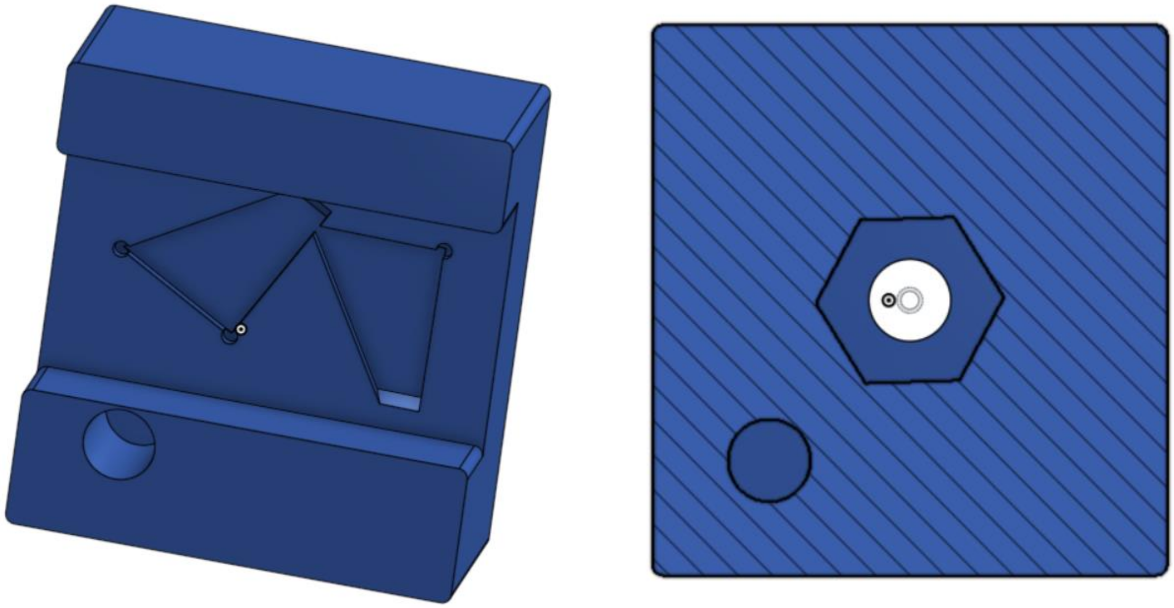

Figure 28: Anamorphic Prism Pair, Bottom Half with Section View

For the final optical demonstration, I created a mount for the anamorphic prism pair. The bottom half of this mount is shown in Figure 28. This mount was 3D printed and uses two separate pieces to hold the prisms in their correct alignment needed to shape the beam. These pieces incorporate the same technique as the lens mounts, using nuts to add thread by leaving a hexagonal gap, shown in a section view of the bottom of the mount in Figure 14 on the right. I was able to make indentations to correctly position the prisms by utilizing the Boolean tool in Onshape.

6.1.1 Optical Design: Mirrors and Focusing Lens (Mike)

The mirrors and the focusing lens are the main system contributing to the redirection of the beam onto the desired spot to be cut. The design will use two dielectric E02 coated mirrors to direct the beam in the x and y positions of the fabric canvas, given that the beam is entering the gantry and hits the first mirror horizontally. Below the second mirror is the aspheric focusing lens, 354280-A, which can be adjusted vertically to adjust where the focal spot is vertically. This can be adjusted based on the thickness and type of fabric, which can vary.

For the optical demonstration, a roughly constructed x-y manual moving gantry was constructed using wood planks, steel rods, and 3D printed parts which could traverse along the steel rails.

Figure 29:Rough gantry prototype used for demonstration

Based on Figure 29, the laser would be situated on the bottom right, below the bottom plank. The beam would propagate parallel to the vertical (x-axis) rails onto the first mirror, redirecting the beam horizontally (y-axis). It would then be redirected by the second mirror onto the floor (z-axis) after passing through the focusing lens. The parts which held the optical components would secure them using screws.

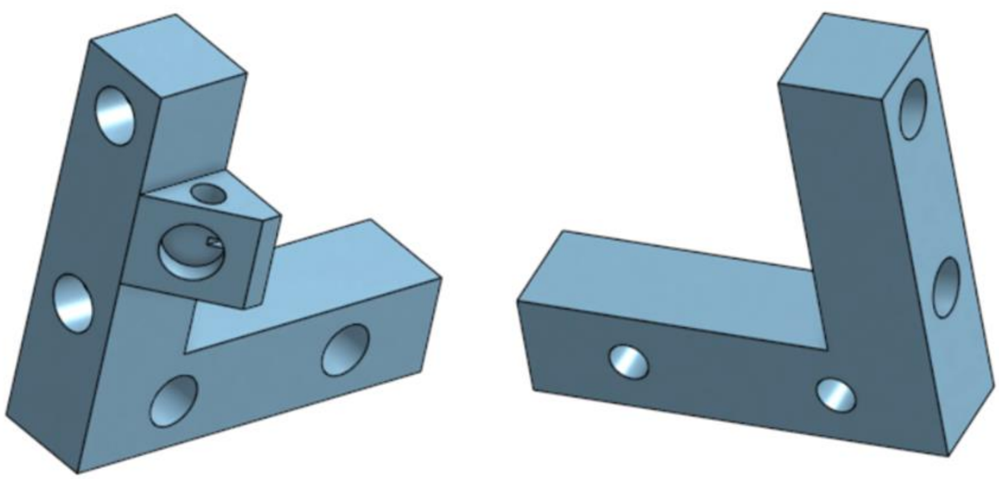

Figure 30: The bracket pieces which would traverse the x-axis and support the y-axis rail. The left bracket holds the x-y mirror

The x-axis rails would slide through the two holes on the bottom of the brackets. Due to the holes being slightly larger than the rails and the rails having slight imperfections, the y-rail could not be consistently perpendicular to the beam going into the system. Due to this issue, these rails will be swapped with higher quality t-slot rails in future demonstrations.

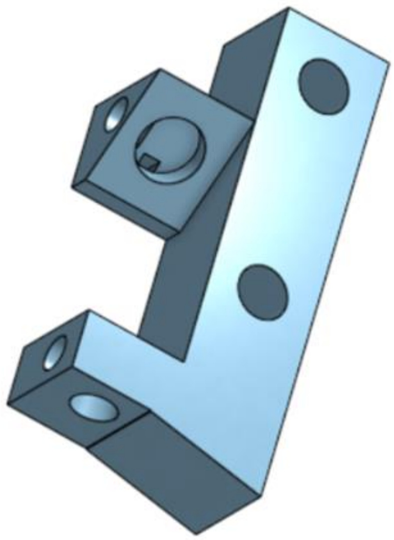

Figure 31: The carriage piece which would traverse the y-axis and support the y-z mirror, the focusing lens, and the photodiode on the slanted surface

This final piece slides across the y-rail, redirects the beam from the y-axis to the z-axis, downward onto a focusing beam and downward on the fabric. To be able to detect the back reflections from the laser off the fabric, a photodiode is placed on the slanted surface on the bottom of the carriage.
Later, a functional gantry with fitted stepper motors was ordered. The same idea from the prototype will be applied to this new gantry.

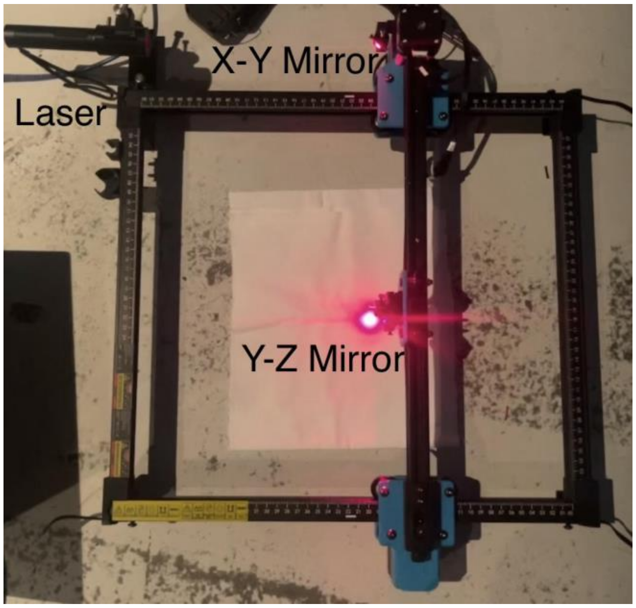

Figure 32 New belt driven gantry with fitted stepper motors with the two moving mirrors mounted. The red laser is used for demonstration.

To ensure that the maximum amount of the beam is incident onto the fabric, the mirrors need to be angled perfectly such that the beam reflects at exactly 90 degrees on all the mirrors. Since the laser is going to be mounted vertically, an additional stationary mirror will be fitted to redirect the beam towards the movable X-Y mirror.

On the same unit as the Y-Z mirror, the focusing lens is mounted to focus the beam down to a small spot size. This focusing lens can have its height adjusted by the user. Next to the focusing lens, the photodiodes are placed facing downwards to read the scattered reflections off the fabric.

Chapter 7: Software Design

7.1 Optimal Programming Languages for image processing (Mike)

Several programming languages can be used for image processing and gantry path generation. The most common languages for this purpose are Python, C++, C, Rust, and MATLAB. Python, through libraries such as OpenCV, NumPy, and many others, offers a high-level, intuitive approach to processing images and extracting relevant features. C++ also supports OpenCV and could execute the same image processing programs significantly faster due to its compiled nature and lower-level memory management. Rust, though newer, provides strong performance and safety precautions which could prevent common programming errors such as memory leaks. C is extremely efficient for embedded systems, but due to the lack of native high-level libraries, image processing becomes cumbersome and so would not be an ideal language. MATLAB, while great for prototyping and algorithm testing, due to its heavy runtime and licensing constraints, would not be suitable for use in a real-time embedded environment such as a Raspberry Pi.

Table 21: Programming Language Comparison Table

Programing Language				
Specifications	**Python**	**C++**	**C**	**Rust**
Recommended Compiler	CPython	GCC	GCC	rustc
Runtime Performance	Very slow, high overhead	Fast	Fast, low overhead	Fast and optimized
Complexity	Easy and intuitive	Like C, but less complex/basic	Complex and low level	Strict syntax, ownership model
Computer Vision and Image Processing	Extensive number of dedicated libraries (OpenCV, NumPy, SciPy, TensorFlow, many more)	Variety of libraries (OpenCV, Dlib, VXL, VIGRA)	Very limited, would require custom code	Limited, could use Open CV
Memory efficiency	Poor, high overhead	Good	Excellent, direct access to memory	Safe and efficient
Error handling	Safe	Needs manual management	Prone to errors	No nulls, enforced checks
Hardware control	Possible through libraries	Can access hardware efficiently	Excellent, direct hardware access	Safe low-level access

For image processing and generating gantry paths, the optimal programming language would be Python, at least during early development. Python integrates seamlessly with the Raspberry Pi OS, has native support for the camera through libraries such as picamera2 and OpenCV. Its simplicity makes it ideal for tuning thresholds, filtering noise, and identifying marker coordinates before converting them into a usable path. However, Python's major drawback is runtime performance due to being a very high-level language. This can cause severe lag when handling large images or complex operations. For real-time operation, the image processing program could later be converted to C++.

7.2 Possible Bugs and Solutions (Mike)

Running into bugs during image acquisition, path generation, and all the steps in between are inevitable. Being able to identify and mitigate these errors in the best way possible is the best defense against the system unexpectedly malfunctioning or breaking. With all the risks of managing a high-power laser, an extremely high intensity spot of light, potentially flammable fabric, and operating delicate components, it is optimal that these bugs can be caught and dealt with and completely avoided ahead of time before they cause any real damage.

7.3 Operational Design (Nick)

The software subsystem for this project focuses on two key aspects. One is a touchscreen-based user interface that provides control, feedback, and laser operation. The second is low-level communication and synchronization between the Raspberry Pi 4B and its peripherals. Together, these elements will ensure tightly coordinated operation of the Fabric Laser Cutter System (F.L.C.S.) with real-time responsiveness and user accessibility.

7.3.1 User Application Design (Nick)

The Human Machine Interface (HMI) serves as the primary point of interaction between the user and the F.LC.S. It is implemented through a touchscreen-based User Interface (UI) that provides full control, monitoring, and feedback of the system's operation. The UI enables the operator to configure job parameters, ensure safety compliance, and monitor the state of the laser cutting process in real time. Specifically, the UI's objectives are:

1. To create a central control panel that displays the current system state and operation in real time
2. To allow the user to configure job parameters such as fabric type, marker color, laser power, and cutting speed
3. To display real-time status of the cutting process, including elapsed time, estimate time to completion, and job progress
4. To allow integration with auxiliary peripherals such as the onboard camera for alignment

Through this interface, users can safely and intuitively configure and operate the system while receiving immediate visual feedback on performance and safety conditions. The UI is designed to be used in kiosk mode operation of the Raspberry Pi 4B touchscreen, ensuring ease of use and reliability.

When launched, the touchscreen application initializes in kiosk mode and presents the **Home screen**, displaying the system status and key control buttons. From this screen, the user may begin a new job, open configuration settings, or access the live camera view. Selecting **Job Setup** transitions the interface to the **Setup Screen**, where the user can cancel or specify laser parameters such as power percentage and feed rate.

Once a configuration is confirmed by the user, the parameters are used to generate G-code instructions, which are transmitted to the ESP32-based GRBL controller through the communication handler. The controller executes these commands in real time, handling motion control and laser operation internally. During operation, the **Status** screen displays live feedback such as estimated job progress, completion time, and system status. This allows the user to monitor the progress and make adjustments if necessary. If an abnormal condition occurs, such as an interlock trigger or system fault, the application immediately halts the job, displays a warning, and disables power to the laser and motion system until safe operation is restored.

Through this design, the UI serves as the bridge between the user and the control system , enabling safe, flexible, and efficient interaction with the laser cutter. It provides control over system behavior ensuring that every operation of the F.L.C.S is executed under monitored and verified conditions.

7.3.1.1 User Application Flowchart (Nick)

This section contains several flowcharts outlining the main functionalities of the UI. Each diagram illustrates how the system responds to specific user inputs, the sequence of operations that occur within the application, and the expected outcomes at each stage.

The figure below demonstrates the software logic for initiating a laser cutting job through the UI. The user begins by launching the main application and selecting the **capture image** button. From there, the user can either choose to cancel the job and go back to the main menu screen, or adjust parameters such as marker type, then go to **job setup** to change number of passes and preset laser settings. Once all parameters are configured and safety checks pass, the user selects **Start Job** to begin the cutting process. Any missing configuration or safety interlock faults trigger an error prompt on the screen until the issue is resolved.

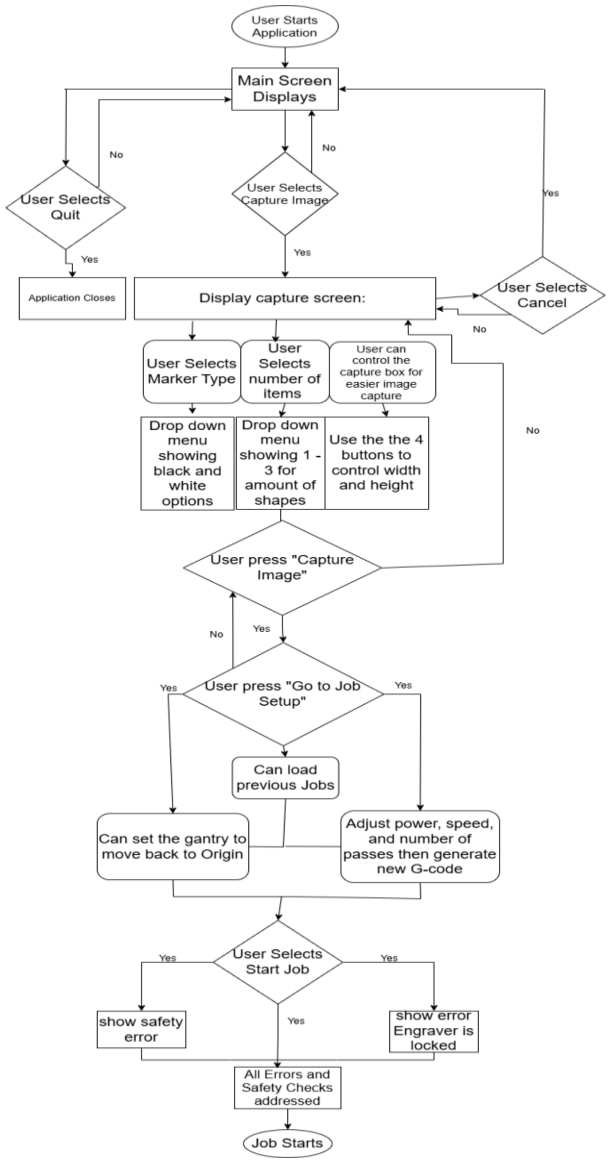

Figure 33: Initiate Job Flowchart

The figure below illustrates the automated marker detection section of the touchscreen interface. When the user selects **Capture Image or Settings,** the application initiates a live video preview from the onboard camera. The system then performs automatic marker detection to identify the alignment trace withing the capture image page. If the marker is not detected or appears unclear, the user may adjust focus or lighting conditions to improve visibility before the detection routine repeats. Once the marker is successfully detected, an overlay is aligned to its position, allowing precise registration between the camera feed and the marker trace.

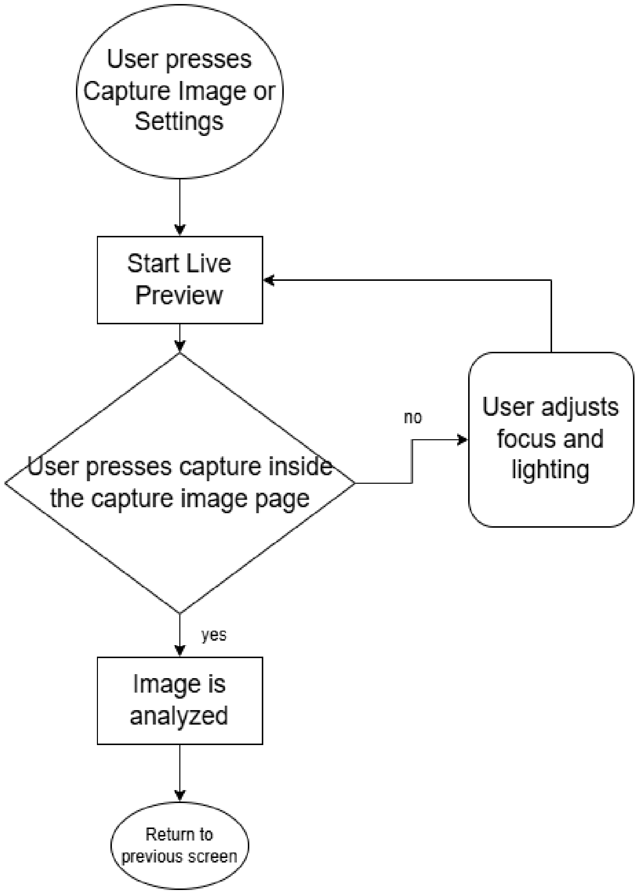

Figure 34: Camera and Alignment Flowchart

The figure below shows the logic implemented for job monitoring and safety management. When the user performs an action such as **Start, pause, Resume,** or **Cancel,** the Raspberry Pi 4B sends the corresponding command to the microcontroller, which controls laser gating and motion timing. During active operation, the system displays live feedback including progress, estimated time to completion, temperature, and error information. A continuous completion check ensures that once the job finishes, the system logs results and returns to the main menu.

In parallel, the software monitors all safety interlocks. Any detected fault triggers an **Abort** command to the microcontroller, disabling the laser and halting all activity. This structure ensures deterministic safety behavior and prevents dangerous accidents during unattended operation.

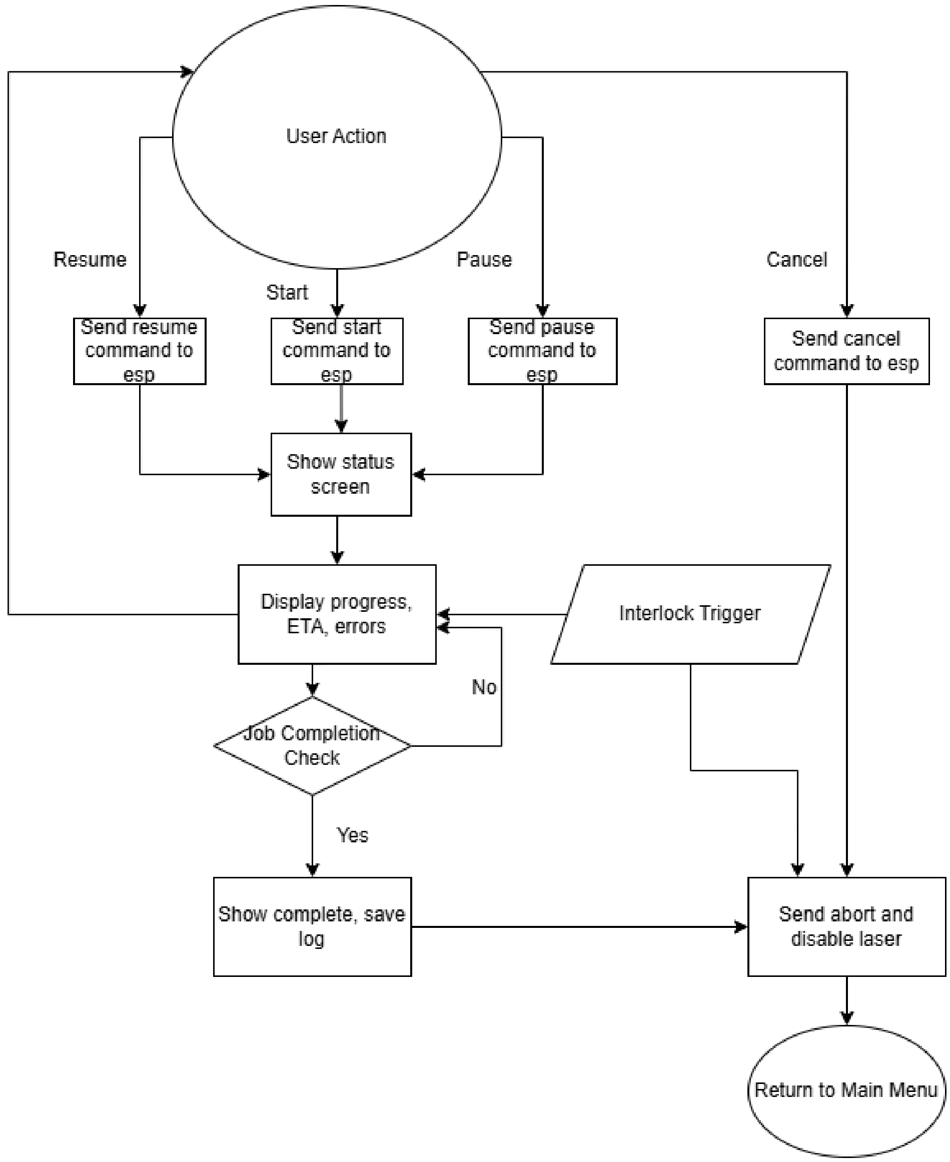

Figure 35: Job Monitoring Flowchart

The following flowchart illustrates the shutdown routine for the touchscreen interface. When the user presses the shutdown button, the system first requests confirmation in order to avoid unintended exits. If confirmed, the software performs a check to see if any cutting job is currently active. If a job is running, an abort command is sent to disable the laser and motors, then save operational logs before completely powering down.

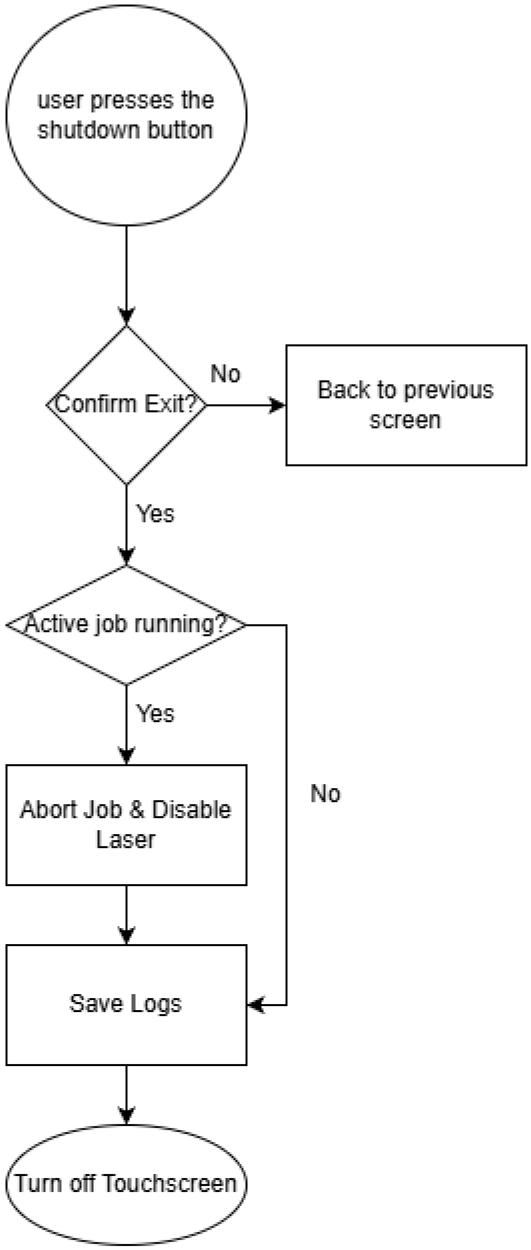

Figure 36: Shutdown Flowchart

7.3.2 Communication between the Pi 4B and the motion controller (Nick)

Reliable communication between the Raspberry Pi 4B and the motion control system is essential for coordinating real-time control of the laser, motors, user interface, and safety subsystems. The Pi 4B will act as the supervisory controller and mostly run the user interface, image processing, and G-code generation. The ESP32-based board will operate as a deterministic embedded microcontroller where it will oversee the execution of tasks such as PWM laser gating, laser control, and motion timing.

Communication between the two devices is performed via serial USB. These characteristics make it suitable for safety-critical operations that must occur without jitter. The Pi 4B transmits instructions such as start job, pause job, resume, abort, and motor step instructions. The microcontroller responds with "ok" and other status messages in order for the UI to be updated.

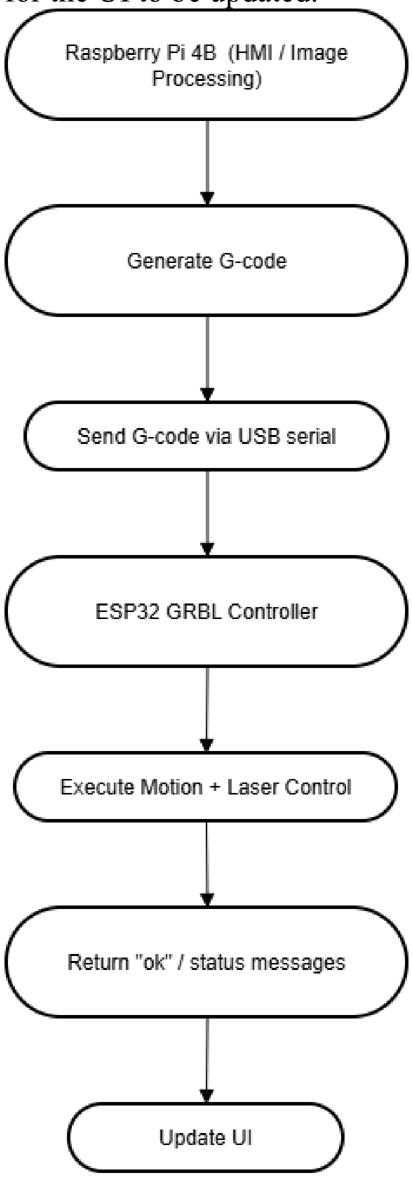

Figure 37: High-level UART communication between the Raspberry Pi 4B and the GRBL microcontroller

7.3.3 HMI Architecture Overview (Nick)

The touchscreen interface is structured as a multi-page application running on the Raspberry Pi 4B in kiosk mode. Rather than operating as a single script containing all functions, the HMI is divided into "pages" that directly correspond to the operational flowcharts presented earlier in this chapter. This improves reliability, simplifies the testing process, and ensures that each functional block (job setup, capture image, job monitoring, shutdown, etc…) can be validated independently.

The core UI pages include:

- **Home Page:** Displays the overall system state, current job status, and top-level user actions such as “Job Setup”, “Capture Image”, and “Settings”.
- **Job Setup Page:** Allows selection of cutting parameters. User inputs are passed as configuration packets to the ESP board
- **Capture Image Page:** Provides real time imaging, marker detection, and visual overlays to ensure material alignment before a job starts.
- **Job Monitoring Page:** provides live data including progress, estimated time to completion, and any active interlocks or warnings.
- **Settings Page:** Also has a live camera view and the user can manually move the gantry, set the origin, change between light and dark mode and turn the laser on or off
- **Shutdown Page:** implements the safe shutdown process defined in the shutdown flowchart. The HMI checks for active machining, issues an Abort if necessary, then powers down the system.

All pages communicate with two backend controllers:

- **Communication Controller:** Manages USB serial communication between the Raspberry Pi 4B and the ESP32-based GRBL controller. It is responsible for streaming G-code commands, handling acknowledgements such as “ok” responses, and managing job control actions such as start, pause, resume, and cancel.
- **Camera Controller:** Handles image acquisition, processing, marker detection, and alignment overlays.

7.3.4 Software Components (Nick)

Table 22: Software Components Descriptions Table

Component	Description
UI Handler	Displays all screens and manages button interactions. Will also provide job and error states.
Configuration Handler	Collect job parameters from the user such as marker color, laser power, and feed rate.
Camera Preview Module	Streams live video from the onboard camera. Supports alignment overlays.
Communication Handler	Manages USB serial communication between the Raspberry Pi 4B and the ESP32-based GRBL controller. Handles G-code streaming, command acknowledgement, and error detection
Job Execution Controller	Oversees job lifecycle including start, pause, resume, and cancel. Coordinates G-code transmission and ensures proper sequencing of commands.
Status Handler	Processes incoming messages from the GRBL controller such as acknowledgments, errors, and job progress. Updates UI in real time

Safety Interlock Module	Monitors system conditions. Automatically halts the job when a fault is detected.
Logging & Diagnostics Module	Records job parameters, including G-code and image

7.3.5 Kiosk Mode Operation (Nick)

To ensure the HMI behaves as a dedicated appliance rather than a general-purpose computer, the Raspberry Pi 4B is configured to run in kiosk mode. In this configuration, the operating system boots directly into the touchscreen HMI without exposing the standard desktop computer environment that allows the user to do anything.

On startup, the Raspberry Pi 4B automatically launches the Fabric Laser Cutter System (F.L.C.S) HMI entry point (main.py) in full-screen mode. This script creates the multi-page interface described in section 7.3.3, including the Home, Job Setup, Capture Image, Job Monitoring, Settings, and Shutdown pages. The user never sees the Linux desktop but will instead have an interactable touchscreen that behaves as a dedicated control panel whose only visible elements are those defined by the HMI.

Kiosk mode is implemented using an AutoStart mechanism that invokes the HMI as soon as the visual interface becomes available, which guarantees that after any power cycle, the system returns to a known state with the HMI ready for operator interaction. The underlying operating system will remain accessible to developers or anyone who knows how to access it for maintenance and debugging; however, these access paths are not directly exposed through the normal user's workflow.

Because the Raspberry Pi does not include a physical power button, system shutdown is handled entirely in software or terminating the power supply. The Shutdown page of the HMI follows the sequence defined in the shutdown flowchart in Section 7.3.1.1. It first checks whether an active cutting job is in progress, issues an Abort command to the GRBL controller, if necessary, logs the job status, and then finally shuts the system down. Afterwards, the user can safely halt power to the touchscreen using an added external switch or button, and re-applying power causes the Raspberry Pi to reboot and re-enter kiosk mode. This ensures a consistent and predictable user experience.

Chapter 8: Optoelectronics Feasibility Study

8.1 Laser Diode (Jacqui)

Our laser diode requires an operating voltage of 4.4-5.2 volts and a typical operating current of 2.1 amps. Our laser diode driver will ensure that the maximum operating current of 3 amps is not reached, as that would burn out our laser diode. We will be using a copper heat sink to ensure the laser diode does not exceed temperature threshold limits. If our copper heat sink proves to be too difficult with our laser diode, we will use the copper heat sink for the rest of the system and then utilize a laser diode heat sink that is designed specifically for our TO-5 style laser diode.

8.2 Image Acquisition System and Focusing Lens

Our camera will be just under a foot and a half over the canvas to ensure the entire area is captured in the camera frame. This leaves sufficient space above the camera height for other essential components since the enclosure is approximately two feet tall. With the camera module 3 connected to the Raspberry Pi 4B with 4Gb of RAM, it would process and recognize the traces drawn using Python or C++ programs.
Since the fabrics may potentially not be completely smooth, a longer focal length is favorable so that the lens has no chance of bumping into the fabric and potentially scratching the lens.

Chapter 9: Integration and Testing Plan

9.1 Integration (Jacqui)

The main goal of this project is to successfully integrate our subsystems so they may operate smoothly to carry out their functions. Once the power is on the touchscreen will prompt the user to choose the cut settings. These settings will include choosing whether the camera should detect white or black marker lines, which fabric type the user is cutting, and if they want a specific available laser power and motor speeds. When the camera and touchscreen have communicated that the image processing is done, the laser power system can be turned on and the job can begin.

We will be utilizing a photodiode system to measure reflectance returning to the system while it is cutting the fabric. The image acquisition system will collect data regarding the location of the fabric to be cut, and this information will be communicated to the mirror system to direct the beam. The power system will supply power to our components, including the laser system which will be dormant until the touchscreen communicates to start a cut. Regarding temperature regulation for the whole system, we will utilize a set of fans and a copper heat sink with a heat tube that utilizes a sponge and water system to dissipate heat. In addition to this we may use a thermal coupler with a copper head to create our own temperature gauge.

Integration is a concern due to the lack of communication throughout senior design one. Communication to the project lead is very important, especially if you happen to have any gaps in understanding during the project, it is best to mention your concerns early. When group members do not communicate their questions or concerns it can lead to a delay in project completion due to not understanding the group project until November when the majority of research is supposed to already be done. There has been consistent communication from the project lead throughout the semester which has been met with minimal communication from group members. This occurs even after the project lead asks for more communication and consideration since this is a project where the subsystems can depend on each other.

9.2 Testing (Jacqui)

The main goal of this project is to successfully integrate our subsystems so they may operate smoothly to carry out their functions. We will be utilizing a photodiode system to measure reflectance returning to the lens system while it is cutting the fabric. The image acquisition system will collect data regarding the location of the fabric to be cut, and this information will be communicated to the mirror system to direct the beam. The power system will supply power to our components, including the laser system which will be dormant until the touchscreen communicates to start a cut. Regarding temperature regulation for the whole system, the original idea was to have an aluminum heat sink which may be used for initial testing. However we were gifted a set of fans, a copper heat sink with a heat tube that utilizes a sponge and water system to dissipate heat, as well as a thermal coupler with a copper head that we can use to create our own temperature gauge.

9.2.1 Considerations for Optical Components (Jacqui)

During our first in person meeting that focused on the demo, we were planning on using a laser diode driver from CREOL's undergraduate lab to test our diode since we do not have the designed driver ready. Since our laser diode only has two pins we could not use the laser diode drivers that the undergraduate lab provides. To use those specific drivers, the Thorlabs TCLDM9, we would have needed to short two pins by soldering them together inside the housing of the driver. This was clearly not an option when using borrowed equipment, and we instead must pivot. Another senior design group had an extra laser diode driver at the time, and we thought this may be used to power our diode, however upon further examination that laser diode driver was not an option.

We originally planned on buying a laser diode driver and within the month of November our EE decided he could make one, however we pivoted as the design Tony had in mind was not compatible with our laser diode. We have purchased our laser diode driver and are waiting for it to arrive to take the miniature demo video. The figure below shows the optical system designed by Jacqui Harper being tested. This was shown in both the optical demo as well as the miniature demo video. We were able to get a focused point that expands slowly as the distance increases. When using the laser diode we purchased we will be able to use this beam to cut fabric with the addition of Mike's system.

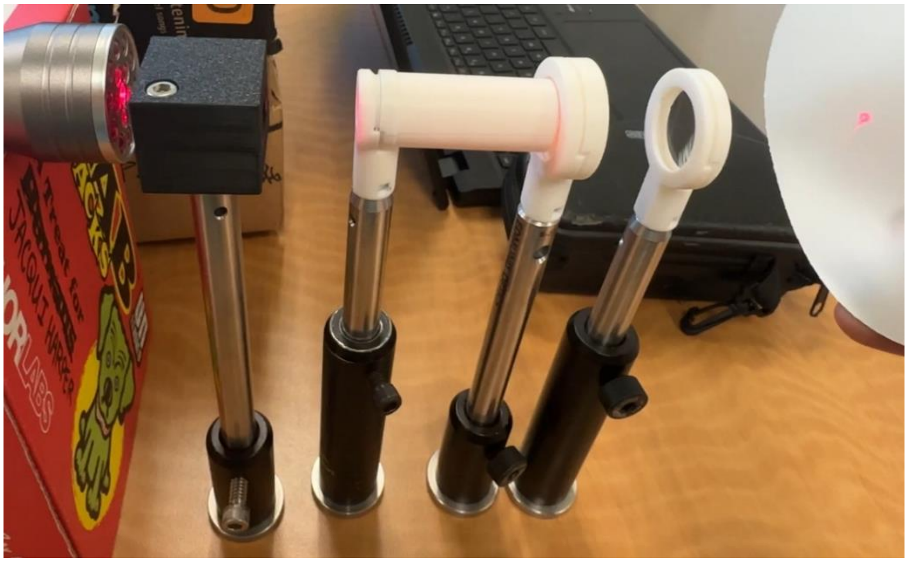

Figure 38: SD1 Optical System Testing (Jacqui)

9.2.2 Optical Testing (Jacqui)

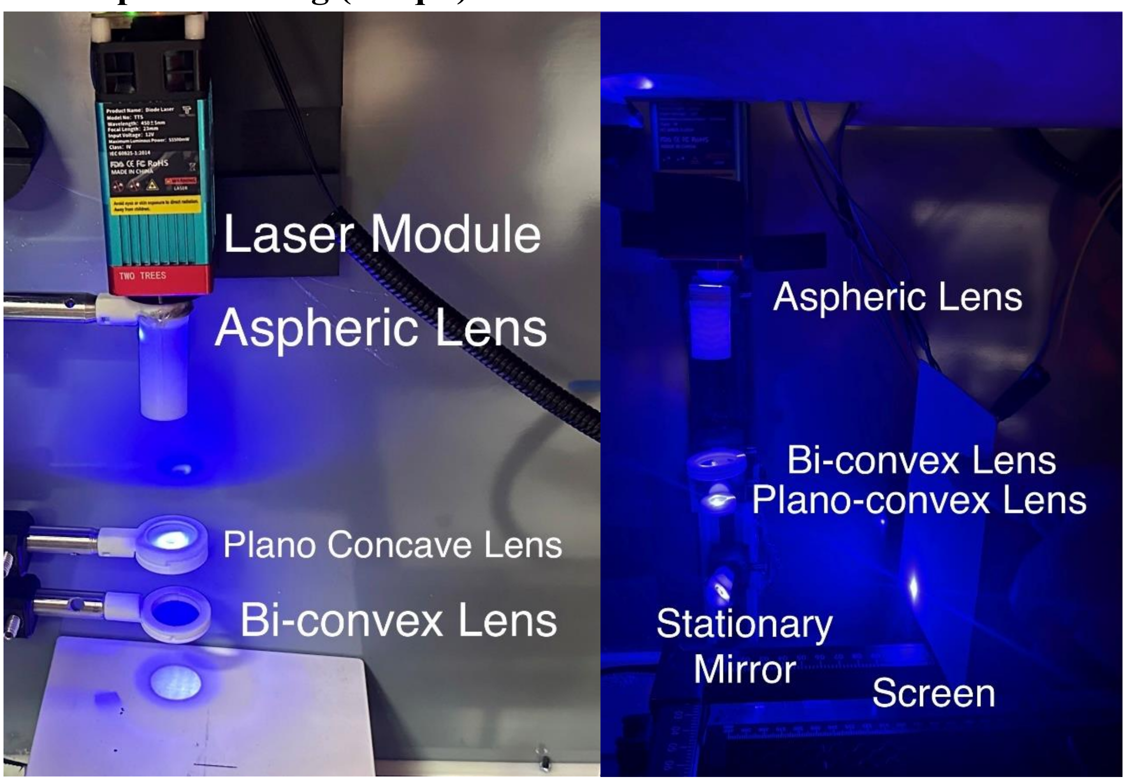

Figure 39: Initial Optical Setup (Left), and Final Optical Setup (Right)

When testing our optical system we discovered that the laser module included with the engraver system has a diverging laser. This diverging laser meant our beam that was assumed to be collimated is actually getting bigger as the distance from the laser increases. We initially enlarged this beam as planned, shown in Figure 38 on the left, resulting in large amounts of stray laser light in our enclosure and a large spot corresponding to large amounts of power loss. To minimize this and ensure the beam would safely be delivered to the mirrors, shown in Figure 39. With the setup shown on the right, we minimize the beam size by switching the placement of the bi-convex and plano lens. In this image we can see the laser beam on the screen, which appears larger than it is. This is due to the reflection off the white screen. In short, the optical system needed to be adjusted to accommodate unforeseen issues with the laser module.

Many iterations of the lens mount system had to be created to find something that would have enough support and precision to work for laser alignment. Additionally, we experienced too much heat on the initial lens mount when running the first few tests. This resulted in melting of the 3D printed lens mount. We mediated this by using heat resistant PLA to create a lens mount that could stand the heat. We also added a supplemental battery operated fan into the enclosure to help with cooling.

When testing the mirror guidance and focusing system, various iterations of the mounts had to be created due to the optics being incredibly sensitive to movement, vibrations, and deviations. The slightest change in angle in the mirrors could be the difference in the gantry cutting fabric and not making a mark on the fabric at all. The mirrors and lenses were all made to be adjustable so that the user could align the mirrors perfectly and then tighten them into place using screws.

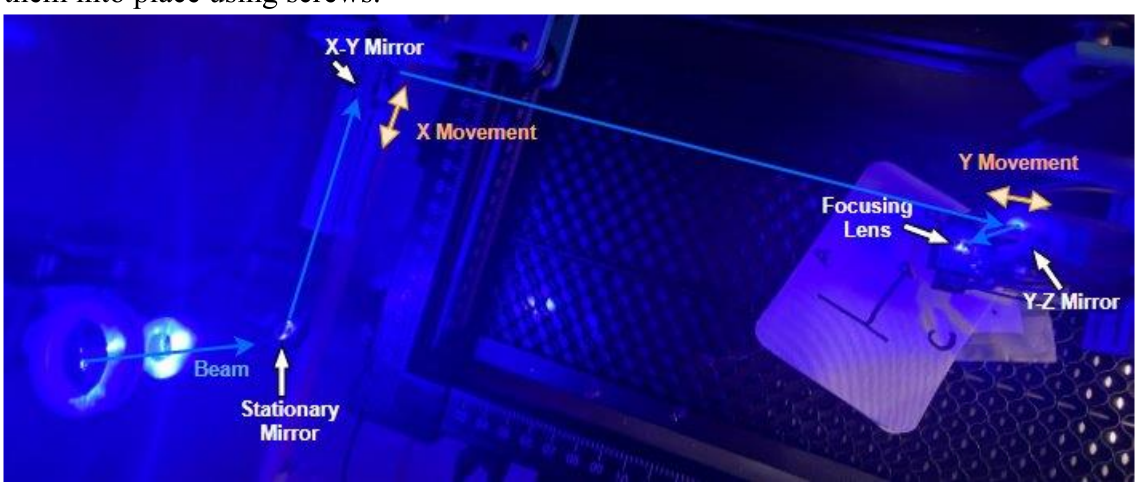

Figure 40 Top-down view of the final gantry with the laser on at low power.

9.3 HMI Hardware Testing (Nick)

9.3.1 Touchscreen Electrical and Video Connection (Nick)

The Raspberry Pi Touch Display 2 was connected to the Raspberry Pi 4B using the MIPI-DSI ribbon cable that came with the latter and powered using the 5 V and GND pins on the Pi's 40-pin header. The following tests were conducted

- T1: Power-on and Display Output
    - After the initial boot, the Raspberry Pi OS desktop rendered correctly on the Touch Display 2 without flickering or any artifacts. This confirmed proper DSI communication and power delivery
- T2: Touch Input Validation
    - Touch functionality was verified by opening the system menu, typing on the onscreen keyboard, and interacting with a few built-in apps such as the file manager. All regions of the screen responded accurately, confirming that the touch controller was functional
- T3: Orientation and Scaling
    - The display was tested in both portrait and landscape orientations. This was done easily through the onboard settings that allow us to switch orientation and quality. Touch mapping remained correct after rotation, confirming that display rotation and touch calibration were properly synchronized

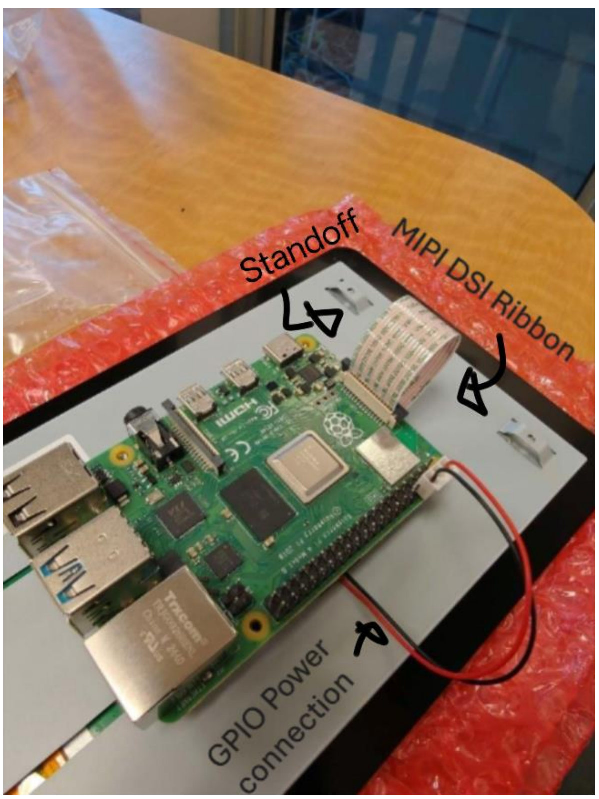

Figure 41: Touch Display 2 to Raspberry Pi 4B Connection

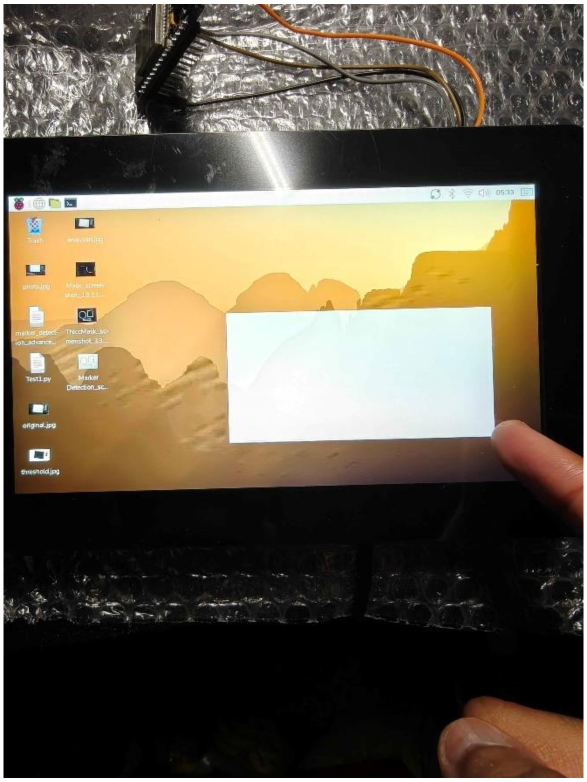

Figure 42: Touchscreen in Landscape mode with touch input

9.3.2 Raspberry Pi power and Touchscreen Mounting

The Raspberry Pi 4B itself is powered the 12V power brick of the Twotrees engraver. The 12V is split by a splitter where one end goes to the engraver and the other is connected to a power supply adapter. The adapter is then connected to a step down 12V to 5V buck via a double wire wago nut. To secure the touchscreen, brackets with counterbored 2.5mm holes were created and secured over the standoff holes on the back of the touchscreen. After mounting the touchscreen, we did various shaking tests to ensure that it would not fall out during use. We also made sure there were no noticeable problems such as touchscreen flickers and laser power loss due to the split power.

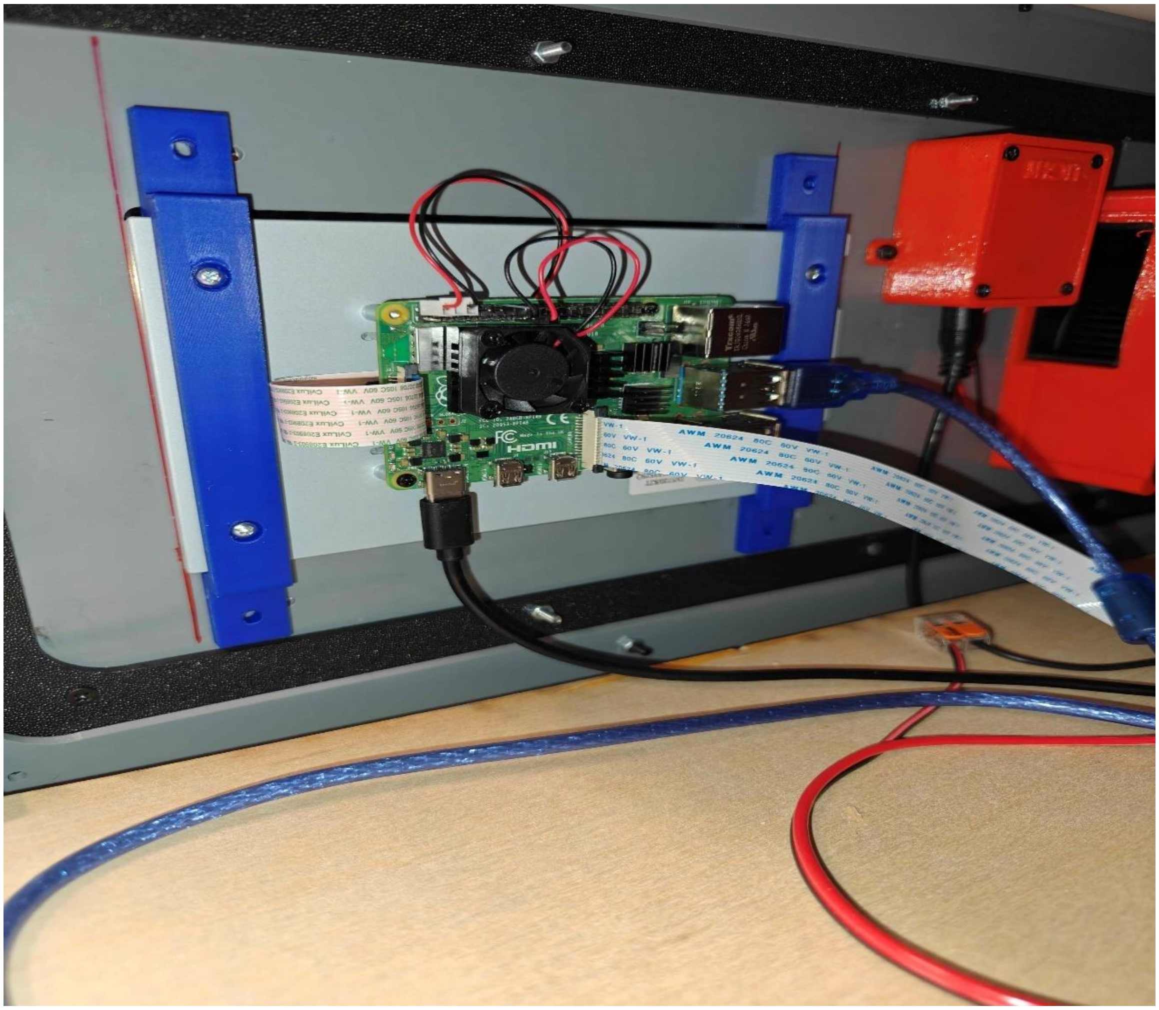

Figure 43: Mounted Touchscreen

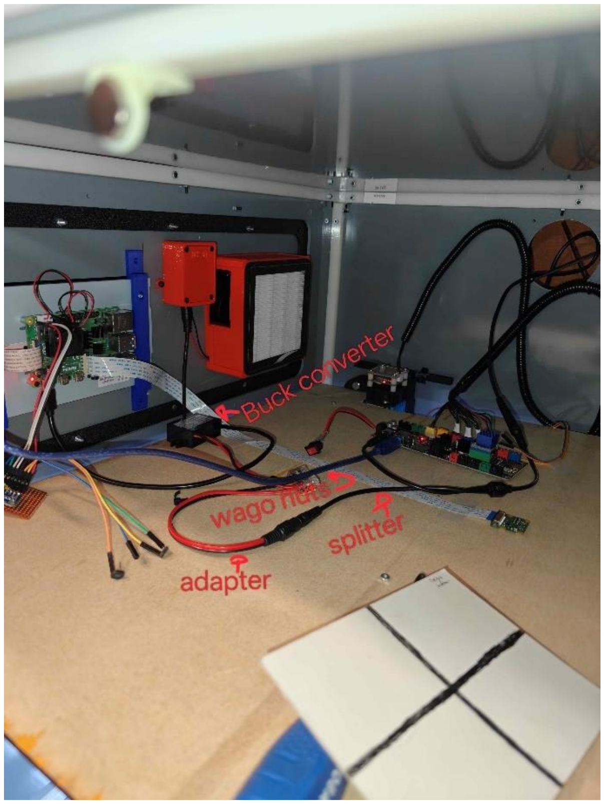

Figure 44: Raspberry Pi 4B Power

9.4 Main UI and Software Functionality (Nick)

This section documents the initial testing of the HMI software that runs on the Touch Display 2. The current prototype is a python-based full screen application that also includes an on-screen shutdown button intended for operator use at the end of a job. Currently, the shutdown button allows for the immediate shutdown of the Raspberry Pi without a console command or cutting the power supply. The goal of this test phase was to verify that the UI launches reliably, responds correctly to touch input, and triggers a clean system shutdown when requested by the user.

9.4.1 Test Objectives (Nick)

The following objectives were defined for this stage of UI testing

- **Application Startup:** Confirm that the HMI application launches successfully from the Raspberry Pi desktop and occupies the entire touchscreen area
- **Page Navigation & Touch Responsiveness:** Ensure all four UI pages (Home, Job Setup, Camera Alignment, Status) load correctly and respond reliably to touch
- **Camera Capture & Marker Analysis:** Confirm that pressing "Camera Alignment" triggers camera_analysis.py, performs image capture, applies thresholding, and attempts to detect alignment markers
- **Image Display Behavior:** Verify that the captured/processed image displays on the touchscreen and test the "Back" button functionality

- **Shutdown Button Operation:** Confirm that pressing the Shutdown button calls the underlying shutdown command and powers the Raspberry Pi off cleanly, without errors or hangs
- **Remote development compatibility:** Ensure that the UI can be edited and relaunched over VNC from a laptop while still being usable directly on the touchscreen

9.4.2 Test Setup (Nick)

- Hardware
    - Raspberry Pi 4B running Raspberry Pi OS
    - Raspberry Pi Touch Display 2 connected over MIPI-DSI and powered from 5 V and GND pins on the 40-pin header
    - USB power supply
    - Raspberry Pi Camera Module connected via CSI ribbon cable
- Software
    - Python 3 HMI prototype (main.py)
    - Camera_analysis.py for image capture and marker thresholding
    - Tkinter-based UI pages
    - Fullscreen mode enabled for HMI testing

9.4.3 Testing & Results (Nick)

T1 – Application Launch

- The HMI launched correctly from the desktop.
- The UI filled the entire Touch Display 2 area.
- Touch input functioned across the whole display

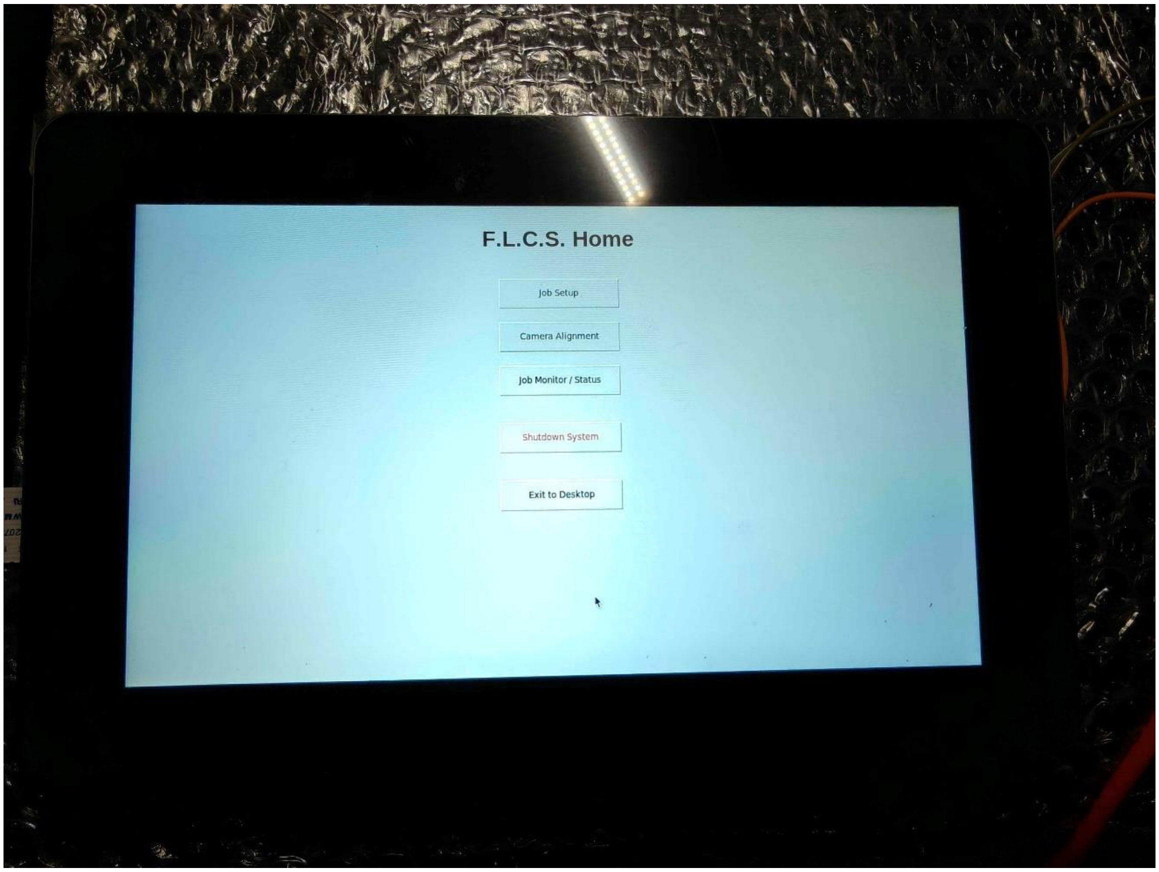

Figure 45: User Interface Test

T2 – Page Navigation

- All four pages are loaded correctly via touchscreen input.
- Buttons responded immediately to taps, registering with no noticeable latency.
- Page transitions behaved as expected.

T3 – Camera Alignment Execution

- Selecting Camera Alignment successfully ran camera_analysis.py.
- The Raspberry Pi Camera captured an image.
- Thresholding and marker-detection code executed.
- An image with processed markings (highlighted regions) displayed on the screen
- This confirmed proper integration between the UI and the camera-analysis backend.

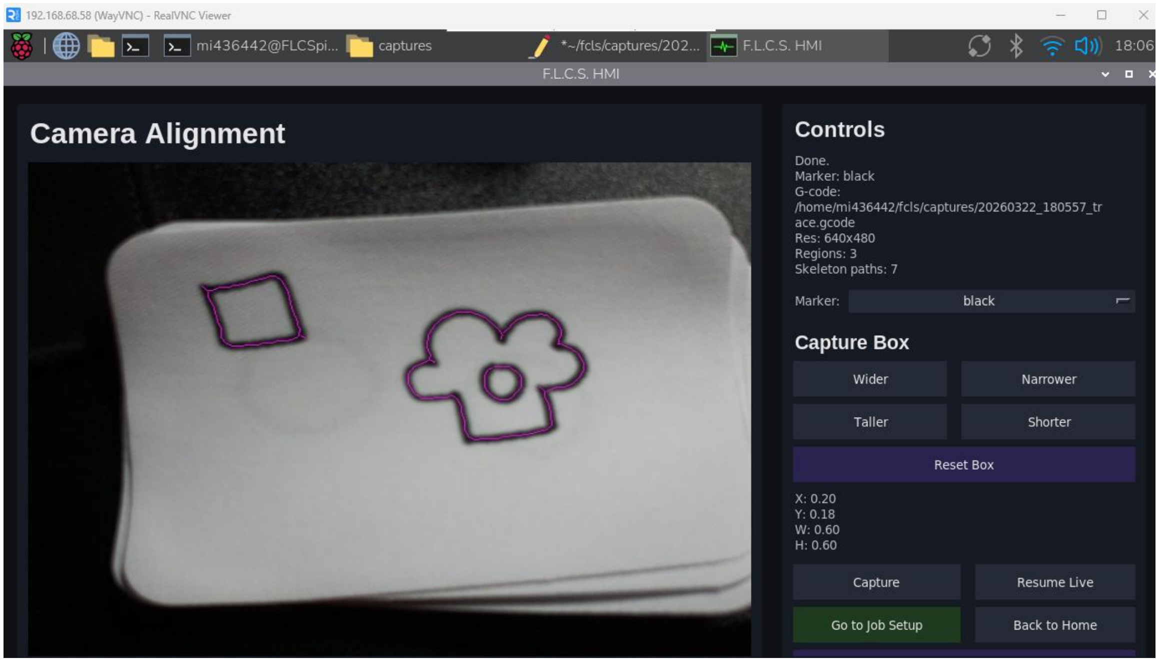

Figure 46: Image Capture and Analysis

T4 – Shutdown Button Validation

- Pressing the Shutdown button executed the underlying system shutdown command.
- The Raspberry Pi powered down cleanly with no file-system errors upon reboot
    - A reboot is achieved by unplugging the device and plugging it back in after using the Shutdown button directly from the UI.
- This demonstrated successful linkage between UI events and system-level commands.

T5 – Remote Development Testing

- The UI was tested both locally (touchscreen) and remotely (over VNC).
- Both controlled paths successfully launched and interacted with the interface.
- Remote development did not disrupt touchscreen responsiveness.

9.4.4 Summary of UI Test Results (Nick)

The initial HMI software prototype successfully demonstrated:

- Reliable startup
- Correct touchscreen interactions
- Working multi-page navigation
- Functional camera capture and marker analysis
- A proper system-shutdown workflow
- Stable operation during both local and remote development

These results confirm that the HMI subsystem is operational and provides a solid base for integrating additional project functionalities such as job control, safety interlocks, and motor/laser coordination.

9.4.5 Path Generation From Captured Image (Nick)

We conducted extensive path generation testing to ensure that the captured image could be accurately translated into G-code for precise gantry movement. During this process, several challenges were encountered. One major issue was that the camera height was too low to capture the full 300x300mm workspace, resulting in incomplete and improperly scaled paths. This was addressed by redefining the effective capture area to match the true field of view. In addition, we experienced inconsistencies in trace positioning. This was due to discrepancies in the machine's coordinate system and the generated pathing. To resolve this, we implemented a user-defined origin feature, allowing the user to set the origin at the bottom left corner of the camera view. This ensured proper alignment between the capture area and the machine workspace. We also observed cases where generated paths appeared flipped or rotated due to mismatches in axis orientation between the camera and the gantry, This was corrected through axis remapping and orientation adjustments in software. These combined improvements resulted in a stable and repeatable pipeline, where generated G-code consistently aligns with the intended geometry and produces accurate cuts on the physical workspace.

9.5 Raspberry Pi-ESP32 Communication Testing (Nick)

It was decided to test basic communication protocols using the ESP32 DEVKITV1. This section documents the initial communication tests between the Raspberry Pi-4B and the ESP32 microcontroller. The goal of this phase was to confirm that a reliable serial link exists so that higher-level subsystems (such as motion/laser control) can exchange data in later stages.

9.5.1 Test Objective (Nick)

- Verify that the Raspberry Pi 4B can open a serial connection to the ESP32
- Confirm that bytes sent from the Pi are received by the ESP32 and echoed back correctly
- Capture and inspect the returned data to ensure formatting is as expected

9.5.2 Test Setup (Nick)

- Hardware
    - Raspberry Pi 4B running Raspberry Pi OS
    - ESP32 dev board, powered via USB
    - UART data connection over GPIO pins
        - Pi TXD0 (GPIO14) → ESP32 RX pin
        - Pi RXD0 (GPIO15) → ESP32 TX pin
        - Common GND between Pi and ESP32
- Software
    - uart_test.py: single byte test
    - uart_test2.py: string test
    - Esp32sketchecho: flashed to the Esp32 via Arduino IDE

9.5.3 Testing (Nick)

- T1 (uart_test.py): Confirm that the Pi can send a single test byte and that the ESP32 receives and echoes it back repeatedly

- Resulted in the message “Received: b'Echo: A\r\n'” printed on the terminal until the code was manually stopped
- This showed that the Pi successfully received and printed each echoed line as a Python bytes object

- T2 (uart_test2.py): Verify that longer messages (a full ASCII string) can be transmitted over UART and that each character is echoed back individually by the ESP32
    - Resulted in the full string being echoed with each having their own line in the form of “b'Echo: x\r\n'” until a final trailing blank line “b'\r\n'”
    - This was a success as the results showed all characters (H, E, L, L, O, 1, 2, 3, and the newline) appearing in the correct order. The trailing blank line indicates that the ESP32 printed an extra newline after handling the message

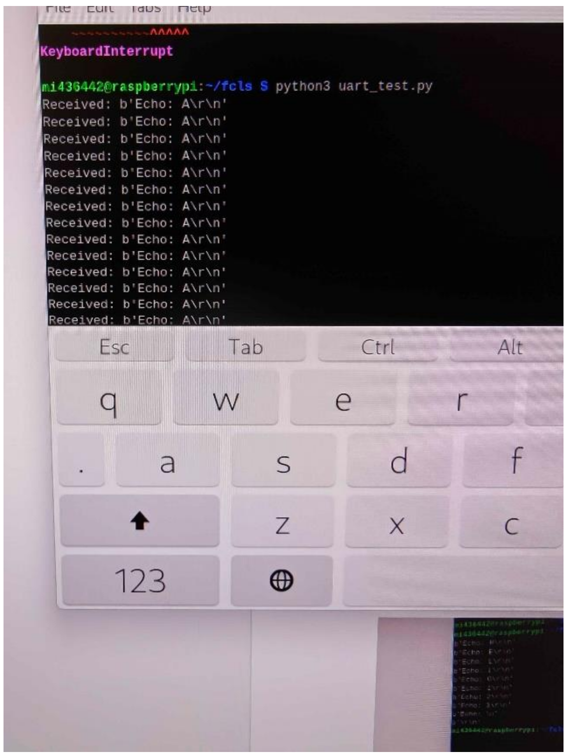

Figure 47: UART test 1 result

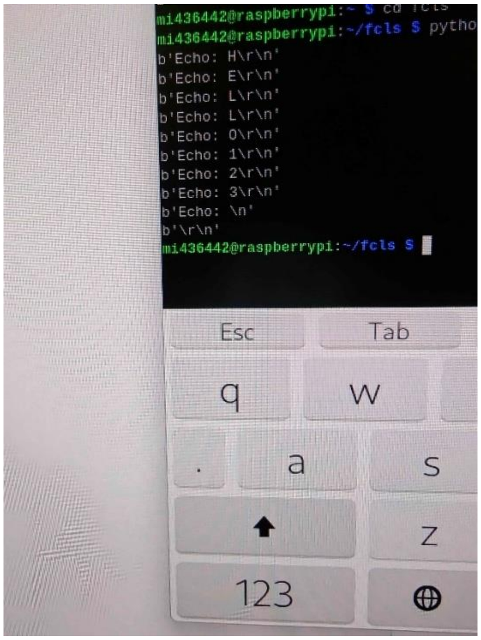

Figure 48: UART test 2 result

9.5.4 Summary of Communication Test Results (Nick)

From these two UART tests, the following were verified:

- The hardware UART connection over GPIO pins between the Raspberry Pi 4B and ESP32 is connected properly
- The Pi can transmit data over to the ESP32, where it is interpreted.
- The ESP32 can send structured responses back to the Pi, and the Pi can read and parse them reliably

These tests establish a working low-level communication channel that will be used later to:

- Send higher-level control commands from the Pi
- Receive status, data, and acknowledgements from the ESP32

9.6 Kiosk Mode/Auto-Launch Behavior Testing

This section documents the testing performed to configure the Raspberry Pi 4B to automatically launch the HMI application upon boot. Although the system is not yet running in a fully locked-down production kiosk mode, these tests validated a pseudo-kiosk mode configuration in which teh interface becomes available immediately after startup without requiring a manual launch of the application.

9.6.1 Test Objectives (Nick)

The objectives for kiosk-mode testing were:

- **Automatic Application Launch:** Ensure main.py starts immediately after graphical login, without requiring terminal commands.

- **Touchscreen Responsiveness After Auto-Lauch:** Confirm the UI remains fully interactive when started automatically.
- **Stability and Restart Behavior:** Determine whether the auto-launch process reliably recreates the application after reboot
- **Compatibility With Development Workflow:** Ensure that kiosk-style auto-launch does not interfere with remote development (VNC)

9.6.2 Test Setup (Nick)

- Hardware
  - Raspberry Pi 4B running Raspberry Pi OS
  - Raspberry Pi Touch Display 2 (MIPI-DSI)
  - USB power supply
  - Laptop ready to run VNC
- Software
  - Python 3 HMI application (main.py)
  - Autostart folder
    - /.config/autostart
  - Desktop entry for the HMI
    - /.config/autostart/flcs.desktop

9.6.3 Testing and Results (Nick)

T1 – Auto-Launch on Boot

- After creating the autostart folder and the desktop entry, the HMI successfully launched upon boot.
  - Timing consistently hovers around 8s for main.py to appear on the touchscreen upon desktop boot. This is within reason in compliance with the specification table 2.
- The full screen UI appeared without requiring a terminal or desktop interaction
- This confirmed that the Pi executed main.py automatically during session initialization.

T2 – Behavior Upon Reboot

- Upon reboot, the application launched correctly and remained fully touch responsive.
- Navigation between pages (Home, Job-setup, Camera Alignment, Status) worked as expected.
- The exit application button remains operational.

T3 – Camera Alignment in Auto-launch Mode

- The Camera Alignment Page correctly triggered camera_analysis.py.
- Image capture and thresholding produced the same results as in manual launch testing.

T4 – Shutdown Behavior Under Auto-Launch

- Pressing the Shutdown button from the auto-launched UI initiated a clean Raspberry Pi shutdown.
- No filesystem warnings appeared upon reboot, confirming proper termination.

T5 - Stability Across Multiple Reboots

- The system was rebooted multiple times.
- The UI launched reliably after every reboot with no crashes.
- This confirmed that the auto-start mechanism is stable for ongoing development.

T6 – Remote Development Compatibility

- The auto-launch configuration did not interfere with VNC testing.
- VNC remains fully accessible, only requiring a re-connection.

9.6.4 Summary of Kiosk-Mode Findings (Nick)

Although not a full production kiosk environment, the pseudo-kiosk configuration successfully achieved:

- Automatic HMI availability
- Full touchscreen interaction
- Reliable behavior across reboots
- Compatibility with camera and shutdown subsystems
- Support for ongoing development via VNC

This provides a strong foundation for implementing a complete kiosk mode later, which would include restrictions on desktop access, cursor hiding, and prevention of exiting the HMI.

9.7 Beam Guiding System (Mike)

This section demonstrates the testing of the prototype manual gantry beam guiding system. The goal of this test is to demonstrate the beam being guided by the mirrors onto a specific point on fabric. This demonstration also shows the photodiode responding to the back-reflections off the fabric.

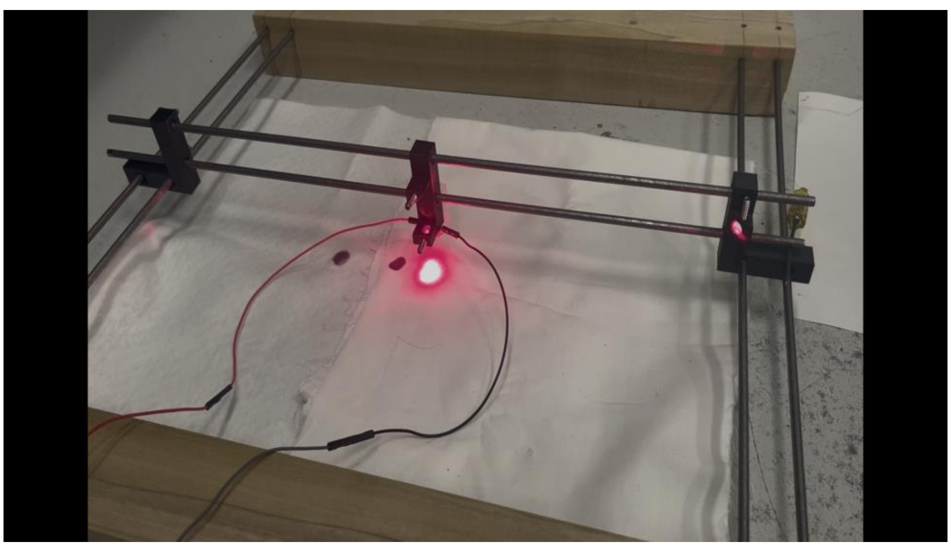

Figure 49:Mirrors guiding beam onto specific spot on the fabric. Fabrics not placed at focal length for demonstration purposes.

In the figure above, the beam, in this case a 650nm laser, is guided directly onto fabric. On the right is cotton and on the left is felt. When the carriage or the y-rail is moved, the beam is redirected to a different point on the fabric. The two cables are connected to a photodiode on the bottom of the carriage which are both directly connected to an Elegoo Uno. The negative end is connected to ground, and the positive is connected to the A0 pin, which reads the current generated by the photodiode. The Elegoo then can show a live display of the voltage through the serial monitor on the Arduino IDE.

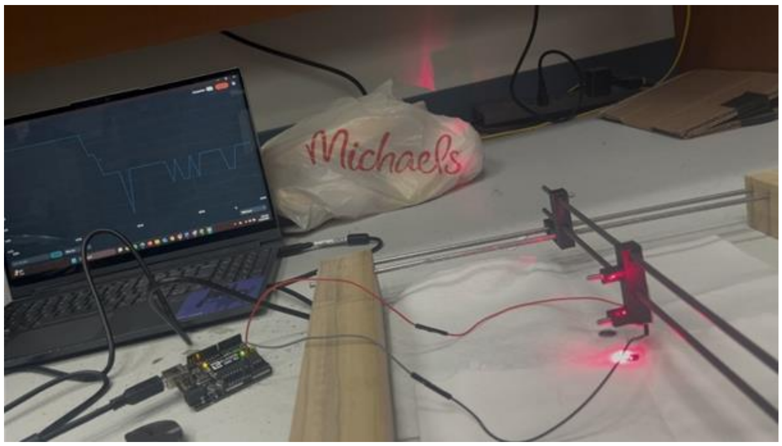

Figure 50: The carriage was just moved onto a black spot on cotton fabric. Photodiode readings on the graph on the left show significantly reduced back-reflections.

Chapter 10: Administrative Content

10.1 Work Distribution

Table 23: Work Distribution Table

Computer Engineering	
Nolphky Nicolas	***Responsible for:*** Touchscreen subsystem Controller and sub-controller Implement serial communication HMI Interface
Electrical Engineering	
Anthony Martinez-Garcia	***Responsible for:*** PCB design Motor research and selection Motor driver research and selection Laser diode driver research and selection Design power supply unit
Photonic Science and Engineering	
Jacqueline Harper	***Responsible for:*** Facilitating group meetings and encouraging time management Group document formatting

	Project motivation and background Laser diode system with beam expansion lenses and prism pair Integration of LD system into housing Housing selection Laser Diode System Feasibility Study
Mike Rodriguez	***Responsible for:*** Mirrors for guiding beam Final focus lens onto the fabric Image acquisition and gantry path generation Photodiodes for scattered beam light detection

10.2 Budget and Financing

This project is not sponsored and is funded by the students who complete each subsystem. The budget sets a target to keep costs below a certain price while not compromising on quality. Total cost is kept in mind to make the final product affordable to a common customer. The budget could change due to design changes or economic factors such as a tax on imported goods.

10.3 Bill of Materials

The table below shows the components that make up the bill of materials.

Table 24: Bill of Materials

Bought By	Item	Details	QTY	Price (USD)
Mike	Raspberry Pi 4/4GB	Main processor for touchscreen HMI and image processing	1	55.00
Mike	Sandisk ImageMate PRO (64GB)	Storage for Raspberry Pi	1	15.00
Nick	Raspberry Pi Touch Display 2	Main touchscreen	1	99.07
Nick	Dofiki Honeycomb Laser Bed 400 x 400	A protective layer that minimizes contact between the fabric and the enclosure during cutting	1	42.79
	Pi Bezel for 7" Pi touchscreen	Frame for the touchscreen (optional, 3d printing)	1	9.99
	Samsung PRO Endurance (256GB)	Internal storage for the touchscreen	1	29.99
	Passive Buzzer	Provides feedback for user actions and errors	1	0.95
	standoffs and screws	Standoffs, screws, etc	1	14.95

	Touchscreen Power (TBD)	Powers the touchscreen (integrated into system PSU)	TBD	TBD
J.H	Laser Diode	Burns/Cuts fabric	4	225.00
J.H	Aspheric Lens	Collimates beam into prism pair	1	104.30
J.H	Anamorphic Prism Pair	Shapes the beam	1	202.10
J.H	Plano-Concave Lens (Lens 1 of Beam Expander)	Expands beam	1	28.00
J.H	Bi-Convex Lens (Lens 2 of Beam Expander)	Nearly collimates beam	1	45.00
Mike	Dielectric Mirrors	Redirects laser beam	3	150.00
Mike	Aspheric Focusing Lens	Focuses laser beam	1	84.00
J.H	Lens/Prisms Holders and Mounts	3D Printed	4	Filament Costs
J.H	Housing/Enclosure	Holds components together in with easy to use features	1	180.00 + Shipping
Anthony	NEMA 17 Stepper Motors	Serves for movement of laser	3	27.39
Anthony	TB67S581FNG Stepper Motor Drivers	Drives the stepper motors to the necessary current	3	20.85

10.4 Project Milestones (Jacqui)

Below are two tables that outline timeframes for tasks to be completed in Senior Design 1 and Senior Design 2. The project is broken into several parts that will come together to realize a final product. Breaking the project into smaller parts allows for weekly progress to be made by a certain timeframe.

Table 25: SD 1 Project Milestones

Senior Design 1 (Fall 2025)					
Week (s)	**Milestone:**	**Assigned to:**	**Start Date:**	**End Date:**	**Progress:**
1	Form Project Idea	Everyone	8-19-25	8-25-25	DONE
2	Form Group	Everyone	8-26-25	8-28-25	DONE

2/3	Reach Out to Reviewers	J. Harper, A. Martinez-Garcia, N. Nicolas	8-29-25	9-4-25	DONE
3	Complete Divide & Conquer Initial Draft (Submit)	Everyone (M. Rodriguez)	9-2-25	9-5-25 (noon)	DONE
4	Senior Design Bootcamp	Everyone	9-9-25	9-12-25	DONE
4	Create Project Website	N. Nicolas	9-8-25	9-28-25	DONE
4	Equipment Loan (if needed)	Everyone	9-8-25	9-12-25	DONE
5	Divide & Conquer Final Revision (Submission)	Everyone (A. Martinez-Garcia)	9-8-25	9-12-25 (noon)	DONE
7	Email D&C to Reviewers (add to Website)	A. Martinez-Garcia, (N. Nicolas)	9-12-25	9-19-25	DONE
7	5 Pages Completed (total, per person, Deadline by J. Harper)	Everyone	9-30-25	10-2-25	DONE
8	Optical Demo	J. Harper, M. Rodriguez	9-27-25	10-7-25 (10AM SHARP)	DONE
8	10 Pages Completed (total, per person, Deadline by J. Harper)	Everyone	9-29-25	10-9-25	DONE
9	15 Pages Completed (total, per person, Deadline by J. Harper)	Everyone	9-29-25	10-16-25	DONE
10	20 Pages Completed (total, per person, Deadline by J. Harper)	Everyone	9-2-25	10-25-25	In Progress
11	(Submit) Midterm Report First Draft	Everyone (J. Harper)	9-2-25	10-31-25 (noon)	DONE
12	Midterm Report Meeting	Everyone	11-3-25	11-5-25	DONE
12	(Submit) Midterm Report Revision	Everyone (N. Nicolas)	11-3-25	11-7-25 (noon)	DONE
13	25 Pages Completed (total, per person, Deadline by J. Harper)	Everyone	9-29-25	11-14-25	DONE
13	Weekly Report 1(Send to Profs. Chan, Kar, and Saleem)	J. Harper	11-10-25	11-14-25	DONE

13	Final Optical Demo	J. Harper, M. Rodriguez (Everyone Present)	11-18-25	11-18-25 (10AM SHARP)	DONE
14	30 Pages Completed (total, per person, Deadline by J. Harper)	Everyone	9-29-25	11-21-25	In Progress
14	Weekly Report 2(Send to Profs. Chan, Kar, and Saleem)	J. Harper	11-17-25	11-21-25	DONE
14	Peer Reviews	Everyone	11-24-25	11-25-25	DONE
14	Upload report and video (YT Link) to website + email for Reviewer Feedback	(N. Nicolas) A. Martinez-Garcia	11-17-25	11-21-25	DONE
15	(Submit) 120-page Final Report	Everyone (A. Martinez-Garcia)	9-2-25	11-25-25 (noon)	In Progress
15	(Upload) Demo Video	Everyone (A. Martinez-Garcia)	11-17-25	11-25-25 (noon)	DONE
15	Upload Demo to Website and Email to Committee	N. Nicolas	11-17-25	11-25-25	DONE
15	Submit Evaluations	N. Nicolas	11-17-25	11-25-25	DONE

Table 26: SD 2 Project Milestones

Senior Design 2 (Spring 2026)					
Week (s)	**Milestone:**	**Assigned to:**	**Start Date:**	**End Date:**	**Progress:**
1	Purchase Components	Everyone	9-25	4-15-26	Done
TBD	Test Experimental Setup, Adjust	Everyone	1-26	4-15-26	Done
TBD	Assemble Housing	Everyone	1-26	3-26	Done
TBD	CDR Video Submission	Everyone	1-26	1-26	Done
TBD	CDR Video on Website and Sent to Committee	N. Nicolas	1-26	2-26	Done

TBD	Review Final Submission Documents with Committee	Everyone	4-26	4-21-26	In Progress
TBD	Upload all Documents to Project Website	N. Nicolas	3-26	4-28-26 (noon)	In Progress

Chapter 11: Conclusion (Jacqui)

This senior design project is a combination of effort from two photonic science and engineering students, as well as an electrical engineering student and a computer engineering student. Each contributed their expertise in their field to help bring this functional and innovative project to fruition. Due to the absence of an industrial engineer or project manager, one of our photonics students acted as the project manager. This project brought together optical design, embedded electronics and software engineering to create a machine capable of precisely cutting fabric using a 3.5-watt laser diode paired with a mirror gantry system to deliver the beam to the fabric precisely. This is done without the need for any file upload to the machine, since the fabric cuts are imaged from the lines drawn on the fabric using the image acquisition, or camera, system. Built with an intuitive user interface on the touchscreen, this project is intended to be useful in all types of applications or creative spaces.

A central accomplishment of the project is the implementation of a beam expansion and directed-optics assembly, which includes a pair of beam shaping prisms, two-lens expander, and a mirror-based gantry system for accurate beam steering. These components allow the laser to maintain a tightly focused spot, with a diameter less than .2 millimeters, across the working area, enabling consistent cutting performance across a variety of fabric types by adjusting the height of the focus lens. In addition to heat management considerations, the PSE students led the characterization and alignment of the optical path, ensuring proper divergence control, safe operation, and compatibility with the mechanical motion system. This was in addition to image-processing logic that allows users to load patterns just by drawing on the fabric. With the camera's ability to see the entirety of the 400x400 honeycomb base, this system will be able to cut pieces of fabric within over a square foot area. This broadens the range of fabric cutting applications for hobbyists and small business owners who may want to utilize F.L.C.S. The PSE students' work was critical in achieving the balance between cutting efficiency, optical stability, and system safety.

Equally important was the development of the electronic and computational subsystems. The Electrical Engineering student designed and implemented the power delivery architecture, laser driver integration, and safety interlocks that ensure stable and protected operation of the Class 4 laser source. Meanwhile, the Computer Engineering student created the control software, touchscreen interface and interactions so that a user can interact with the device intuitively. The resulting user interface prioritizes clarity and accessibility, making it suitable for both novice and experienced users.

This project can set a precedent for future laser cutting systems, with its innovative approaches. These approaches include keeping the laser stationary and using image processing to gather data to direct the laser. The fabric laser-cutting system developed in this project has the potential to benefit a wide range of users and creative environments. Small textile businesses could use a compact, relatively low-cost cutter like this to streamline custom garment production, patch creation, or small-batch manufacturing without investing in industrial CO_2 systems. Freelance makers and hobbyists would gain access to a tool that enables precise textile manipulation for cosplay, quilting, wearable art, and personalized fabric design. In prototyping environments, our system's ability to directly interpret hand-drawn lines on fabric provides rapid iteration capabilities, allowing designers to go from concept to physical pattern with minimal preparation time. Additionally, accessibility-centered creative spaces, including community workshops, arts centers, and educational labs, could adopt a system like this to make textile fabrication more inclusive by eliminating the complexity of vector-file generation or Computer Aided Design software. With its simple touchscreen interface and image-acquisition workflow, F.L.C.S lowers the barrier to digital fabrication and encourages creative expression across diverse user groups.

While the system meets its major design objectives, several limitations point toward valuable areas for future work and refinement. Increasing the laser diode power or improving mechanical efficiency could broaden the range of cuttable materials and increase cutting speed, bringing the system closer to industrial performance. More time dedicated to research would allow us to include diverse fabric types, depending on research findings available. Automating material recognition through color analysis, reflectivity measurement, or machine learning would enable adaptive cutting parameters optimized for each fabric type. Specific enhancements to the motion system—such as higher-stiffness gantry mechanics, improved stepper motor control, or closed-loop feedback—would help reduce vibration and improve dimensional precision. Further refinement of the beam-shaping optics could yield a smaller or more stable spot size, improving edge quality and reducing charring. Collectively, these improvements would elevate the system's performance, durability, and overall usability, and they present clear opportunities for continued research and development beyond the scope of this senior design project.

The team faced several challenges throughout development, including workflow delays and uneven subsystem progress, which required adjustments in task distribution and timeline planning. These obstacles ultimately strengthened the project by highlighting the importance of adaptability, documentation discipline, and communication among team members. The completion of this fabric laser-cutting system highlights the importance of being an effective member of interdisciplinary teamwork and represents a significant accomplishment for the students involved, as well as a meaningful contribution to the fields of photonics, electronics, and embedded systems design.

Appendices

Appendix A – References

[1] "Buildlog.net 2.x Laser". *Buildlog.Net Blog*, https://www.buildlog.net/blog/2011/02/buildlog-net-2-x-laser/. Accessed 1 Sep. 2025.

[2] “Epilog Fusion Pro Lasers”. *Innovative Cutting Systems*, https://www.innovativecuttingsystems.com/epilog-laser/fusion-pro-laser-series.ht m. Accessed 1 Sep. 2025.

[3] “GFL FIBER LASER”. *Dener Machinery*, https://dener.com/catalog/Gantry_Fiber_Laser.pdf. Accessed 10 Sep. 2025.

[4] “Wattsan 6090 LT”. *Wattsan*, https://wattsan.com/product/wattsan-6090-lt/?srsltid=AfmBOory9nmu9Siww-hZrptmbuj_zTc-xi6FvI4JbPgQV08FTDa5Ga4x. Accessed 10 Sep. 2025.

[5] Felipe Mosquera, A. M., Kavinaash Jesurajah, Jackson Gilliland, Nolan McGinley, Amir Mohd (2024). "UCF Senior Design Group 5 Fall 2023 - Spring 2024." from https://www.ece.ucf.edu/seniordesign/fa2023sp2024/g05/.

[6] J.L. Perry, J. H. A., R. Vijayakumar (2016). Submicron and Nanoparticulate Matter Removal by HEPA-Rated Media Filters and Packed Beds of Granular Materials**:** 28.

[7] 7*inch HDMI LCD (C) - Waveshare Wiki.* (n.d.). https://waveshare.com/wiki/7inch_HDMI_LCD_(C)

[8] Elecrow. (n.d.). *RC070M 7 inch 1024 x 600 Touch Screen Display with 720P Camera for Raspberry Pi/MacBook Pro./ Windows 10 – Elecrow Wiki.* https://www/elecrow.com/pub/wiki/rc070m-7-inch-1024-x-600-touch-screen-display-with-720p-camera-for-raspberry-pi-macbook-pro-windows-10.html?h=7

[9] Raspberry Pi Ltd. (2025). *Raspberry Pi Touch Display 2 Product Brief.* https://datasheets. Raspberrypi.com/display/touch-display-2-product-brief.pdf
[10] *Touch Display 2.* (n.d.). https://www.raspberrypi.com/documentation/accessories/touch-display-2.html

[11] Pounder, L. (2024, November 4). *Raspberry Pi Touch Display 2 Review: A Touch of class.* Tom’s Hardware. https://www.tomshardware.com/raspberry-pi-touch-display-2-review-a-touch-of-class

[12] Dean McClements, A. L. (2022, 2024). "CO2 Laser Vs. Fiber Laser: The Main Differences." from https://www.xometry.com/resources/sheet/co2-laser-vs-fiber-laser/?utm_source=chatgpt.com.

[13] Verdeyen, J. T. (1995). Laser Electronics, Prentice Hall: 74.

[14] El Sherif, M., et al. (1997). "Prediction of absorbance from reflectance for an absorbing-scattering fabric." Color Research & Application **22**(1): 32–39.

[15] Liu, Y., et al. (2010). "UV/visible/near-infrared reflectance models for the rapid and non-destructive prediction and classification of cotton color and physical indices." Transactions of the ASABE **53**(4): 1341–1348.

[16] Lasers, R. (2024). "Why a Larger Beam Results in a Smaller Spot Size in Laser Designation?". from https://www.rpmclasers.com/blog/why-a-larger-beam-results-in-a-smaller-spot-size-in-laser-designation/.

[17] Ng, B. (2023). "Laser Beam Expanders: Keplerian vs. Galilean Beam Expanders and Other Configurations." from https://wavelength-oe.com/laser-beam-expanders-keplerian-vs-galilean/.

[18] Safety, U. E. H. a. "Laser Safety Manual." from https://www.unf.edu/ehs/policies/laser-safety-manual.html#:~:text=UNF:%20Laser%20Safety%20Manual

[19] Hadler, J. (2023). "Laser Safety Facts." from https://www.lasersafetyfacts.com/laserclasses.html#:~:text=Laser%20classes,for%20updated%20info%20April%202023.

[20] Cerqueira, F., Brandenburg, B., & Max Planck Institute for Software Systems (MPI-SWS). (n.d.). A comparison of scheduling latency in Linux, PREEMPT RT, and LITMUS RT. *Abstract*. https://people.mpi-sws.org/~bbb/papers/pdf/ospert13.pdf

[21] https://www.thorlabs.com/newgrouppage9.cfm?objectgroup_id=139&pn=BB03-E02

[22] https://www.thorlabs.com/newgrouppage9.cfm?objectgroup_id=3810
[23] https://www.opmtlaser.com/laser-galvanometers/)

[24] https://www.popularwoodworking.com/techniques/what-why-hows-of-cnc-machines/

[25] https://www.thorlabs.com/newgrouppage9.cfm?objectgroup_id=6430

[26] https://www.edmundoptics.com/f/sill-optics-f-theta-lenses/40163/

[27] https://www.edmundoptics.com/knowledge-center/application-notes/lasers/gaussian-beam-propagation/?srsltid=AfmBOoq8YUaQ3TCxzE1MoZ7RZCdAx4hO-KCN_3dgRsXpdhulatVNL20k

[28] https://www.ipgphotonics.com/newsroom/stories/why-should-we-care-about-spot-size-in-fiber-laser

[29] https://www.thefabricator.com/thefabricator/article/lasercutting/the-importance-of-focal-positions-in-laser-cutting

[30]https://www.xometry.com/resources/sheet/laser-parameters/, https://www.thunderlaser.com/choose-by-industries/the-impact-of-laser-on-the-fabric1/

[31]https://www.researchgate.net/publication/258105599_A_study_on_laser_cutting_of_textiles

[32] McCracken, K. "Kiva's Website: Accessible Optics." from https://kivamccr.xyz/accessible-optics/.

[33] Jiajun Fu, C. L., Runhan Zhao, Huixin Wang, Zhongjie Yu, and Qinghua Wang (2024) Laser Cutting of Non-Woven Fabric using UV Nanosecond Pulsed Laser.

[34] Zoghi, M. and A. Dehkordi (2023). CW CO2 Laser Cutting of Multiple-Layer Blended Fabric.

[35] Khalaf, T., et al. (2023). "Performance Evaluation of Input Power of Diode Laser on Machined Leather Specimen in Laser Beam Cutting Process." Materials **16**(6): 2416.

[36] https://www.raspberrypi.com/documentation/accessories/camera.html